This project has received funding from the Euratom research and training programme 2014-2018 under grant agreement No 662287.

EJP-CONCERT

European Joint Programme for the Integration of Radiation Protection Research

H2020 – 662287

D9.62 – Methodology to quantify improvement*

*Guidance on uncertainty analysis for radioecological models

Lead Author: Laura Urso (BfS)

With contributions from: Cagatay Ipbüker, Koit Mauring, Hanno Ohvril, Martin Vilbaste, Marko Kaasik, Alan Tkaczyk (UT), Justin Brown, Ali Hosseini, Mikhail Iosjpe (DSA), Ole Christian Lind, Brit Salbu (NMBU), Philipp Hartmann, Martin Steiner (BfS), Juan Carlos Mora, Danyl Pérez-Sánchez, Almudena Real (CIEMAT), Justin Smith (PHE), Christophe Mourlon, Pedram Masoudi, Marc-André Gonze, Mathieu Le Coz, Khaled Brimo (IRSN), Jordi Vives i Batlle (SCK-CEN)

Reviewers: Juan Carlos Mora (CIEMAT), Marie Simon-Cornu (IRSN), and CONCERT coordination team

Work package / Task	**WP 9** **T9.3** (TERRITORIES)	**SST 9.3.1.3**
Deliverable nature:	**Report**	
Dissemination level: (Confidentiality)	**Public**	
Contractual delivery date:	**M47**	
Actual delivery date:	**M47**	
Version:	**1.0**	
Total number of pages:	**117**	
Keywords:	**Radioecological models; Propagation of uncertainty; Analytical approach; Probabilistic approach; Bayesian approach; Sensitivity analysis; Parameter uncertainty; Conceptual model uncertainty; Monitoring uncertainty.**	
Approved by the coordinator:	**M47**	
Submitted to EC by the	**M47**	

* Along the progress of the TERRITORIES project, clarification of the initial plans appeared necessary to avoid overlap between TERRITORIES Task 1.2 (CONCERT 9.3.1.2 "*Guidance to select the appropriate level of complexity in models***"**) and its deliverable D9.61 ("*Guidance to select level of complexity*") versus TERRITORIES Task 1.3 (CONCERT 9.3.1.3 "*Uncertainties propagation and sensitivity analysis in modelling***"**) and its deliverable D9.62 ("*Methodology to quantify improvement*"). Comparison between existing and advanced models, and then quantification of improvement, was included in the scope of D9.61. That is why the present document, D9.62, was renamed "*Guidance on uncertainty analysis for radioecological models*".

Abstract

This document presents the results of the work undertaken in CONCERT sub-subtask 9.3.1.3 (Task 1.3 of the TERRITORIES project) that deals with propagation of uncertainties and sensitivity analysis for radioecological models that are used to carry out risk assessments of long-lasting exposure situations. It is written in the form of a guidance to support developers and users of radioecological models for uncertainty analysis. This guidance combines in a comprehensive form the approaches and methodologies for carrying out uncertainty analysis with experts' knowledge specifically in the field of radioecology. Structured information about parameter uncertainty, conceptual model uncertainty, scenario uncertainty as well as role of variability are provided together with analytical, probabilistic and Bayesian approaches and methodologies to quantify and (where possible) to reduce these uncertainties. This guidance includes several references and various test cases, which show how quantification of these uncertainties can be handled in practice. It also provides an overview of the tools and software available to quantitatively address uncertainty analysis for radioecological models. Special attention has been given to the specific challenges that need to be accounted for when dealing with radioecological models. By producing results that account for the uncertainty of the radioecological model outputs, the trust and confidence of the public and stakeholders can be increased considerably.

Table of Contents

1 Executive Summary

Radioecology is the discipline that deals with quantifying the transport of radionuclides in the environment and their transfer from one environmental compartment into another. The endpoints of radioecological models, i.e. activity concentrations and ambient doses rates, provide the basis for calculating the doses to humans and non-human biota, which in turn are the input for carrying out an environmental risk assessment and support decision-making for management activities at contaminated sites.

The activity levels of radionuclides in the environment can either be quantified via measurements or via radioecological models, if measurements are not possible or not feasible with reasonable effort. Radioecological models need to account for many physico-chemical and biological processes that occur in nature and their large variability.

Depending on the goal of a risk assessment and the extent to which environmental processes are understood in detail, radioecological models range from extremely simplified representations of reality (e.g. transfer factor model) to rather sophisticated and complex ones (e.g. geochemical speciation models). Radioecological models are often implemented using simulation software that facilitates the development of compartment models by automatically generating the corresponding system of ordinary differential equations or written from scratch using programming tools and languages such as Python, C++ or R. In any case, radioecological models are a simplified representation of reality associated with an uncertainty budget, which in turn will affect the uncertainty of the risk assessment.

This report summarises the efforts of the CONCERT sub-subtask 9.3.1.3 (= TERRITORIES Task 1.3) participants towards quantitative analyses of uncertainties of radioecological models and structures them in form of a guidance document. In fact, a careful analysis of the uncertainty budget is the prerequisite to assess the quality and robustness of model predictions and/or forecasts. It also helps to critically evaluate the underlying scientific basis and increases confidence and acceptance when communicating scientific results to stakeholders and the public.

Uncertainty in the output of a radioecological model arises from many different contributions, which are briefly outlined in Chapter 4: uncertainty due to the choice and range of model parameters, uncertainty due to the inevitable simplification in model structure and conceptualisation (conceptual model uncertainty), uncertainty due to sampling and monitoring of input variables, uncertainty in the knowledge of the scenario to be modelled, uncertainty in the subjective interpretation of the assessment problem (modeller's uncertainty) and uncertainty in the mathematical/numerical implementation of the model.

The prioritisation of the various types of uncertainty that contribute to the total uncertainty budget of a radioecological model depends on the model under consideration, the data available and the specific assessment situation. In this guidance document, propagated parameter/input uncertainty, conceptual model uncertainty and scenario uncertainty are treated in more detail and are prioritised with respect to other contributions to uncertainty. This is done on the one hand because these types of uncertainty certainly contribute largely to the total uncertainty budget of radioecological models applied to long-lasting exposure situations, which are the main focus of the TERRITORIES project. On the other hand, the analysis of these types of uncertainties requires a structured effort that would definitely benefit from a compilation of potential approaches and a guidance document, which has been so far missing in radioecology. Nevertheless, the authors acknowledge that mathematical/numerical uncertainty and modeller's uncertainty are important. Readers of this guidance document and users of radioecological models should not neglect these two types of uncertainty.

The type of approach to carry out a quantitative uncertainty analysis, either probabilistic or Bayesian (seldom an analytical approach), needs to be chosen depending on the information and data available.

Some approaches require a minimum quality of data and will not work properly otherwise. Effort should also be spent on retrieving information about potential correlations of the model parameters. Sensitivity analyses provide insight into the impact of varying parameter values on the model output (parameter sensitivity analysis) as well as into the importance of a specific process for the model output (process sensitivity analysis). Sensitivity analyses are often the first step before proceeding with the detailed uncertainty analysis. Chapter 5 and Chapter 6 are dedicated to these topics.

In Chapter 7, more detail is provided about the state of the art for coping with propagated parameter uncertainty and conceptual model uncertainty in the field of radioecology. In particular, available methodologies are explained and literature references from the field of radioecology are provided to the reader.

In Chapter 8, test cases give examples of how the methodologies for dealing with the quantification of different types of uncertainty, including probabilistic and Bayesian approaches, can be applied to real situations and models in the field of radioecology. The test cases consider to a large extent NORM situations and post-accidental situations, for which data are available from the TERRITORIES Library Database (TLD).

In Chapter 9, recommendations in form of a list of good practices are provided to support the reader in carrying out uncertainty analysis of radioecological models. Software and tools for uncertainty analysis are listed in Chapter 10.

2 Introduction

2.1 The decision-making process in radiation protection and the role played by radioecological models and their uncertainty

Decision-making processes in the field of radiation protection are step-wise approaches that start either with measurements at radioactively contaminated sites or are based on the evaluation of an environmental (radioecological) model outputs. In fact, when measurements are not available or not suitable for risk assessments, radioecological models are used to quantify the transfer of radionuclides from one environmental compartment to another and ends with a qualitative/quantitative estimate of the risk to human and/or non-human biota associated to the presence of naturally-enhanced or anthropogenic radioactivity.

Within this context, the work undertaken in CONCERT sub-subtask 9.3.1.3 (Task 1.3 of the TERRITORIES project) dealt with propagation of uncertainties and sensitivity analysis for radioecological models that are used to carry out risk assessments of long-lasting exposure situations.

Risk assessments in the field of radiation protection are carried out prior to or during a release event, in the short or long term after deposition or disposal of radioactive substances, or before and after remediation activities and are needed for cost-benefit analysis, compliance with dose criteria, for optimisation of radiation protection. Based on the risk assessment carried out, the risk manager can then make a motivated decision on actions to be undertaken (or not).

A schematic representation of the stages required for decision-making process is shown in Figure 2.1-1.

The first stage of a decision-making process is the evaluation of an environmental model output and the characterisation of exposure scenario. The output quantities in the first stage refer to the radiological characterisation, have units such as Bq L^{-1}, Bq kg^{-1}, Bq m^{-2}, Gy h^{-1} and are more specifically outputs of radioecological models.

The second stage is the quantification of the effective dose (E in Sv for effective dose to people or D in Gy for absorbed dose for non-human biota), which is obtained from the radioecological model output multiplied by the dose coefficients either for humans (ICRP, 2012) or for non-human biota (ICRP, 2017).

The dose coefficients involved in the dose-assessment are considered errorless by convention, hence the uncertainty on the dose comes primarily from the total uncertainty budget of the radioecological model and the uncertainty involved in the characterisation of the exposure scenario.

In order to characterise an exposure scenario it is necessary to account for human and wildlife behaviour and living habits in order to establish which population and/or individuals are exposed to radiation and it considers aspects like food consumption, indoor/outdoor occupancy times, spatial and temporal variability of human/animal activities, respiratory rates, etc. For long-lasting exposure situations more details on exposure scenarios and uncertainties related to it are addressed in CONCERT-TERRITORIES deliverable report D9.63.

The third stage if decision-making process is the environmental or human risk assessment obtained by considering the dose for human and /or non-human biota and by making use of the LNT hypothesis and the relevant risk factors (ICRP, 2005) for humans and the dedicated framework for assessing the risk for non-human biota (ICRP, 2014).

In this guidance, the focus is on the total uncertainty budget of radioecological models.

The quantification of the total uncertainty budget of a radioecological model output is basis for good scientific practice and important for communication of results but is also necessary as output model values characterised by good confidence are the starting point of the decision-making process or alternatively indicate that further refinement (e.g. uncertainty reduction, radioecological model improvement) is necessary before moving on with the analysis.

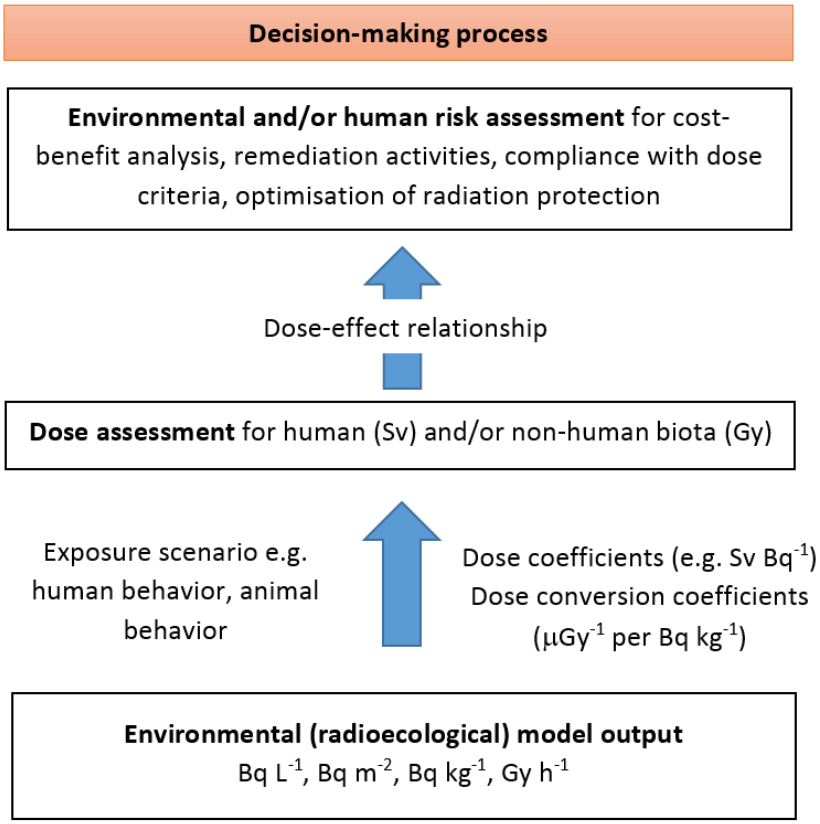

Figure 2.1-1: Schematic representation of the necessary steps to be accounted for within the management of radioactive contaminated sites.

2.2 How the term "uncertainty" is defined and used in this guidance

TERRITORIES focuses on the determination of uncertainties that play a role in the decision-making processes for the control of radiation safety in existing exposure situations. Within this context the term "uncertainty" is used in a very broad sense in relation "*to any situation for which a fact, data or phenomenon and their causes or consequences are not known with certainty by a specific actor in her/his decision context*" (cf. CONCERT-TERRITORIES deliverable report D9.65).

Some reviews on uncertainty classifications in environmental modelling and more in general for environmental risk assessments can be found in (Ascough et al., 2008; Cullen & Frey, 1999; EPA, 2009, 2014; Maier, 2008; Morgan et al., 1992). The reader should be aware that a unique and well-established definition for each type of uncertainty is missing: Ascough et al. (2008) summarised the large number of different definitions and philosophies adopted for the quantification of uncertainty in scientific studies.

In addition some references rely on uncertainty being a multi-dimensional concept of e.g.(Strauss, 1997), and suggest the use of the so-called *uncertainty matrix* (van der Sluijs et al., 2003; Walker et al.,

2003) to obtain a systematic overview of all the types of uncertainties that play a role in the risk assessment. In this matrix, the following concepts are considered necessary to characterise fully uncertainty:

- the *level* of uncertainty i.e. statistical uncertainty, scenario uncertainty, recognised ignorance,
- *the location of the uncertainty* i.e. where the uncertainty manifests itself within the model system (model structure, model parameters, model inputs and model context),
- *the nature of uncertainty* i.e. whether the uncertainty is epistemic i.e. due to imperfection of our knowledge or due to inherent variability of the phenomena being described.

In the present guidance the term “uncertainty” is used in a narrower sense than the one presented in CONCERT-TERRITORIES deliverable report D9.65. In the present work, uncertainty relates specifically to the uncertainty contributions that accumulate/propagate to radioecological model output and that refer to the level statistical uncertainty as in (Walker et al., 2003). The contributions coming from scenario uncertainty are considered only in relation to possible different types and amounts of releases (source terms) whereas the choice of exposure scenario is not considered here in detail as it is main topic of CONCERT-TERRITORIES deliverable report D9.63.

3 Objective of this guidance

Quantification of the uncertainties in radioecology and in particular quantification of total budget of radioecological model output has been considered as a major challenge within the radioecological community (Hinton et al., 2013). In recent years, effort has been dedicated to this topic and the first aim of this guidance is to provide an insight into the efforts that have been undertaken so far. Thus, examples taken from the literature are quoted along Chapters 5, 6 and 7, and original case studies are provided in Chapter 8.

This guidance is meant to provide support not only for modellers and students in the field of radioecology but also to risk assessors and managers who have to develop, select and apply radioecological models. Its main objective is to provide the reader with adequate background and easy-to-use tools that allow either a qualitative or, if enough information is available, quantitative estimation of the total uncertainty budget of a radioecological model output. On the other hand, this guidance does not deal with how to communicate uncertainties on risk assessments nor with uncertainties that play a role at other stages of risk assessment. Also extensive discussion on philosophical meaning of uncertainty is not included. Definitions of various types of uncertainties given here do not attempt to be general and valid outside the context of this deliverable report.

Uncertainty in the output of a radioecological model arises from many different contributions, which are briefly outlined in Chapter 4. Chapter 5 is dedicated to quantitative uncertainty analysis, either probabilistic, analytical, Bayesian, or non-statistical. In Chapter 7, more detail is provided about the state of the art for coping with propagated parameter uncertainty and conceptual model uncertainty in the field of radioecology. Cases studies of Chapter 8 illustrate various applications of uncertainty analysis. In addition, the guidance provides a broad overview of literature that focuses on the quantification of uncertainties in environmental modelling including radioecological modelling.

The use of sensitivity analysis (SA) can be considered as an integrated part of uncertainty analysis. The aim of sensitivity analysis is two-fold. Sensitivity analysis guides the process of model development and it provides information about the influence of the selection of exposure scenario, of the structure of the models and of the parameter choices on the model output (Heinemeyer et al., 2018). In this work, the focus is on sensitivity analysis for the quantification of the impact of parameters' values to model output. Such a sensitivity analysis is detailed in Chapter 6, and illustrated by two cases studies of Chapter 8 (Sections 8.1 and 8.3). However, sensitivity analysis can be used also to improve model quality through analysis of different model structures and two examples of this type of application are also presented (as illustrated in two of the cases studies of Chapter 8 (Sections 8.3 and 8.5)).

The test cases in the document provide practical examples of applications of available software and methodologies described in the guidance. However, no pre-established standardised procedures exist that deal with the quantification of uncertainties for radioecological model. Hence examples are seen as supportive and as clarifying of the theoretical aspects described in the guidance.

Final recommendations provided in Chapter 9 are the most important outcome of the present deliverable report. The reader is strongly encouraged to account for these while carrying the uncertainty analysis for his/her radioecological model.

4 Radioecological models and their uncertainties

Radioecological modelling can be considered as a branch of environmental modelling, with specific challenges related to the peculiarity of radioactive substances and their transfer in the environment.

Radioecological models need to account for processes (biological, chemical and physical) which are intrinsically heterogeneous. Often only a small number of experimental data exists to carry out model calibration and validation as data for radioactive substances is rather limited (luckily) or radiation levels are so low that detection threshold is not exceeded.

Sometimes the outputs of radioecological models can differ between each other in terms of calculated endpoints because they are often embedded in tools that deliver directly the dose to human on non-human biota instead of the radioecological quantities mentioned in Chapter 2.

Last but not least, radioecological model are usually based on simple mathematical structures, e.g. multiplicands, parametric (linear or exponential) equations, linear ordinary differential equations. Partial differential equations are rarely used.

The total uncertainty budget of a radioecological model output is to be considered the accumulated uncertainty caused by all the uncertainty types that affect the model output. An important assumption that is often made (and is valid also in the present document) is that if adequate (i.e. representative) experimental data is available the total uncertainty budget can be quantified by the difference between the model output and the experimental values (i.e. residuals).

4.1 Uncertainty types contributing to total uncertainty budget of radioecological models

Uncertainty types that contribute to the total uncertainty budget of a radioecological model are:

These are:

- Parameter uncertainty
- Input uncertainty (i.e. monitoring uncertainty[1])
- Conceptual model uncertainty (structural uncertainty)
- Scenario uncertainty
- Numerical/technical uncertainty
- Modeller uncertainty

In radioecological modelling, variability plays an important role because of the inherent variability of the human and natural system under analysis. Natural variability is related to the inherent randomness of nature (e.g. temporal, spatial, inter or intra-individuals …), whereas variability associated with human factors comes from current political climate, attitudes of the policy-makers, and requirements from stakeholders. A reduction of variability occurs if the exposure scenario is determined e.g. if the selection criteria for the target population of an assessment is restricted - e.g. with observation of a sub-population (Heinemeyer et al., 2018; Simon-Cornu et al., 2015). Within the scenario of interest, variability cannot be reduced.

4.1.1 Parameter uncertainty

Parameter uncertainty refers to the uncertainty related to the model parameters and their correlations. As an example, in the case of a radioecological model of the form: $y = a \cdot x + b$ in which *x* is the „model input“, *a* and *b* are the „model parameters“ and y is the „model output“, the parameter

[1] For broader definition of monitoring uncertainty cf. CONCERT-TERRITORIES deliverable report D9.74.

uncertainty is the uncertainty associated to the uncertainties in the quantification of *a* and *b* and their propagation along the model. Parameter uncertainty refers to model parameters used as input to the mathematical model that cannot be experimentally controlled (Salbu, 2016) and that are chosen a priori or calibrated. Often, in fact, these parameters are subject to calibrations needed for the different scenarios where the model is applied. Section 7.1 provides details about propagation of parameter uncertainty. Even if more general, Chapter 5 is mostly applicable to parameter uncertainty. Last, all case studies of Chapter 8 include some consideration of parameter uncertainty.

4.1.2 Input (monitoring) uncertainty

Input uncertainty arises in radioecology because of uncertainties in experimental measurements (cf. Section 5.1) as well as uncertainties in representative sampling (cf. CONCERT-TERRITORIES deliverable report D9.60), and uncertainties in interpolation/extrapolation when data is missing (Salbu, 2016). Uncertainty arising from model input(s) comes from monitoring (and sampling) uncertainty if the model input(s) is/are based on measurements. Input uncertainty in fact accounts for inconsistencies between measured values and those used by the model (level of aggregation/averaging). It is also closely related to inherent process variability i.e. spatial and temporal (EPA, 2009; Martuzzi, 2006). In the present guidance input, monitoring/sampling uncertainty and measurement uncertainty are treated together since for long-lasting exposure situations dose assessment calculations rely on measured inputs at the time of interest, or at a time posterior to the very beginning of contamination. However, for quantifying the overall uncertainty of dose calculations, one can often treat model parameter(s) and model input(s) in a "technically" similar way. Uncertainty related to monitoring and sampling activities can be reduced by optimising their design (Oughton et al., 2008). Optimal design is highly dependent on the purpose of the assessment to be carried out i.e. no optimal design is valid in general. Section 7.1 provides details about propagation of input uncertainty. Even if more general, Section 5.1 is mostly applicable to measurement uncertainty. Last, the first three case studies of Chapter 8 (Section 8.1, 8.2 and 8.3) include consideration of input uncertainty, with specific focus on sampling uncertainty in Section 8.2.

4.1.3 Conceptual model uncertainty (structural uncertainty)

Conceptual model uncertainty arises from a simplified, incomplete or even wrong translation of the real world into a conceptual model and its mathematical representation. In literature it is also called structural uncertainty or model uncertainty. Conceptual model uncertainty includes the simplifications introduced when describing environmental processes with mathematical expressions and techniques that are developed to represent the system of interest, namely misspecification of the model boundary conditions like the range of input parameters; misapplication of the model developed for other purposes (Cullen & Frey, 1999). The (EPA, 2009) mention contributions from incomplete knowledge about factors that control the behaviour of the system being modelled; limitations in spatial or temporal resolution; and simplifications of the system. Section 7.2 provides details about qualitative or quantitative approaches of conceptual model uncertainty, and this is illustrated in both case studies of Section 8.4.

4.1.4 Scenario uncertainty

The term scenario uncertainty is used in a variety of contexts with slightly different meanings. For risk assessment analysis, the term scenario is used to describe a particular set of sequence of events and conditions, a different type of release (source term) e.g. (Salbu, 2006). In the management of radioactive waste and safety assessment, scenario uncertainty is related to the uncertainties associated with the possible occurrence of features, events and processes (FEPs) external to the disposal system that may impact the natural or engineered parts of the disposal system over time: scenarios considered may be disruptive events external to the disposal system, such as volcanism, seismicity, human intrusion and climate change. On the other hand, for environmental management

of a radioactively contaminated site, the term scenario is used to describe not only missing knowledge of the type of release but also hypothetical or generic individual exposure. The definition of the "critical group or representative person" in the scenario development also constitutes an important source of uncertainty related to scenario, referred to as exposure scenario uncertainty (which is exhaustively treated in CONCERT-TERRITORIES deliverable report D9.63). In general, these different definitions underlie an incomplete knowledge about the states of the system where the exposure occurs, including not only the situation at the moment of the assessment, but also the situation in the past (for retrospective assessments) and in the future (for prospective assessments). This includes uncertainty in environmental properties, the sources and speciation of contamination, time and spatial variation, etc. This type of uncertainty is usually handled with a 'what-if' methodology (Refsgaard et al., 2007).

4.1.5 Numerical/technical uncertainty

The numerical/technical uncertainty is related with the implementation of numerical approaches used to solve the equations. The numerical methods used to solve systems of ordinary differential equations (e.g. Runge-Kutta methods with and without adaptive time-stepping (Bogacki & Shampine, 1989)) or partial differential equations are numerous and included in available software libraries or simulation software such as Ecolego, GoldSim, Matlab (cf. Chapter 10). These software tools usually provide default settings which are considered by the user without investigating other possibilities (when the tool allows the user to change them). Indeed, when performing environmental impact assessments with radioecological models, the choice of the numerical scheme configuration is often a compromise between the calculation time and the precision and this need to be accounted for. In fact it is easy to inadequately choose/use a numerical method to solve systems of ordinary differential equations as it all depends on the numerical solver used, its configuration and the typical time scales of the process involved in the model application. This is all the more true that when the uncertainty analysis concerns an 'integrating' variable, such as a dose to human population, which can tend to show a narrower range of uncertainties than that of intermediate variables, such as activity stocks or concentrations in a given biosphere compartment - which can often reflect the uncertainty of a specific model parameter. It is easy to obtain 'erroneous' results with a poorly configured numerical solver.

4.1.6 Modeller uncertainty

The modeller uncertainty refers to the (incorrect) way in which modellers translate an assessment situation into a model based on an incorrect interpretation of the assessment situation or the selection of an inappropriate model. An example of this type of uncertainty is the selection of a (conservative) screening model although best estimates of doses to humans are required.

4.2 Prioritisation of uncertainties within this guidance

In this guidance, more detail is provided on how to quantify *parameter uncertainty, input uncertainty, conceptual model uncertainty* and *scenario uncertainty* (in particular uncertainty on source term). Within the TERRITORIES project, in fact, these types of uncertainties contribute largely to the uncertainty of model output. However, parameter uncertainty and input uncertainty are also prioritised because, despite extensive literature and availability of examples within radioecology, a description of these in one unique document has been lacking so far. It is aim of this guidance to fill this gap. On the opposite, for conceptual model uncertainty very little has been done in the field of radioecology and in this guidance effort is undertaken to extend methodologies from other fields of research to radioecology. Scenario uncertainty related to poorly known types of releases and situations is considered as well and examples are provided on how to address it by means of 'what-if' approach in Chapter 8.

5 Approaches to uncertainty analysis (overview)

Several approaches to evaluate uncertainty in the output of mathematical models are available and are applicable to radioecological models: the analytical approach, the probabilistic approach and the Bayesian approach. Information on the model parameters and input variables may be available from either direct measurements, expert judgement, or by indirect observations (Sy, 2016) and choosing among these approaches will depend on these information.

Alternative approaches have been proposed for handling uncertainty in the absence of complete and precise data, based on the Fuzzy set Theory (Zadeh, 1965). Their application in radioecology has been very rare (Ali et al., 2012; Mercat-Rommens et al., 2006), and they are not discussed further in the present deliverable report.

In the following section, the analytic, probabilistic and Bayesian approaches are introduced. Additionally also a qualitative approach is presented which is used whenever the conditions for applying statistical approaches do not hold or statistical quantification is not considered necessary (Section 5.5). Before carrying out the uncertainty analysis, correlations among model parameters need to be understood in order to be properly accounted for in the statistical methods for propagating uncertainty. Also specific features related to the peculiarities of radioecological models need to be considered. Therefore Sections 5.4 and 5.6 are dedicated to these topics.

5.1 Analytical approach to propagate uncertainty to the model output

The analytical approach is used mostly in the analysis of uncertainty related to measurements (JCGM, 2008a) in the form of the classical formulas for propagation of error (Refsgaard et al., 2007). The error propagation formulas are valid if the uncertainties have a Gaussian (normal distribution), if the uncertainties for non-linear models are relatively small: the standard deviation divided by the mean value is less than 0.3 and if the uncertainties have no significant covariance. They can however be extended to allow non-Gaussian distributions and co-variances but become rather complex and cumbersome to use and are seldom found in radioecology especially since computational power has allowed for more straight-forward implementation of probabilistic methods and Bayesian methods.
In general, a measurand Y is not measured directly but is determined from N other input parameters x_1, x_2, …, x_N, through a multivariate functional relationship, a measurement model function *f*,

$$y = f(x_1, x_2, x_3, \dots, x_N) \quad (1)$$

For a measurand y (a result of modelling, forecast, etc.) expressed by Equation (1), each single input *i* has its own uncertainty, $u(x_1)$, $u(x_2)$, $u(x_3)$,…, $u(x_N)$, respectively. Under these conditions, the total (combined) standard uncertainty of the output y is evaluated by Equation (2),

$$u^2(y) = \sum_{i=1}^{N}\sum_{j=1}^{N}\left(\frac{\partial y}{\partial x_i}\right)\left(\frac{\partial y}{\partial x_j}\right)u(x_i, x_j) =$$

$$= \sum_{j=1}^{N}\left(\frac{\partial y}{\partial x_i}u(x_i)\right)^2 + \sum_{\substack{i,j=1 \\ i\neq j}}^{N}\left(\frac{\partial y}{\partial x_i}\right)\left(\frac{\partial y}{\partial x_j}\right)u(x_i, x_j) \quad (2)$$

where: $\left(\frac{\partial y}{\partial x_i}\right)$ – are the first partial derivatives or sensitivity coefficients;

$u(x_i, x_i) = u(x_i)\cdot u(x_i) = u^2(x_i)$ – the variance of x_i;

$u(x_i, x_j); i \neq j$ – the covariance between x_i and x_j.

In practice, within radioecology, the input parameters are often considered mutually uncorrelated:

$u(x_i, x_j) = 0$, when $i \neq j$,

where the "uncorrelation" is not always correct, but enables a considerable computational convenience to rewrite Equation (2) in a simpler form:

$$u^2(y) = \sum_{i=1}^{N} \left(\frac{\partial y}{\partial x_i}\right)^2 u^2(x_i) \quad (3)$$

Equation (3), based on a first-order Taylor series approximation of $Y = f(x_1, x_2, ..., x_N)$, express the basic recommendation for evaluation of uncertainty in the output of a multivariate system. For simple, linear models, they can even be applied using a pocket calculator (Elster, 2014).

When the function is linear in the input quantities and the probability distributions for these quantities are Gaussian, the analytical approach provides exact results. Even when these conditions do not hold, the approach can often work sufficiently well.

From the estimated measurand *y* and expanded uncertainty, $k_p \cdot u(y)$, a coverage interval can be defined:

$$y - k_p \cdot u(y) \leq y \leq y + k_p \cdot u(y) \quad (4)$$

where k_p is the coverage factor, usually taken in the range 2 to 3.

The produced interval (cf. Equation 4) is expected, at a confidence level *p*, to encompass a large, specified fraction *p* of the distribution of values that could reasonably be attributed to the measurand Y. Note that calculation of a coverage factor k_p for a given confidence level *p* requires information about the probability density function (PDF) for the output quantity.

When the PDFs for the uncertainties are asymmetric (cf. Equation 4) cannot be used for the calculation of coverage intervals for measurand *y*. Instead, calculations of appropriate lower and upper limits for y, i.e. quantiles, are used.

Some cases that can be analytically handled for a general number *N* of input quantities are linear functions:

$$y = c_1 x_1 + \cdots + c_N x_N \quad (5)$$

where the PDFs for all input quantities are Gaussian, or all are rectangular with the same width.

Cases where there is only one input quantity (N = 1) can often be treated analytically for relatively simple models, like quadratic forms,

$$y = x^2 \quad (6)$$

reciprocals,

$$y = \frac{1}{x} \quad (7)$$

logarithms,

$$y = \ln x \quad (8)$$

etc., but considering only simple PDFs for input like rectangular, triangular or standard normal PDF (Cox & Siebert, 2006; JCGM, 2008b; Rice, 2006). An advantage of an analytical solution is that it

provides an exact insight through relating the probability distribution for output on parameters to the probability distributions for input.

5.2 Probabilistic approach to propagate uncertainty to the model output

Deterministic approaches for model analysis allow the user typically to select single best estimates, or conservative (high percentile in their cumulative distributions) input values and parameters, for any given calculation thus yielding single point estimate results for that particular scenario and model application.

Probabilistic methods, in contrast, are used to generate samples from the probability distribution functions (PDFs) for each of the model inputs (which include input data and mathematical model parameters), run the model based on one random value from each probabilistic input, based in their respective PDFs, and produce one corresponding estimate of the model outputs. The process is then typically repeated hundreds or thousands of times to create a statistically representative sample of model outputs. These output data are themselves presented as a probability distribution of the output of interest (EPA, 2014).

Whereas the result of a single calculation of a modelling system is a qualified statement ("if we run for given conditions defined by a given scenario and inputs, then result ‘y’ could occur"), the result of a probabilistic simulation is a quantified probability ("if we run for given conditions defined by a given scenario and inputs, there is a ‘x %’ chance that result ‘y’ could occur "). Such a result (in this case, quantifying the probability of any given output ‘y’) are potentially more useful to decision-makers who utilise the simulation results although sometimes the ability of decision makers to deal with concepts of probability and uncertainty varies (EPA, 2014).

The impact of the variation of model inputs and parameters on the model output is then the estimate of how the uncertainty of these quantities propagates to the model output.

The technique of a kind of trial-and-error statistics known as Monte Carlo Method (MCM) or Monte Carlo Simulations (MCS) is the most well-known and most often applied tool (Kirkup & Frenkel, 2006) for obtaining PDFs from samples over possible input and model parameters. The use of MCM requires the generation of a large amount N of random input values by means of statistical sampling following an appropriate statistical distribution in order to run a simulation (a trial) for each of the N input.

To generate samples the most often used methods are the Monte Carlo Markov Chain (MCMC) method, the Latin Hypercube Sampling (LHS) method (McKay et al., 1979) and the bootstrap method (Efron & Tibshirani, 1994). One of the criteria to consider in order to choose among the sampling methodology is the rate with which convergence of the obtained parameter distribution can be obtained. Also one of the main issues related to the use of MC sampling methods is whether there remain important parts of the parameter space unsampled. On the other hand, some other considerations may be important, e.g. whether a methodology is already included in a software, what extent the user has already experience with the available methodology. However, whatever the applied sampling strategy, it is important to consider thoroughly the sampling properties of the algorithm used (Beven, 2007).

In the following sections, the bootstrap method, the MCMC method and the Latin Hypercube Sampling methods are briefly described. The descriptions are by far not exhaustive as different variations of these methods are available but aim only at elucidating the concept behind the methodologies. The reader can find in the referenced material much more detailed descriptions.

5.2.1 The bootstrap method

The bootstrap method is statistical technique for estimating quantities about a population by averaging estimates from multiple small data samples. These samples are constructed by drawing observations from a large data sample (at least 200 data points (Barthel & Thierfeldt, 2015)) one at a time and returning them to the data sample after they have been chosen. This allows a given observation to be included in a given small sample more than once. This approach to sampling is also called sampling with replacement and is a discrete form of sampling. When applying this method it is especially important to analyse the available data for its representativeness.

5.2.2 Monte Carlo Markov Chain (MCMC)

The Monte Carlo Markov Chain (MCMC) algorithms are based on the theory of Markov chain and enable the creation of a sequence of correlated variables with the aim to approximate a target distribution that well encompasses these variables (Vose, 2008). These algorithms aim to choose samples with a density that varies through the model space, dependent on the likelihood (cf. Section 5.3) and hence their possible use depends also on data availability. The Monte Carlo Markov Chain starts with a proposal distribution (transitional kernel) for the Markov Chain. Random samples of model parameters are generated in the model space consistent with the proposal distribution. At each sample point, the model is run to determine the value of likelihood of model prediction at that point. The initial sample of points is then used as the basis for selection of new samples, using the proposal distribution to choose new points around each current sample. After a further sampling sequence, the method is checked for convergence on a consistent distribution. If not, another iteration is carried out.

The MCMC algorithms mostly used are e.g. the Metropolis-Hastings (Hastings, 1970; Metropolis et al., 1953) and the Gibbs-sampling algorithm (Gelfand & Adrian, 1990). In the first one a Markov Chain is generated, in which the set of samples at step *t* is dependent on the samples at (*t*-1*)*. At each step the samples are randomly generated from a proposal distribution that depends on the results obtained at step *t*. The critical step is the choice of whether a new point should be accepted or rejected. The second algorithm is a variant of the Metropolis-Hastings algorithm. In the Gibbs sampler it is assumed that the form of the distribution of the parameter is given *a priori*. The algorithm then chooses a random parameter, picks a new value for that parameter from the current estimate of the marginal distribution and continues to the next parameter. This algorithm is useful if all the distributions can be assumed to be normally distributed, but the marginal distributions and covariance are unknown.

5.2.3 Latin Hypercube Sampling (LHS)

The Latin Hypercube sampling (LHS) is a method that ensures that the search for sampled values is carried out all over the parameter space. In LHS, each parameter dimension of the model space is split into a number *N* of discrete values. Where a prior distribution is assumed, discrete intervals of probability are used. Parameter sets are chosen based on sampling an interval randomly for each parameter and hence *N* sets of parameter values will be generated and run, with the sample being scattered through the model space.

5.2.4 Monte Carlo Methods for discerning between parameter uncertainty and variability

Recent efforts in relation to the application of Monte Carlo methods have been carried out concerning the separated treatment of uncertainty and variability. In an earlier report EPA (2001), it was recommended that appropriate methods should be applied to quantify uncertainty and variability separately, and that both components should then be propagated through the selected model to estimate the uncertainty and variability in the model result. As considered by (Simon-Cornu et al.,

2015), two-dimensional (or second-order) Monte Carlo simulation (2D MC) approaches have been developed to estimate the uncertainty in the risk estimates stemming from parameter uncertainty. These 2D MC approaches can be applied so that distributions reflecting variability and uncertainty are sampled separately and can thus be represented independently in the model output. Nonetheless, as (Simon-Cornu et al., 2015) also underlie, the net separation of variability and uncertainty in the inputs of exposure assessment is often very challenging. Some headway appears to have been made on this theme albeit recognising that the difference between variability and uncertainty is subjective and depends on the scope of a scenario. More details on 1D MC method and 2D MC method is provided in Chapter 7.

5.2.5 Example of propagation of uncertainties using analytical and probabilistic approach

A simple example is provided here to show the equivalence in simple cases of the analytical approaches and the probabilistic approaches.

A simple counting of the disintegrations of a beta emitters is performed with a proportional counter. Two measurements are carried out, one with the sample M±u(M) and one without the sample to determine the background F±u(F). The net counts corresponding to the sample are therefore

$$N = M - F \quad (9)$$

The uncertainty would then be analytically computed as:

$$u(N) = \sqrt{u^2(M) + u^2(F)} \quad (10)$$

That value of $N \pm u(N)$ should be corrected by the efficiency of the detector ε (together geometrical and intrinsic) to obtain the activity of the sample

$$A = \frac{N}{\varepsilon} \quad (11)$$

The final uncertainty of the activity would therefore be:

$$u(A) = A \cdot \sqrt{\frac{u^2(M)+u^2(F)}{(M-F)^2} + \frac{u^2(\varepsilon)}{\varepsilon^2}} \quad (12)$$

If:

For measurements of T= 1000 s

M = 3452 ± 59

F = 643 ± 25

(and by considering that the measurements follow Poisson distributions, which can be approached by Gaussian distributions when the number of events is big enough) one obtains N = 2809 ± 64, by using the analytical expression (cf. Equation. 10) for the uncertainty.

If the detection (geometric and intrinsic) efficiency is determined by measuring 100 times a certified standard obtaining ε = 0.02345 ± 1%, the activity would then be A = 120 000 ± 3000 using Equation (12).

It can also be done by using the MC method, assuming all the measured values follow Gaussian distributions (the example was carried out by using the crystal ball plug-in in Microsoft Excel – cf. Chapter 10).

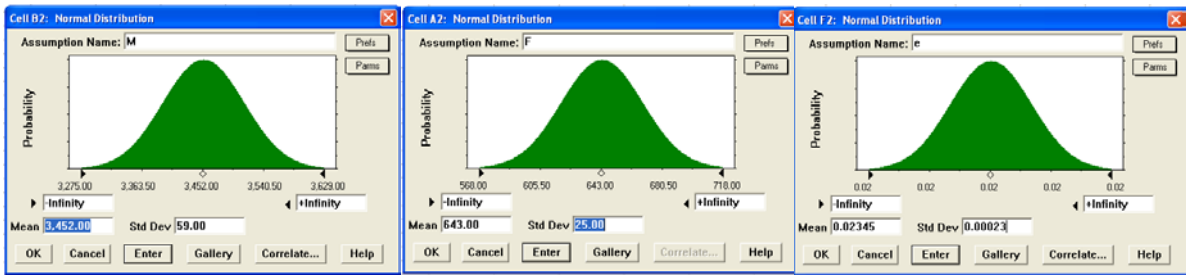

Figure 5.2-1: Gaussian pdfs assigned to the measurement of the sample M (left), the background F center) and the efficiency ε (right).

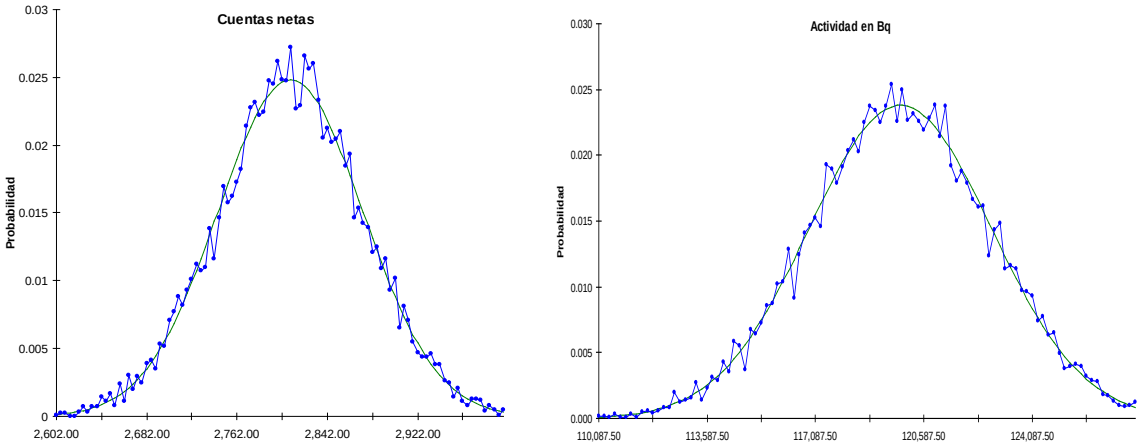

Figure 5.2-2: Net counts of the sample N (left) and total activity of the sample A (right).

The application of a pure MC method to the formula used for the calculation of the net counting (cf. Equation 9) and the total activity (cf. Equation 11) provides the result in Figure 5.2-2.

If the values of the histogram represented in Figure 5.2-2 are fitted to a Gaussian distribution, a mean $\mu = 119825$ and a standard deviation $\sigma = 2947$ are obtained. Rounding the values an activity of A = 120 000 ± 3000 is obtained, exactly the same obtained by propagating the uncertainty using the analytical methods.

5.3 Bayesian approach to propagate uncertainty to the model output

Risk characterisation, achieved partly or wholly through the application of modelling tools, is part of any robust environmental impact assessment. A common approach in this regard is to assign probability density functions (PDFs) to uncertain parameters and to perform probabilistic simulations to get PDFs of the model output. The techniques for conducting such simulations are well developed, as discussed in Section 5.1, and various software are available (cf. Chapter 10) to apply these methods. However, a main challenge in these approaches is how to assign PDFs to uncertain parameters. In many cases, a distribution type, such as normal, uniform, triangular, etc. can be easily used to characterise a parameter or variable. However, assigning values to the distribution parameters is a much harder task, as often the data coverage is insufficient (especially in radioecology) for estimating the values using standard fitting techniques. A widespread approach to overcome such challenges is to make use of Bayesian statistics.

Generally speaking and based on the definition of probability, statistical approaches can be divided into two main schools (Suter-II, 2007): Frequentist and Bayesian. While probability from a Frequentist

point of view is understood as an expression of frequency, Bayesian statistics defines it as an expression of belief. The Bayesian definition of probability is more flexible than the frequentist one as beliefs concerning various sources of uncertainty and variability can be expressed in units of probability (Suter-II, 2007).

In the Bayesian approach, parameters are treated as random variables. This is not a description of their variability alone, but a description of the uncertainty and lack of knowledge about their true values (Bernardo, 2003). Quantifying this uncertainty, by making use of probability, is the essential characteristic of all Bayesian methods (Gelman et al., 2003).

Bayesian statistics provides a method for modification of probability in the light of existing and /new evidence and it is based on the Bayes' Theorem (Bayes, 1763), which is developed from the concept of conditional probability (Sivia & Skilling, 2006).

Consider inferences are to be drawn on the unknown parameter (or parameter vector) θ in light of vector of independent and identically distributed empirical data values $\mathbf{y} = \mathrm{y}_1, \ldots, \mathrm{y}_\mathrm{n}$ and the prior probability distribution $p(\theta)$. Bayes' theorem combines information from the prior and the likelihood to give the posterior density of the parameter conditioned on the data:

$$\mathrm{p}(\theta|\mathrm{y}) = \frac{\mathrm{p}(\mathrm{y}|\theta)\cdot\mathrm{p}(\theta)}{\int_{-\infty}^{\infty}\mathrm{p}(\mathrm{y}|\theta)\cdot\mathrm{p}(\theta)\mathrm{d}\theta} \text{ or posterior} = \frac{\text{likelihood} \times \text{prior}}{\int_{-\infty}^{\infty}(\text{likelihood} \times \text{prior})\mathrm{d}\theta} \quad (13)$$

Here, the posterior distribution describes our state of knowledge about the truth of the parameter θ after considering the data. The likelihood function describes how likely the current data are given the parameter θ. The prior represents the present state of our knowledge based on an initial consideration of the parameter θ. The denominator is the probability of the data, a normalising constant. Hence, the combined (posterior) probability distribution of the parameter given the empirical data is proportional to the prior probability distribution times the likelihood function of the empirical data values:

$$\mathrm{p}(\theta|\mathrm{y}) \propto \prod_{\mathrm{i}=1}^{\mathrm{n}} \mathrm{p}(\mathrm{y}_\mathrm{i}|\theta) \times \mathrm{p}(\theta) \quad (14)$$

The power of the Bayes' Theorem lies in the fact that it relates the quantity of interest (the probability of each specific value of the distribution parameter given the measured data) to a term that we have a better chance of quantifying (the probability of the measured data given that the distribution parameter has a specific value). Note that in this way we are implicitly recognising that the value of the distribution parameter is an uncertain quantity, meaning that different values are possible with different probabilities.

To individuals not familiar with Bayesian methods the inclusion of information based upon belief about the relevancy of data may seem rather subjective. However, this is exactly the process that is employed during 'classical' pooling of datasets wherein knowledge/belief about congruity of transfer factors between taxonomically similar organism groups is used to delineate the extent to which data are combined. For example, in building wildlife transfer databases, as exemplified by the work of (Copplestone et al., 2013), there is a tacit assumption that there is some rationale in grouping mammals in terms of feeding strategy. This assumption is made based upon prior knowledge/belief regarding the importance of the ingestion pathway in determining internal radionuclide body burdens and similarities in physiology dictating uptake. Hence, while the 'classical' approach implicitly uses judgment, the Bayesian approach explicitly acknowledges the role of judgments made.

Given the inherent large variability of transfer parameters, Sheppard (Sheppard, 2013) advised against basing assessments solely on a few site specific data and not consider many generic data which might exist. Bayesian approach allows for such considerations and provides a framework for systematic and

consistent pooling of site specific and generic data. Given that the prior knowledge is valid, this approach is a valuable mean for acquiring more robust parameter values in cases where the available data are scarce.

Furthermore, in parallel to common practice of construction confidence intervals in classical statistics, Bayesian approach allows for construction of credible intervals. However, in contrast to classical confidence intervals, credible intervals can be interpreted as the set of likely values of an unknown quantity with associated probabilities.

For relatively simple models, however, there is little advantage to get upon applying Bayesian statistics compared the classical probabilistic one. However, the power of Bayesian approach becomes more evident as we consider more and more complex models. This is due to the capacity of the Bayesian approach to accommodate complexity (Clark, 2005) and in efficiently exploiting and combining information from multiple sources (Kruschke et al., 2012). Given the availability of today's powerful computational hardware and sophisticated software, the Bayesian methods for data analysis are now easily accessible and should be considered as a valuable option. In the present report, the case study of Section 8.4.2 is Bayesian.

The Bayesian approach is also commonly used for building hierarchical models, which are useful for data structures with multiple levels and parameters of a model have meaningful dependencies on each other, such as data from individuals who are members of groups which in turn are in higher-level organisations. Hierarchical models have parameters that meaningfully describe the data at their multiple levels and connect information within and across levels (Klugman, 1992).

5.4 Methods for analysing and calculating correlations between model parameters

The prerequisites of good results of statistical modelling are suitable PDFs of model parameters. In addition, there is a need to estimate whether these model parameters are dependent or independent from one another.

Frequently it is presumed that the model parameters are independent. This can result in errors of model output if dependencies actually exist (Ferson, 1994; Ferson & Burgman, 1995; Ferson & Ginzburg, 1996). A variety of articles concerning the risk analysis models have tackled the importance of including correlations in MC simulations since it has been shown that ignoring existing dependencies can lead also to miscalculation of total uncertainty budget of radioecological models (Apostolakis & Kaplan, 1981; Kraan & Cooke, 1997).

In general, correlations can be ignored if the uncertainties of the correlated parameters in question are low compared to the uncertainties of the other parameters. In addition, (Smith et al., 1992) have indicated the rules of thumb when correlations can be ignored:

- if the correlations are weak,
- if the parameters have relatively little influence on the outcome.

From joint measurements of the stochastic parameters, their correlation can be statistically calculated (direct dependence between parameters). Dependencies between parameters can be caused by the joint causal influence of another (third) parameter that is not an explicit model parameter (hidden parameter). Dependencies between several variables can also implicitly result from common restrictions (Borgonovo, 2008). Sometimes the need in considering correlations between variables X and Y can be replaced by the explicit calculation of Y as a function of X, resulting from the biological and/or physicochemical essence of the model. For example, in the case of the constant sum of two parameters the second parameter could be expressed by the constant sum and the first parameter,

thus avoiding the complications of considering two correlated parameters. The probabilities of extreme and rare events are determined by tails of the probability distribution functions. The purpose of the risk analysis is to characterise these extreme events in the tails. The tails of the probability distributions depend sensitively on the shapes and dependencies of probability distributions (Bukowski et al., 1995; Ferson, 1994). Unfortunately, in practice, there is often not enough information concerning the distribution tails.

When there is not enough information concerning the correlations between the parameters, it may be practical to calculate bounds of the risk without making preliminary assumptions about the dependencies (Tucker & Ferson, 2003). In that case, the interval analysis or probability bounds analysis could be applied. An example of problems arising from ignoring the correlation between model parameters is the sensitivity ratio calculation, which generally requires independent model parameters. If model parameters are actually correlated, then keeping one parameter fixed while changing the others gives an erroneous result.

5.4.1 Correlation coefficients

Correlation is a quantitative expression of the statistical dependence between two model parameters. In the case of linear models, it can be represented by the Pearson correlation coefficient. For nonlinear models the Spearman rank correlation coefficient is used. The statistical dependence about parameter can be non-linear and even non-monotonous (Dowdy et al., 2004).

The Pearson's correlation coefficient or **linear correlation coefficient *r*** characterises the strength and direction of linear dependence between the values of two model parameters. It is calculated as:

$$r = \frac{\sum_i (X_i - \bar{X})(Y_i - \bar{Y})}{\sqrt{\sum_i (X_i - \bar{X})^2} \cdot \sqrt{\sum_i (Y_i - \bar{Y})^2}} \quad (15)$$

where $\bar{X}$ and $\bar{Y}$ are the average values of parameters *X* and *Y* and index *i* count the values of the parameters from 1 to *n*. A correlation coefficient *r* characterises the degree of relationship linearity between *X* and *Y* and therefore *r* value close to 0 does not mean that parameters are independent of each other.

Spearman rank-order correlation coefficient *ρ* measures the strength and direction of the association between the ranks of the values (not the values themselves) of two model parameters. Thus, values X_i and Y_i are replaced by corresponding ranks. Ranking refers to the data transformation in which numerical or ordinal values are replaced by their rank when data is sorted. Positive correlation coefficients indicate that two model parameters are changing in the same direction (e.g. both parameters are increasing) while in case of negative correlation coefficients the two model parameters change in opposite directions (one parameter is increasing while the other is decreasing).

5.4.2 Methods of estimation of correlations/dependencies

The **scatter plot** can be applied for graphic analysis of two parameters of the model. It is a simple but still efficient tool for identifying dependencies between parameters of the model. A simple visual analysis of scatterplot gives information on the positive or negative correlation between these model parameters. The slope characterises the strength of the correlation. It is also possible to draw conclusions about the linearity – nonlinearity as well as monotonicity of the dependence.

Multivariate (joint) probability distribution function describes the frequency of occurrence of model output values dependent on several model parameters. The joint distribution function contains complete information about the dependencies between model parameters. For example, a set of correlated quantities may be modelled by a multivariate normal distribution (Figure 5.4-1). This implies that the marginal distribution for each quantity X_i alone will be a simple univariate normal distribution. The dependencies are specified by a covariance matrix between each pair of model parameters, X_i and X_j. However, in order to construct the joint distribution, one needs dependence information between all model parameters. This is usually not known when the number of model parameters is large.

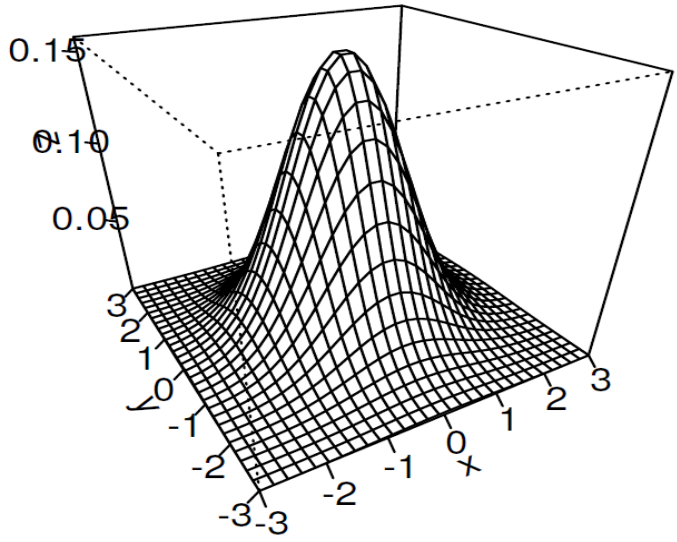

Figure 5.4-1 Bivariate distribution function (Kerns, 2018)

5.4.3 Implementing correlated model parameters in Monte Carlo analysis

To handle the correlations coupled with 1D MC method it is convenient to use either the Iman-Conover method (Iman & Conover, 1982) or simulation from elliptical Copulas (Nelsen, 2006).

The calculation algorithm of the Iman-Conover method involves Cholesky decomposition, matrix algebra and, in case LHS is used, rearrangement of the initial uncorrelated Latin hypercube sample. It generally uses Spearman's rank correlation coefficients in the correlation matrix. The Iman-Conover method has several good properties: (a) it does not depend on the shape of the distribution function, (b) it can characterise complicated correlations between several parameters, (c) it is applicable to both random and Latin hypercube sampling, and (d) it preserves the intervals of Latin hypercube sampling. Due to its favourable properties, Iman-Conover method is implemented in many probabilistic modelling software packages (cf. Chapter 10).

In general, a copula is a multivariate probability distribution that joins univariate probability distributions into a multivariate distribution and takes into account dependence (correlations) between univariate margins (Nelsen, 2006).

According to Cherubini et al. (2004), five steps are needed to apply the Gaussian Copula method:

1. The first step is to apply the Cholesky decomposition on correlation matrix $\mathbf{R}$ such that correlation matrix $\mathbf{R}$ can be expressed as the product of lower triangular and upper triangular matrices: $\mathbf{R} = \mathbf{A}^{\mathrm{T}}\mathbf{A}$.

2. *r* independent random variables $\mathbf{z} = (z_1, z_2, ..., z_r)$ are generated from N(0,1) where *r* is equal to the number of model parameters and input data.
3. Vector $\mathbf{x}$ is calculated as the product of matrix $\mathbf{A}$ and column vector $\mathbf{z}$: $\mathbf{x} = \mathbf{Az}$. Column vector $\mathbf{x}$ has the desired correlation structure. The purpose of the next two steps is to set the values of real model parameters' distribution functions in the same order.
4. The probability values $u_i = \Phi(x_i)$ are calculated at values of vector $\mathbf{x}$, where $\Phi(x_i)$ is the univariate standard normal distribution function (with mean 0 and standard deviation 1) at vector $\mathbf{x}$ values.
5. The quantile functions corresponding to the *r* margins of distribution functions of model parameters and input data $\mathrm{F}_1^{-1}(u_1)$ to $\mathrm{F}_r^{-1}(u_r)$ are applied on the probabilities u_1 to u_r in order to find the quantiles t_1 to t_r in correct order (taking into account the correlation structure): $(t_1, t_2, ..., t_r)^{\mathrm{T}} = (\mathrm{F}_1^{-1}(u_1), \mathrm{F}_2^{-1}(u_2), ..., \mathrm{F}_r^{-1}(u_r))^{\mathrm{T}}$.

The five steps described above are repeated *n* times to get *n* column vectors $(t_1, t_2, ..., t_r)^{\mathrm{T}}$ with model parameters and input data in the correct order. In order to calculate the j-th value of model output, the model is applied on the j-th column of model parameter values, where the index *j* counts from 1 to *n*. There are several types of copulas for describing different types of dependencies.

5.5 Non-statistical approaches for uncertainty analysis

In cases when the mathematical approaches cannot be applied, alternative strategies to obtain acceptable model results have to be applied. As explained in Section 5.2, a probabilistic approach for propagating uncertainty requires a large number of model simulations, in order to achieve statistical significance. Some types of models may not be amenable to apply such statistical methods for a variety of reasons:

a) Large number of parameters combined with too long time of execution of the model,

b) Model embedded in a design platform with limited capacity to do multiple runs for large models (cf. Chapter 10),

c) Models that are not designed for making predictions, but to understand how a system works, in which the emphasis is not so much on the accuracy of the parameters but on studying the processes involved.

An alternative (or complement) to the probabilistic approach of model evaluation for models not amenable to this treatment is non-statistical uncertainty analysis (NUA) and the process uncertainty Analysis (PUA). These two approaches have been developed specifically within the field of radioecology. A similar approach is available in other environmental disciplines e.g. the NUSAP methodology presented in (Refsgaard et al., 2006).

NUA consists of evaluating functionally how the model output would behave if some input parameters are uncertain within a range, without resorting to the more sophisticated method of assigning probability distributions to the parameters and obtaining by a MC method the resulting distribution of the output of interest.

PUA is a tool for analysing the impact of a certain process on the predicted model endpoints. In its widest form, PUA comprises estimating the key processes with the highest uncertainty and estimating the influence of processes disregarded in the course of model development. In other words, A PUA would indicate the amount of uncertainty reduction generated in the model when adding or removing mechanisms. It is possible to use the model reconfigured in this way to explore the impact of various

mechanistic hypotheses. The outcome of a PUA is a more robust, fit for purpose model "sufficiently complex to be realistic and sufficiently simple to be practical".

A combination of NUA and PUA can be a used to study how the parameters and entire processes differ in their influence on the predicted model endpoints (and how the uncertainty can be reduced). In particular, parameter uncertainty analysis approaches applies only to a given model, so no insight beyond the given model is possible from such a method. Conversely, PUA generates knowledge applicable to many models (as many versions of it are produced during the analysis, in order to evaluate the influence of process). Application of this approach will be further elaborated in one case study, Section 8.5.

5.6 Specific challenges in radioecology

Most of the theoretical approaches described in the previous sections require data of sufficient quality. In reality, however, data might be scarce, of low quality or even missing.

5.6.1 Relevance of uncertainty budget

Assessment models in radioecology have been designed for different purposes. Depending on its purpose, the acceptable overall uncertainty of a model varies substantially. Research models aim at representing features, events and processes in detail and calculating their endpoints (e.g. activity levels, dose rates and doses) as accurately as possible. Here, low overall uncertainties of the model results are desirable. Assessment models that support epidemiological studies should also produce dose rates and doses to humans that are as close to reality as possible. Some models for regulatory radiation protection purposes have deliberately been designed in such a way that they overestimate the dose to humans and non-human biota. These models might be legally binding calculation rules. In that case zero uncertainty is assumed from legal point of view. Here, it might be sufficient to demonstrate that the calculated endpoints are conservative, i.e. more unfavourable than is to be expected in reality.

5.6.2 Unknown parameters

It is a quite common situation in radioecology that model parameters, like transfer factors or concentration ratios, have not been measured for the specific radionuclides, the type of specie and/or the type of ecosystem for which an assessment has to be made. In these cases, parameter values have often been extrapolated from species or ecosystems with similar characteristics and/or from chemically similar elements. Sometimes parameter values have been estimated using allometric relations or more sophisticated techniques such as the REML (Residual Maximum Likelihood) approach (Beresford et al., 2016). Often parameter values have been measured in the lab, e.g. the partition coefficient K_d or the time-dependent dissolution of hot particles. Implicitly it is assumed that parameter values measured in the lab can be applied to real ecosystems. The uncertainty arising from the extrapolation approaches described above should be taken into account when assessing the propagated parameter uncertainty of a radioecological model. This contribution to propagated parameter uncertainty, however, is usually hard to quantify.

If a probabilistic assessment has to be made but the available data and supporting information do not allow to derive probability density functions for all necessary parameters, the missing probability density functions are often the result of expert judgement. In order to quantify the resulting contribution to propagated parameter uncertainty, it is recommended to test also plausible alternative probability density functions and check the sensitivity of the model results.

As introduced in Chapter 4, in a mathematical model two kinds of numbers are used: parameters and variables or input values. The term ‘parameter’ refers to numerical values that are part of the mathematical model itself, in many physical well-established models being constant values. Model

parameters are conceptually different from the input of a dynamic radiological model, which of course may depend on time.

Often the parameter values used in actual dynamic radioecological models themselves show time dependence (e.g. transfer factors of a given radionuclide from soil to tree are usually consider a dependence with the age of the tree), sometimes distinct, unpredictable. Consequently, it is hard to make robust long-term forecasts and to assess the resulting uncertainty. Model parameters that depend on time indicate a conceptual oversimplification of the radioecological model, as part of the radionuclide dynamics to be simulated is depicted in an aggregated way by these parameters.

It is one of the objectives to achieve radioecological models with parameter values that are constant in time, especially if long-term concentration levels, or equivalent doses or dose rates have to be forecasted. The focus for model developers should be to try to replace time-dependent empirical parameters with radioecological sub-models which include non-time dependent parameters. Ideally, the sub-model adequately represents the hidden dynamic process and requires only time-independent parameter values. In summary, the mathematical model structure itself should represent any dynamic aspects, with model parameters being constant in time.

5.6.3 Unknown correlations

The methods for analysing and calculating correlations between model parameters described in Section 5.4, are based on meaningful data of sufficient quality. If the available data do not meet these requirements, alternative approaches to take into account parameter correlations should be considered.

Correlations arise, for example, from intrinsic limits that relate to an ecosystem, to physico-chemical processes that determine the fate of radionuclides, or to the physiology of humans and non-human biota. How to use best these intrinsic limits will be explained using the effective dose of humans due to the ingestion of food as an example. The effective dose of humans due to the ingestion of food is given by:

$$E_{ing,r} = e_{ing,r}(\tau) \cdot \sum_n U_n \cdot C_{n,r} \qquad (16)$$

where $E_{ing,r}$ is the effective dose due to the ingestion of radionuclide r with food expressed in Sv per year, $e_{ing,r}(\tau)$ is the dose coefficient for ingestion of radionuclide r expressed in Sv Bq^{-1}, the index n denotes the different groups of food, U_n is the consumption rate of food group n expressed in kg per year, and $C_{n,r}$ is the activity concentration of radionuclide r in food group n expressed in Bq kg^{-1}.

International recommendations, e.g. ICRP Publication 101 (ICRP, 2006) , or legal regulations often require calculating the effective dose of the 'representative person'. A 'representative person' is representative for population groups who receive higher radiation doses as a result of their specific living habits. ICRP Publication 101 recommends calculating a high percentile, e.g. the 95th percentile, of the radiation exposure of members of the public. Selecting the 95th percentile of the consumption rate of each food group will result in an unrealistically high caloric intake. In an ideal situation, the consumption rates of different groups of food, including their correlation are known. If the correlations between the consumption rates are unknown, the maximal caloric intake that is physiologically reasonable should be taken into account. In the case of probabilistic assessments using Monte Carlo simulations, combinations of consumption rates exceeding the maximum caloric intake should be rejected. In the case of deterministic assessments, e.g. calculation rules for legal purposes, it is sensible to use the 95th percentile of the consumption rate for the food group that dominates the effective dose due to ingestion and average values for all other food groups. This robust approach will be implemented in official calculation rules in Germany.

5.6.4 Optimum model structure

Model complexity is always a compromise between having a sufficient flexible description of the ecosystem and the processes being modelled and minimising the number of uncertain and/or variable parameters. On the one hand, an oversimplified model will lack the capability to adequately represent relevant radioecological processes in the ecosystem under consideration. On the other hand, as the number of parameters increases, additional uncertainty and/or variability will be introduced and forecast accuracy will be diminished. In other words, an optimum model structure, neither too simplistic nor unnecessarily complex, is one of the keys to minimizing the overall uncertainty budget. Apart from research models that are designed to understand and quantify details of an ecosystem, it is recommended to use and/or to develop radioecological models that focus on the key processes, i.e. those processes that most strongly determine the endpoints of the model. A sensitivity analysis for the processes considered in a model (as described in Section 5.5) helps to identify the most important processes with regard to the assessment task. A FEP list, i.e. a list of features, events and processes that determine the radionuclide behaviour in the ecosystem to be modelled, helps to take into account all important aspects.

The structure of a model not only determines the number of model parameters, but also their nature. Model structures requiring only 'robust' parameters should be preferred. Model parameters are usually termed robust if they are only moderately sensitive and moderately variable/uncertain. Sensitivity here refers to the extent to which the model results are dependent on changes in the value of the parameter. Parameter sensitivity analysis is explained in detail in Chapter 6.

As has already been mentioned, parameters used in dynamic radioecological models may ideally show a distinct, unpredictable time dependence, which makes reliable long-term predictions impossible. In this case, developers of long-term forecast models are highly recommended to revise the model structure and/or replace time-dependent model parameters with sub-models. An ideal forecast model should have a mathematical model structure that represents any relevant dynamics but model parameters should be constant in time.

6 Tools and methods for sensitivity analysis

The theory underlying sensitivity analysis has been developed mainly by (Saltelli et al., 2008). The author defines the sensitivity analysis as the study on how the overall uncertainty of a given model (in other words, the uncertainty of model output) is divided into the uncertainties originating from the model input(s). Sensitivity analysis enables the user to rank the model inputs or parameters in order of importance. The model parameters that have little to no effect on the uncertainty of model output can be treated as constants in the model. This effectively enables to simplify the uncertainty estimation for the model. Sensitivity analysis also permits to find critical or otherwise interesting regions in the model input space, identifying interactions between model inputs (Saltelli et al., 2008). Additionally, sensitivity analysis can be useful for testing model performance as it facilitates to ascertain whether or not the model is robust or highly dependent on weak assumptions (Saltelli et al., 2008).

6.1 Local and global sensitivity analysis

The sensitivity analysis (SA) can be divided into local SA and global SA. Local SA is an analysis that is performed adjacent to a given point of the space of model parameters or inputs, based on calculating partial derivate at the same point of the space of model parameters and inputs (EPA, 2009).

Global SA (Hamby, 1994), on the other hand, is an analysis that is conducted over the whole space of model parameters and inputs. In other words, model parameters and inputs are varied over their whole range of variation. Figure 6.1-1 presents the difference between the local SA and global SA.

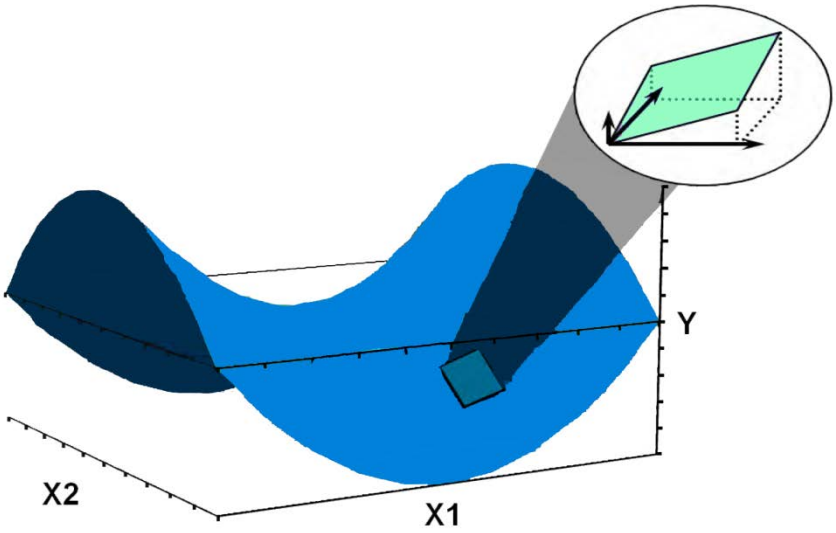

Figure 6.1-1 The difference between global and local SA. Local SA applies for the small green surface of model parameters while global SA applies for the whole (response) surface of model parameters.

The following subchapters briefly describe several SA methods including normalised partial derivative, sampling-based methods, the Morris method and variance-based methods. A summary table of the described methods is also presented at the end, pointing out their strong and weak sides.

6.2 Overview of Methods

6.2.1 Normalised partial derivative

The sensitivity of the model output to a particular parameter or input value can be thought as related to the gradient of the model surface and a traditional single factor for sensitivity measure is obtained by evaluating the local gradient at a particular point in the parameter space, normalised by the value of the parameter at that point (Beven, 2007).

The expression $\frac{\partial Y}{\partial X_i} \cdot \frac{u(X_i)}{u(Y)}$ is called the normalised partial derivative, i.e. the partial derivative of model output with respect to a model parameter $\frac{\partial Y}{\partial X_i}$ is multiplied by the ratio of standard uncertainties (variances) of a model parameter and model output $\frac{u(X_i)}{u(Y)}$. The simple partial derivative characterises the sensitivity of model output with respect to a model parameter but does not take into account the uncertainty in model parameter values. A higher partial derivative value does not necessarily mean that the model parameter or input X_i affects the output Y strongly if the uncertainty of model parameter or input is very low.

For this reason, the normalised partial derivative also called sensitivity index (SI) is a better SA measure than the simple partial derivative. Furthermore, the normalised partial derivative is a dimensionless measure and therefore does not depend on units of model parameters and model output.

The normalised partial derivative can be used as a global SA measure if the model is approximately linear with respect to model parameters or inputs, but it cannot be used as a global SA measure if the model is nonlinear. In the case of nonlinear models, it can only be used as a local SA measure, i.e. it is studied how small variations of the model parameter or input values affect the model output value. The normalised partial derivative method is also called a 'one at a time' (OAT) method, i.e. model parameters or inputs are varied one at a time to observe the corresponding changes in model output values. It is probably the most widely used SA method, but it also has its limitations, as pointed out by (Saltelli & Annoni, 2010).

Examples of application of local and global SI indices are given in Section 8.3.

6.2.2 The Morris method

The Morris method is a type of screening method based on discretisation of the model inputs in levels, allowing for a fast exploration of the model behaviour. The Morris method is based on the so-called "*one at a time*" (OAT) randomised designs. It can be used as a first SA step that enables to find model parameters or inputs of low and high contribution to the model output. It also allows finding model parameters that either nonlinearly affect the model output or are in interaction with other model parameters. The Morris method is computationally cheap and enables to see the results on one plot. If $f(\mathbf{x}) = f(x_1, x_i, .. x_k)$ is the functional relationship between *k* model parameters or inputs, to be able to calculate the model output *f*, the Morris method allows to classify inputs that have negligible effects, inputs that have large linear effects without interactions and inputs having large nonlinear and/or interaction effects. The method consists in discretising the input space for each variable and then performing a number of OAT designs. All the *k* model parameters or inputs are divided into *p* levels. So, the model parameter space is a *k*-dimensional *p*-level grid. The model parameters' values corresponding to the grid can be chosen as quantiles corresponding to probabilities $[1/(p-1), 2/(p-1), \ldots, 1-1/(p-1)]$ of the model parameter's distribution functions (Saltelli et al., 2004).

During a Morris trial each model parameter or input is once varied by Δ to calculate the elementary effect *d* of the j-th variable obtained at i-th repetition, defined as:

$$d_j^{(i)} = \frac{[f(X^{(i)}+\Delta e_j)-f(X^{(i)})]}{\Delta} \quad (17)$$

where Δ is a quantile difference corresponding to an integer multiple of 1/(*p*-1) in the parameter probability space and e_j a vector of the canonical base.

N random Morris trials enable to calculate the average elementary effects for each model parameter or input, quantified with the index $\mu_j^* = \frac{\sum_{i=1}^{N}\left|d_j^{(i)}\right|}{N}$. The larger μ_j^* is, the more the j-th input contributes to the variance of the output. It is also possible to calculate standard deviations of the *N* elementary effects for each model parameter or input, namely:

$$\sigma_j = \sqrt{\frac{1}{N}\sum_{i=1}^{N}\left(d_j^i - \frac{1}{N}\sum_{i=1}^{N} d_j^i\right)^2} \quad (18)$$

which are a measure of nonlinear and/or interaction effects of the j-th input.

In Figure 6.2-1 the Morris plot is presented. It can be seen that parameter x_3 does not practically affect the model output. The effect of model parameter x_1 on model output is the largest.

Various modellers have demonstrated that the number of levels *p*=4 and realisations *N*=10 already give good results (Ekstroem & Broed, 2006). The Morris method is described in more detail in (Ekstroem & Broed, 2006) as well as in (Saltelli et al., 2008; Saltelli et al., 2006).

The Morris method is used as the main SA approach in several radioecological models (Girard et al., 2014; Saltelli & Annoni, 2010; Sy et al., 2016)

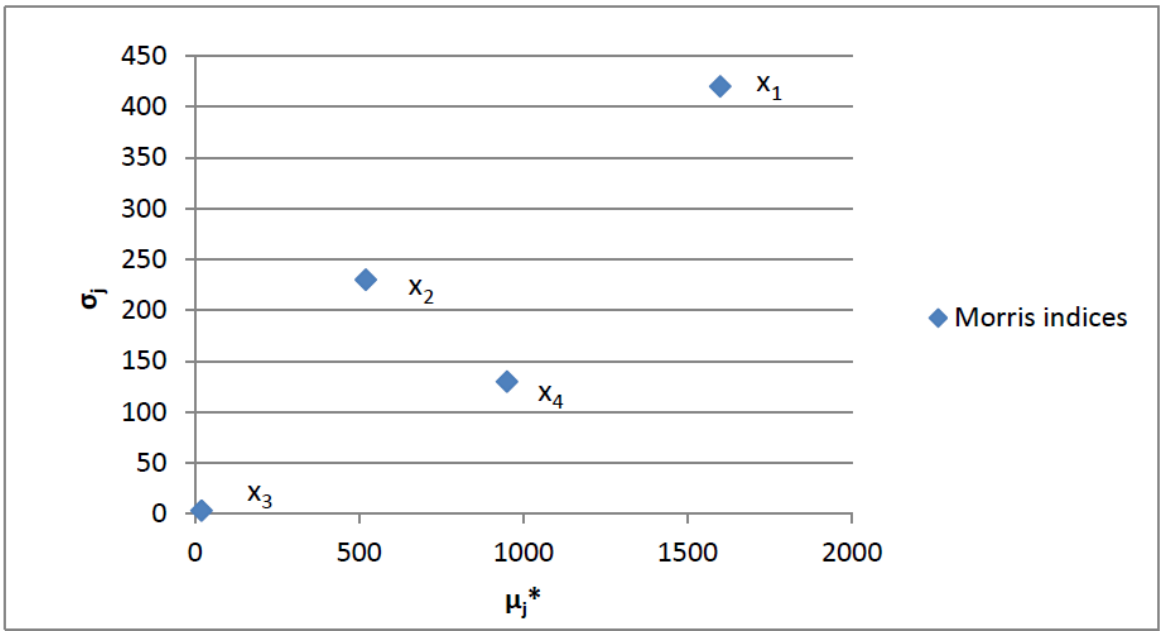

Figure 6.2-1: An example of Morris plot. Model parameter x_1 affects model output most strongly while model parameter x_3 does not practically affect the model output.

6.2.3 Sampling-based methods

Sampling-based methods are based on mapping the relationships between model inputs and output using the Monte Carlo method (Ekstroem & Broed, 2006). Sampling-based methods can be treated as global SA methods because all the model parameters and inputs are varied over their entire range of variation. A good illustrative overview of sampling-based SA methods is presented in (Helton & Davis, 2002). Methods to investigate parameter correlations (as presented in Section 5.4) can be then used such as the scatter plot, the standardised regression coefficient (SRC), the correlation coefficient (CC) and rank transformations.

A **scatterplot** of points $[X_{ij}, Y_j]$ is shown in Figure 6.2-2 between model parameter or input X_i and model output Y_j whereby index *j* counts the Monte Carlo iterations to relate model output to a model parameter. It is perhaps the simplest SA method that allows visualising the relationships between a model parameter and model output. A comparison of Figure 6.2-2 and Figure 6.2-3 shows that model parameter x_1 affects the model output more strongly than parameter x_2. A scatterplot can also reveal a nonlinear relationship between a model parameter and model output. Model parameters are varied over their entire range. So, the scatterplot method can be regarded as a global SA method. A scatterplot does not enable to detect interactions with other model parameters. It can also be rather tedious to plot the many parameter and model output relationships in case of complicated models of many parameters. Nevertheless, this method can be used as the first step of SA.

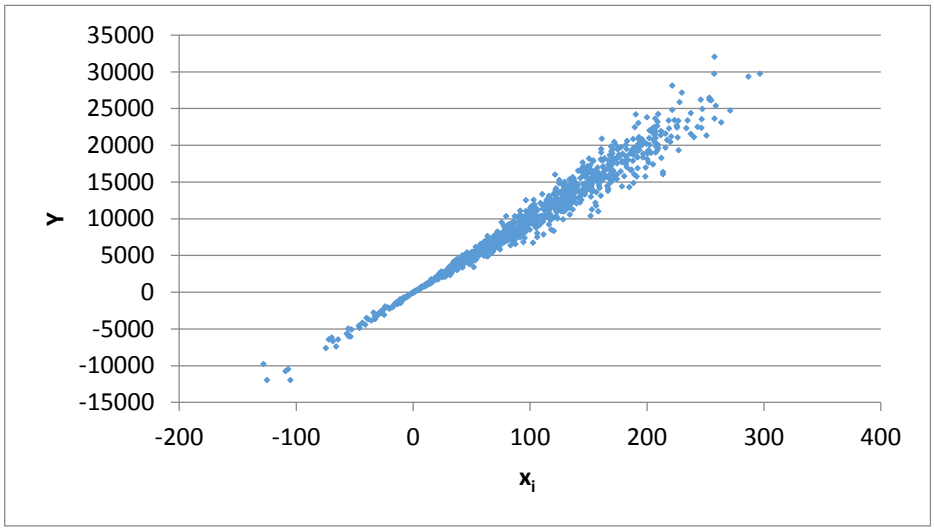

Figure 6.2-2: Scatterplot of the strong relationship between model parameter x_1 and model output Y.

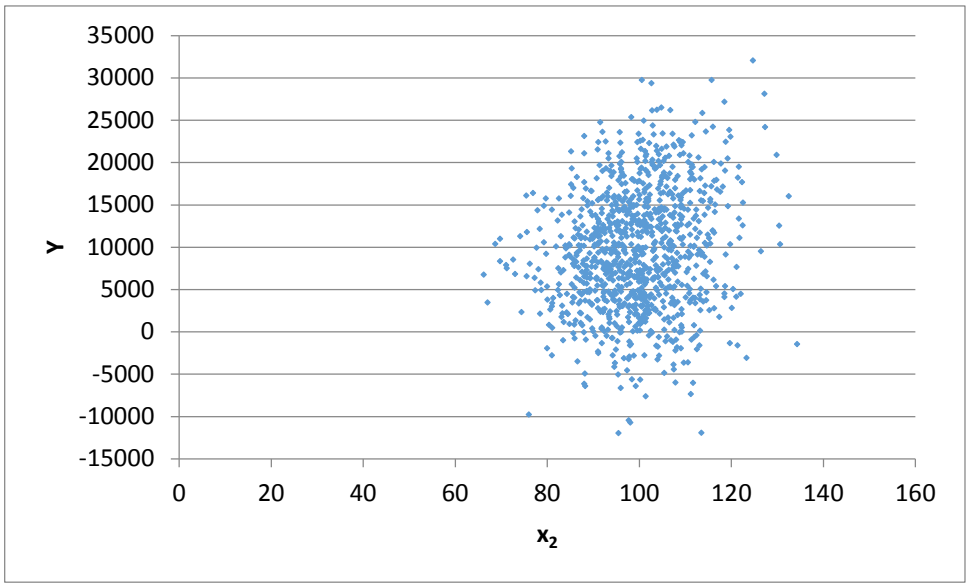

Figure 6.2-3: Scatterplot of the weak relationship between model parameter x_2 and model output Y.

Standardised regression coefficient (SRC) is obtained from multivariate regression analysis, which is used to fit the input data to the theoretical model. The multivariate linear regression formula relates model output value Y_j to the model parameter or input values $X_{i,j}$ where index *j* counts the number of sampled values from 1 to *N* and index *i* counts the number of model parameters or inputs from 1 to *k*:

$$Y_j = \beta_0 + \sum_{i=1}^{k} \beta_i \cdot X_{i,j} + \epsilon_j \qquad (19)$$

where β_0 and β_i are the multivariate linear regression coefficients and ϵ_j is the approximation error. The coefficients β_i measure the linear relationship between model parameters or inputs and the model output (Ekstroem & Broed, 2006). The sign of the coefficient shows whether the model output increases or decreases as the model parameter or input value increases. The coefficients β_i have

dimensions. In order to get dimensionless sensitivity measures the standardised regression coefficients (SRC) obtained from the following formula is used (Ekstroem & Broed, 2006):

$$\frac{Y_j-\bar{Y}}{s_Y}=\sum_{i=1}^{k}\frac{\beta_i\cdot s_{X,i}}{s_Y}\cdot\frac{X_{i,j}-\bar{X}_j}{s_{X,i}} \quad (20)$$

where $s_Y=\sqrt{\frac{\sum_{j=1}^{N}(Y_j-\bar{Y})^2}{N-1}}$ and $s_{X,i}=\sqrt{\frac{\sum_{j=1}^{N}(X_{i,j}-\bar{X}_i)^2}{N-1}}$.

The coefficients $\frac{\beta_i\cdot s_{X,i}}{s_Y}$ are the standardised regression coefficients.

The **coefficient of determination R^2** is calculated by the formula

$$R^2=\frac{\sum_{j=1}^{N}(\hat{Y}_j-\bar{Y})^2}{\sum_{j=1}^{N}(Y_j-\bar{Y})^2} \quad (21)$$

When R^2 approaches to 1, then it can be stated that the regression model stands for most of the variability in *Y* (Ekstroem & Broed, 2006).

6.2.3.1.1 Correlation coefficient-based method

The **Pearson correlation coefficient (CC)** specifies a measure of strength for the linear relationship between model parameter x_i and model output *Y*:

$$\rho_{X,Y}=\frac{\mathrm{cov}(x_i,Y)}{\sigma_{x_i}\sigma_y} \quad (22)$$

where $\mathrm{cov}(x_i,Y)$ is the covariance between model parameters x_i and model output *Y*, σ_{x_i} and σ_y are the corresponding standard deviations. The correlation coefficient is a dimensionless parameter with possible values between -1 and 1.

6.2.3.1.2 Rank transformations

In this instance, standardised rank regression coefficients SRCs and Pearson correlation coefficients CCs are calculated on ranks instead of sampled values of model parameters or inputs x_i and model output *Y*. Ranks are defined by appointing *N* to the largest value in a dataset, whereas 1 and 2 to the smallest and second smallest values, respectively (Ekstroem & Broed, 2006). Standardised rank regression coefficients (SRRCs) and Spearman's rank correlation coefficients (RCC) work significantly better for nonlinear models compared to SRCs or CCs because rank transformations transform a nonlinear but monotonic relationship to a linear relationship (Ekstroem & Broed, 2006).

In radioecology examples of application of RCCs and CCs are to be found in the application of ERICA model (Oughton et al., 2008). These SA measures are also used by (Albrecht & Miquel, 2010). On the other hand, SRCs and SRRCs have been used by (Ciffroy et al., 2005) and (Helton et al., 2012).

6.2.4 Analysis of variance

The functional decomposition of the variance referred to as analysis of variance (ANOVA) and analysis of covariance models is frequently used for the analysis of data that can be best described by a normal distribution and is applicable to nonlinear and non-monotonous models.

It is important to distinguish the difference between regression analysis and analysis of variance before proceeding to the use of ANOVA in SA. Regression analysis aims to relate one or more variables to

variation in response, whereas ANOVA detects variation among mean values of populations. Statistical significance of a variable, in regression analysis, is determined with the square of the residuals from which standard error of each variable is calculated. This approach cannot be used if a variable has random variation (which in turn contribute to the variation in other variables), but ANOVA helps us construct models with variables that have random effects.

ANOVA can be best described as a decision-making and optimisation tool by determining the average difference in performance of a conducted experiment, analysing the variables by their mean squares and estimating experimental errors at specific levels (Mousavi & Parvini, 2016). In addition, several important statistical parameters can be found with ANOVA and these include the significance of model coefficients (and each factor), the coefficient of determination (R^2) and importance of the model in question.

6.2.5 Variance-based methods

Variance-based methods help to understand to what extent each model parameter x_i contributes to the explicit variance of the model output $\mathrm{V}(\mathrm{Y})$ (Ekstroem & Broed, 2006). In the case of additive models only first order sensitivity indices can be calculated (Saltelli et al., 2004).

So the aim of this method (calculating the first order sensitivity indices) is to rank model parameters $\mathrm{x_i}$ according to the amount of variance that would disappear if the true value of model parameter $\mathrm{x_i^*}$ is known (Ekström, 2006). This is achieved by calculating the conditional variances $\mathrm{V(Y|x_i = x_i^*)}$, i.e. variance is taken over all model parameters except $\mathrm{x_i}$. Since the true value $\mathrm{x_i^*}$ is usually unknown, the mean of this conditional variance $\mathrm{E[V(Y|x_i)]}$ is calculated by varying model parameter $\mathrm{x_i}$ over its entire range. So, closer the value of $\mathrm{E[V(Y|x_i)]}$ to unconditional variance $\mathrm{V(Y)}$ is the lower the contribution of model parameter $\mathrm{x_i}$to model output Y is. In statistics, $\mathrm{V(Y) = E[V(Y|x_i)] + V[E(Y|x_i)]}$ whereby $\mathrm{V[E(Y|x_i)}$ is called the main effect. First order sensitivity index is the normalised main effect that is calculated by the following formula:

$$\mathrm{S_i = \frac{V[E(Y|x_i)]}{V(Y)}} \tag{23}$$

In the case of additive models, the sum of first order sensitivity indices is equal to 1. The higher is the first order sensitivity index, the higher is the contribution of that model parameter to the variance of the model output.

In the case of non-additive models, the sum of first order sensitivity indices is less than 1 due to higher order sensitivity indices that characterise interactions between model parameters. The guidance on how to calculate higher order sensitivity indices is provided by (Ekstroem & Broed, 2006; Saltelli et al., 2008; Saltelli et al., 2004). In general, it is mathematically very resource demanding to calculate all the first and higher order sensitivity indices using the brute-force method. Therefore, the so-called Sobol method (Ekstroem & Broed, 2006; Sobol, 1993) and the Fourier Amplitude Sensitivity Test (FAST) (Cukier et al., 1978; Ekstroem & Broed, 2006; Saltelli & Bolado, 1998) are available to calculate the corresponding sensitivity indices in a more efficient way compared to the brute-force method.

6.2.6 Comparison of SA methods

The positive and negative characteristics of different SA methods are presented in Table 6.2-1.

Table 6.2-1: Comparison of selected SA methods.

Method	Positive attributes	Negative attributes
Scatterplot	• Visualises relationship between the selected parameter and model output. • Can be the natural starting point of SA helping to select further SA methods (Frey & Patil, 2002).	• Does not enable to visualise interactions between parameters. • For complicated models of many model parameters or inputs, the number of scatterplots is big.
Normalised partial derivative	• Suitable global SA method for approximately linear models. • Suitable local SA method for non-linear models.	• Does not deal with interactions between parameters. • Does not perform well with nonlinear, non-monotonous models in global SA sense.
Morris method	• Ranks the model parameters or inputs in order of importance. • All the results can be read from a single Morris plot. • Can be the natural starting point of global SA reducing the number of model parameters or inputs to deal with.	Indicates but does not quantify interactions between model parameters or inputs.
Sampling-based methods (e.g. SRC, SRRC, CC, RCC)	• Perform well with linear models. • Rank methods perform well with nonlinear but monotonous models.	Not suitable for non-monotonous models.
Variance-based methods (e.g. Sobol's method, FAST)	• Independent of model assumptions (can be applied to nonlinear and non-monotonous models). • Addresses interactions.	Computationally demanding.

7 Methods to quantify parameter/ input uncertainty and conceptual model uncertainty

The uncertainties listed in Chapter 4 contribute to the total uncertainty of a radioecological model. The uncertainties prioritised in this document as explained in Section 4.2 are parameter/input uncertainty and conceptual model uncertainty. In the present chapter some more details on how to handle parameter/input uncertainty and conceptual model uncertainty are provided.

7.1 Quantification of parameter/input uncertainty

In this section, the estimation of parameter uncertainty is handled in more detail. As mentioned in Section 4, parameter uncertainty and input uncertainty can be handled technically in similar way and therefore the methodology proposed here is valid also for dealing with input uncertainty.

Extensive guidance about parameter uncertainty and variability estimation using the probabilistic risk assessment method is given in (EPA, 1997, 2001, 2014).

The general steps of parameter uncertainty and variability estimation include:

- (Preliminary) sensitivity analysis (SA) to reduce the number of model parameters and input data that are described by PDFs, as presented in Chapter 6,
- Selection of PDFs for model parameters and input data by differentiating between variability PDFs (PDF_V) and uncertainty PDFs (PDF_U) as presented in Section 7.1.1,
- Applying the Monte Carlo method(s) to calculate the distribution of model output values via random numbers generated from PDFs of model parameters and input data. As explained in Chapter 5, the Monte Carlo methods (1D MC and 2D MC) are the most practical approaches for parameter uncertainty and variability estimation. Detailed description on how to apply these is given in Section 7.1.2,
- In case of correlated model parameters and input data, it is necessary to apply a suitable method (cf. Section 5.4) coupled with 1D MC method to take correlations into account for estimating parameter uncertainty.
- A simplified scheme of the parameter uncertainty and variability estimation is presented in Figure 7.1-1. Software that can be used for parameter uncertainty (and variability) estimation is given in Chapter 10.

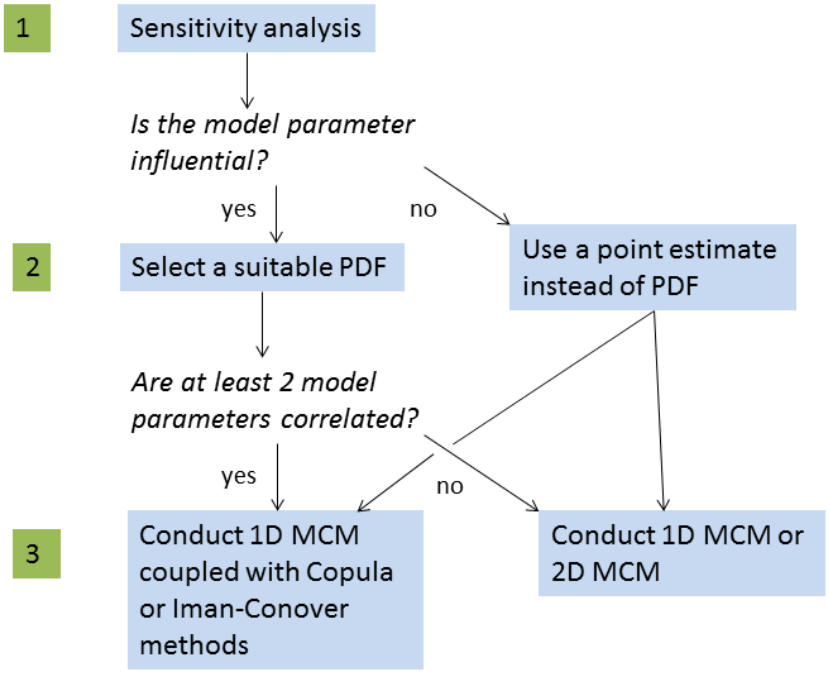

Figure 7.1-1: Simplified scheme for quantifying parameter uncertainty. From step 2, all the uncertainty and variable model parameters and input data should be handled.

7.1.1 Selection of PDFs

The selection of PDFs is an important step in the application of any Monte Carlo methodology. In general, it is not necessary to select PDFs for all the parameters if according to the preliminary SA the model parameters or input data do not significantly contribute to the uncertainty of model output. This helps to save the amount of work related to PDF selection. For a preliminary SA, the preliminary PDFs of parameters can be chosen using the type of information available. Table 7.1-1 provides some examples on how to choose a preliminary distribution based on the limited available data, similar to Appendix B in (EPA, 2001).

Table 7.1-1: Examples on how to choose PDFs if only limited information and/or data is available.

Information / Constraints	**Assumed PDF**
mean, standard deviation	Normal
lower limit, upper limit	Uniform
lower limit, mode, upper limit	Triangular
average rate of occurrence of events	Exponential

In general, the choice of PDFs can be based on repeated measurements and data from the literature. For example (EPA, 2011) contains many data about exposure factors that characterise human behaviour and individual's exposure to an agent. If no site-specific data exists it is possible to use surrogate data to find the distribution function of a model parameter (EPA, 2001). In this case, available

data about other sites (in another region of the World) can be used to find the model parameter PDF for the site with lacking information. For example, it can be assumed that water intake rate (per adult person) is of rather similar distribution in several regions of the World. It is also possible to use expert elicitation to derive the PDFs in case of lacking information about the model parameters (EPA, 2001; Till & Grogan, 2008). Difficulties arise if different experts assume significantly different PDFs. One example of expert elicitation was to derive distribution functions for the model parameters of COSYMA and MACCS codes that estimate risks and other endpoints associated with hypothesised accidents due to nuclear installations (Goossens & Harper, 1998; Goossens et al., 1997) . Different groups of experts derived distributions in different fields of radioecology (atmospheric dispersion, deposition, food chain, etc.) according to their competence.

The three steps of fitting distributions to experimental data are:

- Selection of the family of PDFs,
- Fitting parameters of the selected distribution,
- Assessing the quality of fit of the distributions.

7.1.1.1 Selecting the family of PDFs

The first step to fit PDFs to experimental data is to select the family of distributions that may match with the measured data based on the knowledge. The following questions may help to choose the family of suitable distributions as given by EPA (1997):

- Is there any mechanistic basis for choosing a distributional family?
- Is the shape of the distribution likely to be dictated by physical or biological properties or other mechanisms?
- What are the bounds of the variable?
- Is the variable discrete or continuous?
- Is the distribution skewed or symmetric?
- If the distribution is thought to be skewed, in which direction?
- What other aspects of the shape of the distribution are known?

Knowing the mechanistic reasons about a model parameter (or input data) can help to choose the distribution. For example, normal distribution can be assumed for model parameters that result from the sum of random variables. Log-normal distribution can be assumed for the product of random variables. More information about mechanistic bases of choosing PDFs can be found in the works of Evans et al. (2000) and Morgan and Henrion (1990).

Such a mechanistic base was discussed for the ERICA-tool, (ERICA, 2007), and for SYMBIOSE default database (Simon-Cornu et al., 2015), when it was considered that a TF, a CR or a K_d is the result of multiplication of a large number of unknown positive parameters. Hence, the underlying distributions for these quantities were set to log-normal ones (Simon-Cornu et al., 2015).

The most appropriate PDFs together with relevant mechanistic bases and examples are handled in Appendix B in (EPA, 2001).

7.1.1.2 Fitting parameters of a selected distribution

Once the distribution has been selected it is important to find the distribution parameters that best fit to the measured data.

There are several ways to fit sampled data to the theoretical distribution. The two well-known methods are the *method of moment matching* (MoMM) and *maximum likelihood estimation* (MLE).

The MoMM is based on the following steps (EPA, 2001; Morgan & Henrion, 1990):

- Calculate the moments of a sample distribution (empirical distribution).
- Calculate the parameters (e.g. mean, standard deviation) of a chosen distribution based on the moments. In general, the number of parameters characterizing the distribution must be equal to the number of moments calculated in the previous step.
- These parameters characterise the chosen (fitted) distribution.

The MoMM is rather easy to apply and it always works. On the other hand, MoMM may not provide the best estimates for the distribution function parameters.

The idea of the MLE is to find distribution parameters Θ_1 to Θ_k that would produce the distribution that most closely matches the observed data. In the case of MLE the likelihood function:

$$L(\Theta_1, \dots . \Theta_k) = \prod_{i=1}^{n} f(x_i, \Theta_1, \dots \Theta_k) \quad (24)$$

is maximised (EPA, 2001). According to Equation (24), the likelihood function is equal to the joint probability density function corresponding to *n* observations x_1 to x_n. In order to find the maximum value of likelihood function, it is necessary to set the derivatives of the likelihood function with respect to distribution parameters Θ_1 to Θ_k to zero and solve the system of equations.

MLE is a good method for finding the distribution parameters of the PDF. On the other hand, solving the equations to find distribution parameters Θ_1 to Θ_k of the PDF can be very difficult.

Besides fitting distributions to data, the use of empirical distribution functions (EDF) is also possible (Ciecior et al., 2018; EPA, 2001). EDFs can be recommended to use if the number of repeated measurements of a model parameter is high. On the other hand, if the number of repeated measurements is small it is very probable that the tails of the target distribution extend further compared to the EDF. In this case, it is recommended to use theoretical PDFs instead of EDFs. According to EPA (2001), it is also possible to approximate the tails of an EDF by an exponential distribution.

In an extensive study by (Simon-Cornu et al., 2015), 331 PDFs for the transfer parameters CR, K_d and TF were derived for the SYMBIOSE modelling platform based on the summary data in IAEA documents. For fitting the distributions to the summary data, the method of moment matching was used.

7.1.1.3 Assessing the quality of fit of the distributions

The two main possibilities to assess the quality of fit of the distributions is to use probability plotting and goodness of fit tests.

Perhaps the most intuitive way is to visually study the match between the empirical distribution function (EDF) with cumulative distribution function (CDF) of the fitted distribution. For calculation of the EDF, it is necessary to sort the observations into ascending order. In this case the EDF, corresponding to *n* observations can be calculated by the following formula (Law, 2015):

$$F_n(x_i) = \frac{i-0.5}{n} \quad (25)$$

where index *i* counts the observations from 1 to *n*.

It is possible to present the fitted CDF as a straight line and see the differences of EDF with respect to this straight-line using *probability-probability plots* and *quantile-quantile plots*.

The probability-probability plot (P-P plot) is a graph of fitted model probability $F(x_i) = q_{m,i}$ versus the sample probability $F_n(x_i) = q_{s,i}$ (Law, 2015).

The quantile-quantile plot (Q-Q plot) is a graph of q_i-quantile of the fitted model quantile function $F^{-1}(q_i) = x_{m,i}$, versus q_i-quantile of the sample quantile function $F_n^{-1}(q_i) = x_{s,i}$ (Law, 2015).

The Q-Q plot amplifies changes that exist between the tails of the CDF and EDF while the P-P plot amplifies changes that exist between the middle regions of the CDF and EDF (Law, 2015).

In Figure 7.1-2, the functions of the empirical distribution and the fitted log-normal distribution are compared. In Figure 7.1-3 and Figure 7.1-4 the corresponding P-P plots and Q-Q plots are presented.

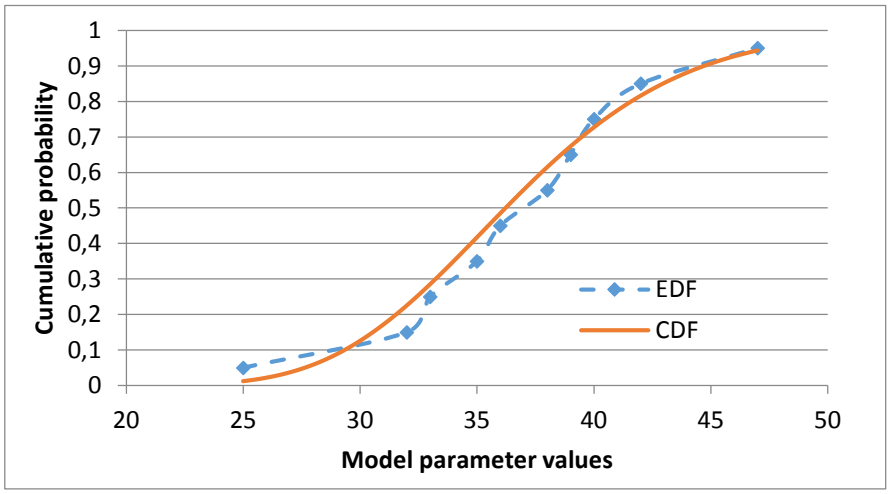

Figure 7.1-2: Empirical distribution function (blue dashed line) is compared to the theoretical log-normal cumulative distribution function with μ=3.59 and σ=0.164 (orange solid line).

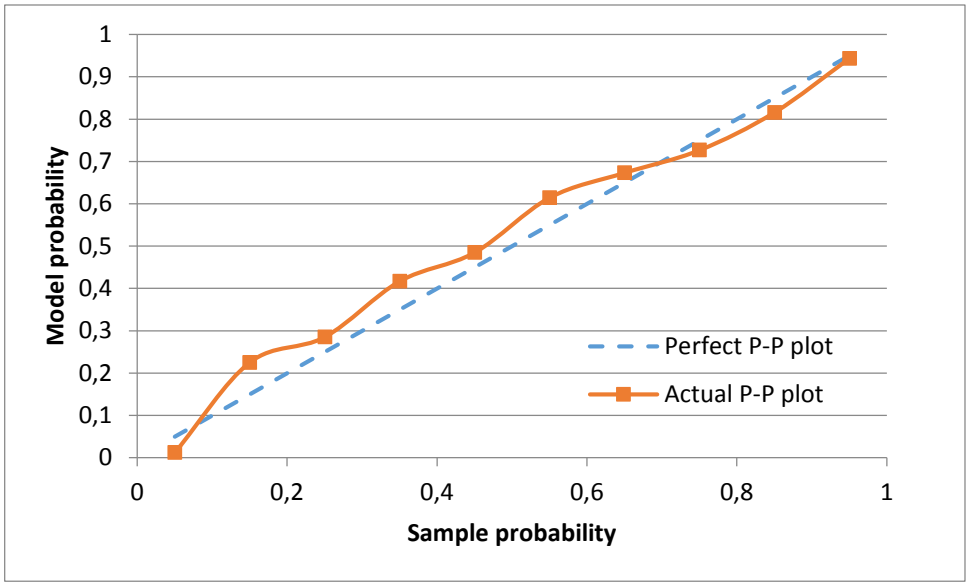

Figure 7.1-3: The fit between the actual P-P plot (orange solid line) and the perfect P-P plot (blue dashed line) in case of log-normal model distribution with μ=3.59 and σ=0.164.

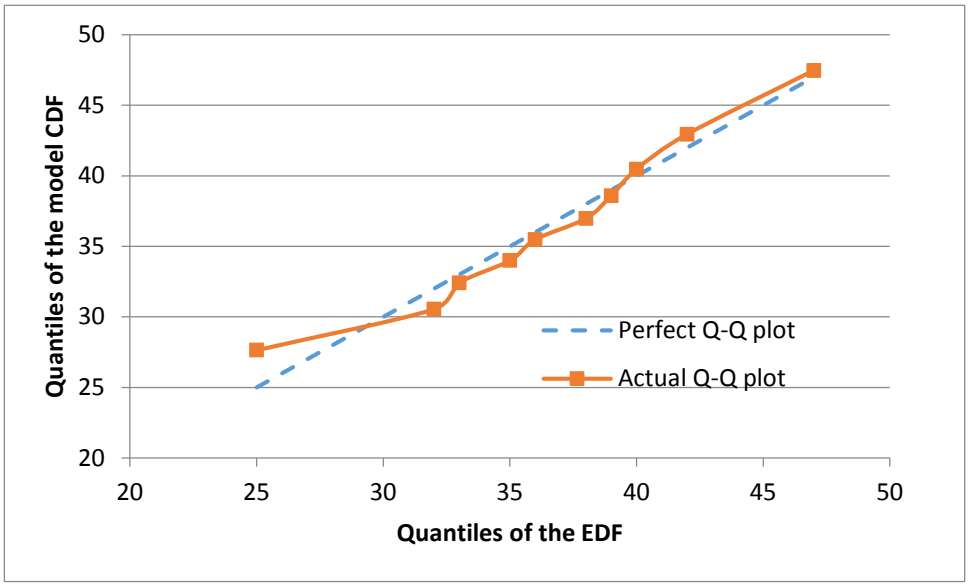

Figure 7.1-4: The fit between the actual Q-Q plot (orange solid line) and the perfect Q-Q plot (blue dashed line) in case of log-normal model distribution with μ=3.59 and σ=0.164.

Goodness of fit tests are used to compare empirical distributions to the theoretical distributions for deciding whether the theoretical distributions represent observed data. In general goodness of fit tests are used to find theoretical distributions that do not represent the observed data good enough (EPA, 2001). The three goodness of fit tests handled in the present guidance are the *Chi-Square test*, *Kolmogorov-Smirnov test* and *Anderson-Darling test*.

According to EPA (2001), „Chi-Square is a measure of the normalised difference between the squares of observed and expected frequencies."

It can be expressed by the following formula:

$$\chi^2 = \sum_{i=1}^{k} \frac{(O_i - E_i)^2}{E_i} \quad (26)$$

where O_i is the observed number of sampled values in bin number *i* and E_i is the expected number of sampled values in bin number *i*, that can be calculated by the following formula:

$$E_i = n \cdot (F(X_U) - F(X_L)) \quad (27)$$

where X_U and X_L are the upper and lower limits for bin *i*, respectively, n is the number of sampled values and *k* in Equation (27) is the number of bins for observed (empirical) and expected frequency distributions (NIST/SEMATECH).

In general, the lower is the Chi-Square value the better is the fit. The Chi-Square value is compared to the Chi-Square critical value $\chi^2_{k-1,1-\alpha}$ where α is the significance level (Law, 2015). The fitted distribution is rejected if the Chi-Square value exceeds the critical value. The Chi-Square test is suitable for discrete and continuous distributions (Law, 2015). It is important to note that the Chi-Square critical value depends on the choice of the number of bins.

In the case of the Kolmogorov-Smirnov test, the maximum difference between empirical distribution function (EDF) and theoretical (fitted) cumulative distribution function (CDF) is calculated. The EDF can be calculated by the following formula (NIST/SEMATECH):

$$F(X_i) = \frac{i}{n} \quad (28)$$

where index *i* corresponds to the observation X_i in the ordered set of *n* observed values.

The large maximum difference between the EDF and CDF (D_n) indicates a poor fit. If $D_n > d_{n,1-\alpha}$ then the theoretical distribution has to be rejected. $d_{n,1-\alpha}$ is a suitable coefficient depending on the significance level *α* and number of observations *n*. More information about calculating $d_{n,1-\alpha}$ can be found in the book by Law (2015).

The Kolmogorov-Smirnov test is most sensitive to the median of a distribution (EPA, 2001).

The Anderson-Darling test works better for the tails of a distribution (EPA, 2001; Law, 2015) i.e. it is more important for dose assessment. It uses the weighted averages of squared differences between the EDFs and CDFs (A_n):

$$A_n^2 = n \cdot \sum_{-\infty}^{\infty} |F_n(x) - F(x)|^2 \cdot \Psi(x) \cdot f(x)\, dx \quad (29)$$

where $\Psi(x) = \frac{1}{F(x)\cdot(1-F(x))}$ is the weighing factor taking higher values for the tails of a distribution (Law, 2015) and $f(x)$ is the corresponding PDF of a fitted distribution. Similar to other tests if A_n exceeds the critical value the theoretical distribution has to be rejected. More details about calculating the critical value can be found in the book by Law (2015).

In an extensive study (Ciffroy et al., 2009) PDFs for the distribution coefficient K_d in freshwater for different radionuclides were derived by considering many literature sources. In this case, the quality of fit of the distributions was assessed by means of the Kolmogorov-Smirnov test.

7.1.1.4 The problem of high percentiles

It is rather probable that the tails of a fitted distribution do not match with tails of a target distribution while the central regions of the distributions match well. The tails of model parameters' distributions can affect the tails of the model output distribution (EPA, 2001). It is a good practice to study how well different candidate distributions affect the tails of the model output distribution (EPA, 2001). According to the study by Ciecior et al. (2018), the approximation of EDFs with log-normal distributions is not recommended if the tails of the EDFs significantly differ from the tails of corresponding log-normal distributions.

Correlations between model parameters can also have an effect on the tails of the model output. A good example of negative correlations between model parameters could be the estimation of radiation exposure from consuming radionuclides-contaminated food. According to the study by Breuninger et al. (2003), the modeller can use the comprehensive dietary datasets which characterise the consumption by population of individual food classes. If upper quantiles of the distributions determined for a population are used for the consumption rates of a reference person, the result is definitely too conservative. It is highly unlikely that one person could be responsible for consumption rates corresponding to upper quantiles of all food classes. According to the study by Breuninger et al. (2003), the overestimation of radiation exposure prediction of 34 % to 53 % was obtained if 95th percentile of total consumption was calculated as the sum of 95-th percentiles of all food classes.

7.1.2 Applying the Monte Carlo methods

In this section, the schematic approach to propagate parameter uncertainty to model output is presented.

7.1.2.1 One dimensional Monte Carlo method

Once the PDFs for model input data and model parameters have been fitted to measurement data or estimated in another way it is possible to apply the 1D MC method to find the frequency distribution of model output. 1D MC method is based on random sampling from PDFs of model parameters and input data and calculating the model output for each set of model parameter and input values based on the model (JCGM, 2008a). The scheme of the 1D MC method is presented in Figure 7.1-5.

The primary result of the 1D MC method is the discrete distribution function. It is possible to calculate the mean, standard deviation and coverage interval out of the discrete distribution function.

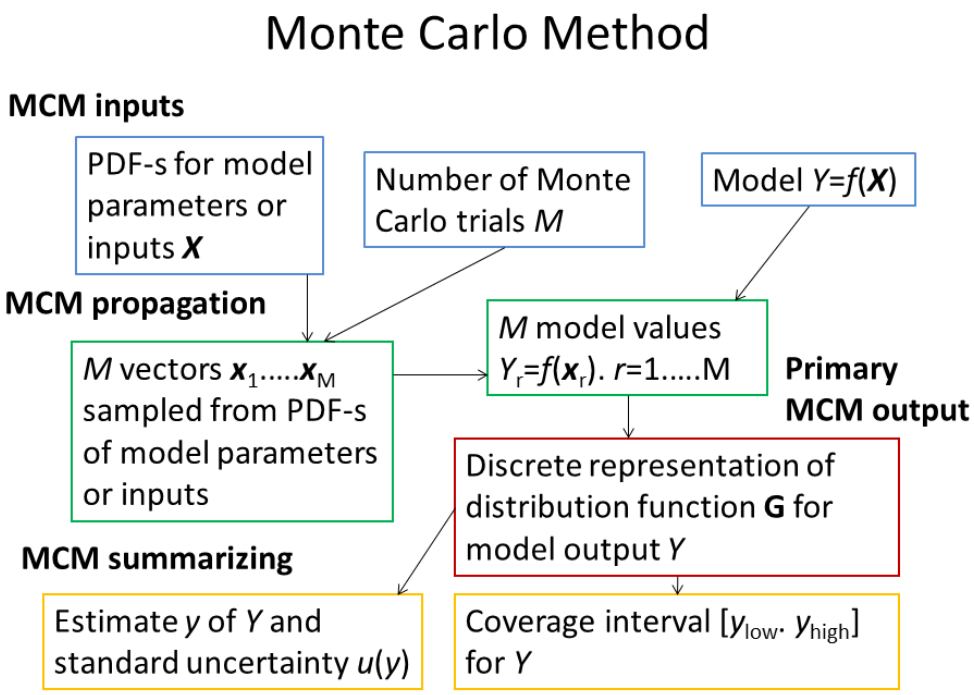

Figure 7.1-5: Schematic representation of the 1D MC method (JCGM, 2008)

An example of application of the 1D MC methodology in radioecology is to be found in (Albrecht & Miquel, 2010). The authors quantified the so-called biosphere dose conversion factors (BCDF) for Cs-135 and Se-79. The BCDF are conversion rates to convert a defined concentration in an aquifer (usually in Bq per unit volume) to an effective dose rate for a specific population and are computed using 1D MC simulations for which the log-normal and triangular PDFs are necessary for radionuclide specific model parameters, physical parameters and societal parameters (food consumption, usage of time). The number of required iterations in their case is set 10.000. In another study by Ciecior et al., (2018) the Biosphere Modelling and Assessment (BIOMASS) models developed with the Ecolego software (cf. Chapter 10) are used to calculate the BDCF for Cs-135. All the model parameters except the soil-plant transfer factor for pasture, soil-plant transfer factor for cereals and animal transfer factor for cow's milk were chosen as log-normal for applying the 1D MC method. Furthermore, most case studies of Chapter 8 are 1D MC.

7.1.2.2 Two-dimensional Monte Carlo method

As briefly outlined in Section 5.1, 1D MC method does not enable the user to handle variability uncertainty and parameter uncertainty separately. Instead, the PDFv and PDFu of a model parameter are combined into a single PDF. In order to separate between variability and parameter uncertainty in model output, the 2D MC can be used. For both methods, it can be assumed that variable and uncertain components of each model parameter are additives (Frey, 1992).

In order to apply the 2D MC method, the model parameters are divided into variable and uncertain parameters (Frey, 1992). The measurement model $\mathrm{Y} = \mathrm{f}(\mathbf{U}, \mathbf{V})$ is a function of vectors of uncertain model input data and parameters $\mathbf{U}$ and variable model input data and parameters $\mathbf{V}$**.** Let the number of uncertain model parameters and input data be *m* and the number of variable model parameters and input data be *n*. Let us also assume that *M* Monte Carlo simulations are run for uncertain model parameters and for all simulated values of uncertain model parameters *N* Monte Carlo simulations are run for variable model parameters or input data. So, the total number of 2D MC trials equals the product of *M* and *N*. The schematisation of the 2D MC method (Frey, 1992) is presented in Figure 7.1-6. In Figure 7.1-6 vectors are shown in bold. For example, $\mathbf{U}_1$ corresponds to the first simulation of all uncertain model parameters ($\mathbf{U}_1$ to $\mathbf{U}_\mathrm{m}$) while $\mathbf{V}_\mathrm{N}$ corresponds to the N-th simulation of all variable model parameters ($\mathbf{V}_1$ to $\mathbf{V}_\mathrm{n}$). The primary output of the 2D MC method is the MxN matrix containing model output values corresponding to *M* sets of uncertain model parameter values and *N* sets of variable model parameter values. It is calculated by replacing the random vectors of uncertain and variable model parameters into the model.

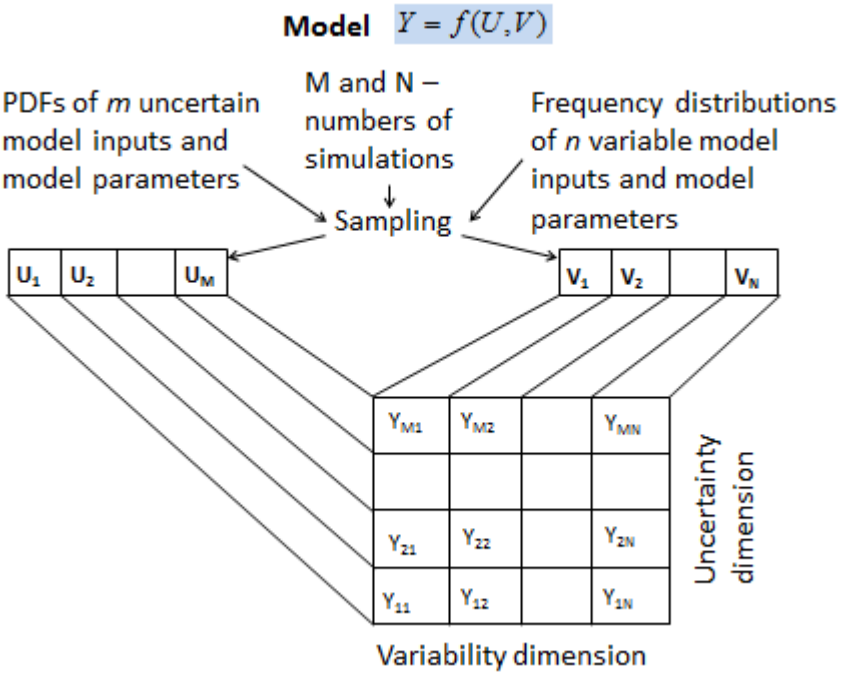

Figure 7.1-6: Schematic representation of the 2D Monte Carlo method similar to the study by Frey (1992). Vectors are shown in bold.

It is possible to present the result of a 2D MC on the graph (Figure 7.1-7). Different cumulative probability curves in Figure 7.1-7 correspond to variabilities at different confidence levels.

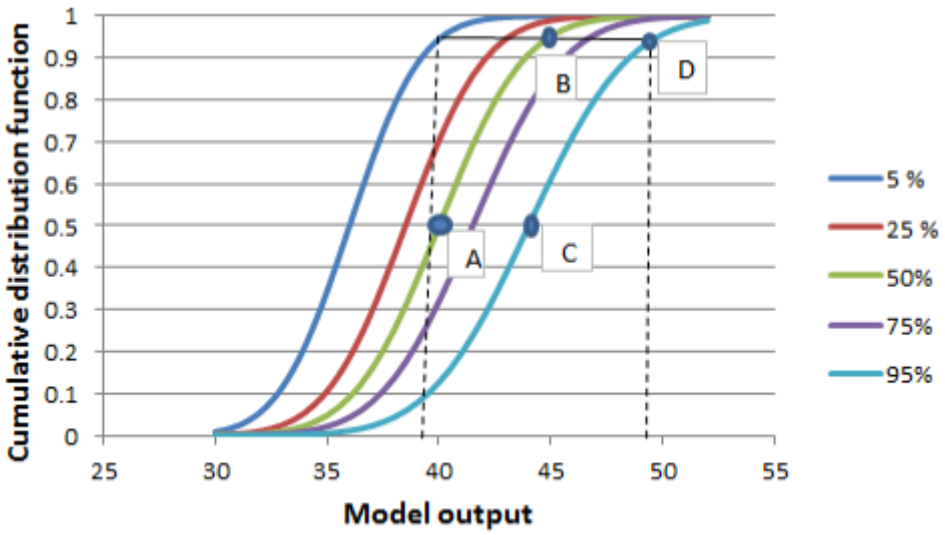

Figure 7.1-7: Possible results of a 2D Monte Carlo method. The coloured cumulative distribution functions correspond to variabilities at different confidence levels. The variability ratio is defined as B/A, the uncertainty ratio is defined as C/A and the overall uncertainty ratio is defined as D/A.

For example, the confidence level can be 95 % that for 95 % of the village wells the contamination concentration is less than 49 concentration units, while the confidence level that for 95 % of the village wells the contamination concentration is below 39 concentration units is only 5 %. According to the study by (Özkaynak et al., 2009) the variability ratio represents the ratio of the 95th percentile of variability to the central tendency (50th percentile of uncertainty for the 50th percentile of variability) that is calculated as B/A in Figure 7.1-7 (in the units of model output). The uncertainty ratio represents the ratio of the 95th percentile of uncertainty to the central tendency (Özkaynak et al., 2009) that is calculated as C/A in Figure 7.1-7. The overall uncertainty ratio (D/A) (cf. in Figure 7.1-7) takes into account the combined effect of uncertainty and variability. It is calculated as the ratio of the 95th percentile of uncertainty for 95th percentile of variability to the central tendency (Özkaynak et al., 2009).

2D MC method has been applied in dose assessment by (Simon-Cornu et al., 2015), Ciecior et al. (2018) and Jang et al. (2008).

In a case study about the daily ingestion dose rate due to ingestion of filtered river water via drinking, consuming cow milk and fish (Simon-Cornu et al., 2015) the SYMBIOSE modelling software was used to run the 2D MC simulations. The model parameter PDFs were chosen from the SYMBIOSE database for calculating the ingestion dose rates for Cs-137, I-129 and U-238. 100 different diets characterised the inter-individual variability dimension and 1000 simulations were performed in the uncertainty dimension. The overall uncertainty ratio was the highest (88) for daily ingestion dose rate due to consumption of fish. The corresponding variability ratio and uncertainty ratio were equal to 18 and 4.8, respectively.

In another study by (Jang et al., 2008) the doses due to ingestion of foodstuffs and drinking water were calculated for Korean infants, children and adults using the 2D MC method. Korean data was used to construct the PDFs due to radionuclide concentrations in different foodstuffs and due to dietary habits of the population. 250 simulations were performed in the uncertainty dimension (outer loop of 2D MC) and 10.000 simulations were performed in the variability dimension (inner loop of 2D MC). The doses for 95 % of infants corresponding to 95 % confidence level were found to be significantly higher than for 95 % of adults corresponding to 95 % confidence level (1.43 mSv y^{-1} compared to 0.27 mSv y^{-1}).

7.2 Quantification of conceptual model uncertainty

7.2.1 Definition of conceptual model uncertainty

In Chapter 4 the definition of conceptual model uncertainty is provided. In the present section more detail is given about this type of uncertainty, based on literature available.

In (Refsgaard et al., 2006), the conceptual model uncertainty is defined as "*the uncertainty related to the structures of environmental models"*. (Refsgaard et al., 2007) also state that "*the conceptual model uncertainty is due to incomplete understanding and simplified description of modelled processes as compared to reality"*. In (EPA, 2014) conceptual model uncertainty is referred to as "*limitations in the mathematical models or techniques that are developed to represent the system of interest*".

Throughout this document the term conceptual model uncertainty will be used, which is synonymous with structural uncertainty. Its definition summarises the information listed above, i.e. the conceptual model uncertainty quantifies missing or improperly formulated processes, structures or equations. Conceptual model uncertainty is the result of simplifications needed to translate the processes involved in the transfer of radionuclides into mathematical terms.

This type of uncertainty is not addressed as often as the parameter uncertainty. In the field of hydrology, however, conceptual model uncertainty has proven to be larger than parameter uncertainty when comparing water balance models (Engeland et al., 2005).

Neglecting conceptual model uncertainty may lead to uncertainty bands that are not sufficiently wide and to over-fitting of the available data (Draper, 1997), in case the model is calibrated by tuning only the parameters' values and no effect of the model structure is considered.

7.2.2 Overview of methods to quantify conceptual model uncertainty in environmental modelling

7.2.2.1 Literature review

Literature consisting of reports and peer-reviewed articles that deal with conceptual model uncertainty of environmental models has been collected by using the SpringerNature and Scopus databases and Google search.

Unfortunately, no reports and peer-reviewed articles dealing practically with the quantification of the conceptual model uncertainty of radioecological models have been found. In order to develop an appropriate methodology to quantify this type of uncertainty in radioecology, information from other research fields, e.g. hydrology and water balance modelling, ecology, epidemiology, environmental engineering and agronomy has been collected.

The reports available deal with the uncertainty assessments in environmental models for more generic pollutants and have been produced by the EPA (2009), (EPA, 2014) and the Netherlands Environmental Assessment Agency (van der Sluijs et al., 2003)

The peer-reviewed articles considered were found in the following scientific journals:

1. Environmental Modelling & Software
2. Advances in Water Resources
3. Journal of Hydrology
4. Ecological Modelling
5. Radiation and Environmental Biophysics
6. European Journal of Agronomy

Some of the documents are guidances to support scientists and decision-makers to quantify the different types of uncertainty. In particular, the reports from the EPA (2009), (EPA, 2014) and RIVM (van der Sluijs et al., 2003) deal with both qualitative and quantitative approaches to quantify conceptual model uncertainty. Also peer-reviewed articles deal with assessment methodologies and general approaches to estimate the overall uncertainty and in particular of the conceptual model uncertainty (Bastin et al., 2013; Refsgaard et al., 2006; Uusitalo et al., 2015) whereas some others deal with practical quantification (Alderman & Stanfill, 2017; Jin et al., 2010; Lindenschmidt et al., 2007; Pulkkinen & Huovinen, 1996).

7.2.2.2 Quantitative approaches

Quantitative approaches to evaluate conceptual model uncertainty are manifold and in general no standard recipe is available on how these should be applied to a specific set of models and to a specific research question. Residual analysis combined with Bayesian or probabilistic techniques and sensitivity analysis are the most applied methods. Residual analysis combined with Bayesian or probabilistic analysis (cf. Chapter 5 for more details on Bayesian and probabilistic approaches) consists in carrying out a statistical analysis of the residuals between model predictions and observations. Analysis of the residual quantifies the overall model uncertainty. The conceptual model uncertainty is then obtained by subtracting the propagated parameter uncertainty from the overall model uncertainty (Refsgaard et al., 2006). The approach based on the residual analysis relies on the assumption that uncertainties are additive. This is a debatable assumption. For example, one could assume that uncertainties are multiplicative, as in (Tian et al., 2013). Indeed the combination of parameter and conceptual model uncertainty is often non-linear due to correlation between variables in a model. Also differences

between predictions and observations may not be caused only by the structural uncertainty but also by uncertainties in the observations.

In order to quantify the conceptual model uncertainty such method is applied in several published works. For example in (Jin et al., 2010), the standard Bayesian methodology and residual analysis is applied to the water balance model WASMOD. In (Alderman & Stanfill, 2017) the Bayesian standard method and the residual analysis are applied to more than one model for predicting wheat phenology.

(Jin et al., 2010) use the residual between hydrological model output and data together with the analytically derived likelihood function to quantify simultaneously the PDFs of the model parameters and the so-called simulation error by applying the Bayes theorem. In this way, the 95% confidence intervals due to both parameter uncertainty and conceptual model uncertainty are calculated by adding the 95% confidence interval due to the parameter uncertainty to the confidence interval due to the conceptual model uncertainty.

In the work by (Alderman & Stanfill, 2017), the PDFs of the parameters are calculated according to the Bayes theorem using a MC algorithm. To quantify the prediction uncertainty of each model, the Mean Square Error of Prediction (MSEP) is calculated. MSEP allows determining the prediction variance which is based on a standard decomposition of the squared error, to which the parameter uncertainty and conceptual model uncertainty contribute:

$$\mathrm{var}\left[\hat{f}(X;\hat{\theta})\right] = \mathrm{var}\left\{E_{\hat{\theta}}\left[\left(\hat{f}(X;\hat{\theta})\middle|\hat{f}\right)\right]\right\} + E_{\hat{\theta}}\left\{\mathrm{var}\left\{\hat{f}(X;\hat{\theta})\middle|\hat{f}\right\}\right\} = \sigma^2_{\mathrm{conceptual}} + \sigma^2_{\hat{\theta}} \quad (30)$$

The contributions to model variance can be estimated based on a simulation experiment: each model is run for the specific prediction situation of interest using $\hat{\theta}$ parameter vectors drawn at random from the parameter distribution for that model.

As described in Chapter 6, sensitivity analysis (SA) is the study of how the variation of the output model can be quantitatively apportioned to different sources of variation in the model inputs and parameters and it is most often achieved with MC calculations. Similarly, the authors of the RIVM report (van der Sluijs et al., 2003), suggest to carry a sensitivity analysis on model structures introducing a switch-parameter to exchange among different model equations representing different conceivable model structures and sample for that switch-parameter from a non-informative type of distribution (for example uniform distribution).

Another example of sensitivity analysis for deriving the conceptual model uncertainty within a wrapper framework is provided by (Lindenschmidt et al., 2007). The term wrapper framework is found explicitly in (Arendt et al., 2012; Bastin et al., 2013). In the field of environmental engineering it is used to indicate the embedding of models in a Monte Carlo generator tool in order to be able to vary the parameters and even the model structures numerous times in order carry out sensitivity analysis. Given each available model and experimental data, a residual analysis is carried out. Three US EPA models for calculating the transfer of pollutants (e.g. heavy metals) in sediment layers are combined in a high-level architecture platform which allows for MC simulations. Randomly generated model outputs for different sets of parameters, boundary conditions and model structures are calculated. The residual term in the linear regression function, that describes a key process empirically, is assumed to quantify the conceptual model uncertainty. A normal distribution probability with mean zero and a predefined variance, is attributed to the residual term. The conceptual model uncertainty is then obtained from the confidence interval of this term.

Other methods exist which are more sophisticated and are mentioned here for completeness. They deal with multi-model simulations and are the Bayesian Model Averaging (BMA), the Generalised

Likelihood Uncertainty Estimation (GLUE) and the Multi-Model Inference (MMI) techniques. Examples of the application of MMI are available in behavioural ecology in (Symonds & Moussalli, 2011) and in epidemiology in (Walsh & Kaiser, 2011). The GLUE methodology is applied in (Jin et al., 2010). The BMA is applied in (McAllister & Kirchner, 2002) in the field of fishery management.

7.2.2.3 Qualitative approaches

When statistical quantification is not possible, only qualitative approaches can be considered to evaluate the conceptual model uncertainty. These rely on a structured analysis of the system considered, which includes

- The description of the critical assumptions within a model,
- The documentation of a model or the model quality and
- The evaluation of how well the model fits the purpose of the assessment.

To qualitatively address conceptual model uncertainty (van der Sluijs et al., 2003) and (Refsgaard et al., 2006) propose model comparison as method.

Model Comparison is an approach in which different model outputs are analysed. The evaluated difference in prediction can be considered as the contribution of conceptual model uncertainty if the parameterization of the models is similar (Refsgaard et al., 2006). If the predictions obtained are similar, then the contribution of the conceptual model uncertainty can be considered small. An example of application of model comparison to quantify conceptual model uncertainty can be found in the field of research related to climate change (IPCC, 2001) or in hydrology (Butts et al., 2004).

The following methods also support the model comparison analysis:

- EE (Expert Elicitation), a structured process to quantify subjective judgments of experts. Expert Elicitation aims at building a proper probability density function (PDF) reflecting the experts' degree of belief.
- Model Quality Checklist (MQC), which takes into account that models need to be assessed in relation to particular functions. The checklist is thus intended to help guard against poor practice and to focus modelling on the utility of results for a particular problem (fit-for-purpose). Also within TERRITORIES a questionnaire very similar to the checklist presented in (Risbey et al., 2005) was developed to gain information on the available radioecological models.

7.2.2.4 Methodology available

(Refsgaard et al., 2006) propose a methodology to handle conceptual model uncertainty based in which the methods presented in the previous sections are included. They indicate that in principle the optimal way to address the conceptual model uncertainty is a six-step protocol to combine the quantitative analysis for multiple models and the pedigree analysis, in order to evaluate the tenability of each model (via expert reviews) and the quantified conceptual model uncertainty.

7.2.2.5 Main aspects to consider for the analysis of conceptual model uncertainty

The list of applicable techniques presented above demonstrates that various methods are possible depending on the types and numbers of models considered.

Several aspects have a major impact:

- If models are available, they can be used to make qualitative/quantitative assessments for conceptual model uncertainty; on the other hand if data is unavailable the quantification of the conceptual model uncertainty is limited.
- The residual analysis can be applied to quantify the overall uncertainty. In this case the assumption of uncertainties being additive is used to quantify the parameter uncertainty and conceptual model uncertainty.
- The quantification of parameter uncertainty is often a prerequisite for determining the conceptual uncertainty.
- The use of the Bayesian or a probabilistic approach is almost inevitable to quantitatively include expert judgment in the analysis, e.g. to attribute a probabilistic function to the quantities of interest.
- Often regression models to make the assessments and/or the use of a wrapper framework is used.

When quantifying the conceptual model uncertainty, some challenges need to be considered:

- For every methodology chosen, it is necessary to translate scientific (physical, biological or chemical) hypotheses into statistical ones to apply the statistical tools properly, cf. Grueber et al. (2011).
- One problem in the application of the Bayesian method is the choice of a prior.
- The assumption that uncertainties are additive may be incorrect. In principle, also a multiplicative assumption may be reasonable.
- Only a limited number of models is available and one cannot be sure that all the model space is covered by the available model ensemble.
- Asserting that models have a “similar parameterisation” is not trivial. Does each model need the same parameters? Or is it only the same number of parameters that matters?

7.2.3 Quantifying conceptual model uncertainty in radioecological modelling

7.2.3.1 Conceptual model uncertainty in radioecology

Uncertainty due to model structure plays an important role in radioecology. (Salbu, 2016) reviewed the following cases, in which conceptual model uncertainty plays a dominant role:

1. Whenever the radioactive particle characteristics are not considered in the quantification of the source term. In particle contaminated areas, inventories can be underestimated, and impact and risk assessments may suffer from unacceptably large uncertainties if radioactive particles are not taken into account.
   Investigations of radioactive particles released from a series of sources show that the matrix composition, the activity concentration and atomic/isotopic ratios of matrix elements and refractory elements reflecting burn-up (e.g. lanthanides, actinides) are source specific (IAEA, 2011).
2. In the assumption of the system being in an equilibrium state when this is not the case (dynamic behaviour). An example is the use of the distribution coefficient K_d, which assumes reversible and equilibrium conditions and neglects system dynamics and process kinetics (EPA, 1999).
3. Whenever radionuclides and co-contaminants such as metals or organics are present in the ecosystem (Salbu et al., 2019). These are capable of interacting during the uptake and/or influence responses in exposed organisms. Thus additive, synergistic or antagonistic effects may appear that affect the total dose but that are not accounted for in the model.

Other sources of conceptual model uncertainty can be:

4. The use of empirical parameters that represent several important processes in an aggregated way, e.g. the so-called concentration ratios. Concentration ratios are very common in radioecology as they quantify the transfer from one medium to another one, e.g. concentration ratio soil-plant, soil-mushroom, soil-cow milk etc. These factors can vary over orders of magnitude and are based on measurements of the total activity concentration in bulk samples (Bq kg^{-1}, Bq m^{-2}).
5. The deliberate exclusion of relevant processes, e.g. resuspension. Resuspension (Pröhl, 2003) is the process by which contaminated particulate material in soil or sediments are re-entrained into the air or the water column, respectively, by mechanisms such as wind action, sea currents and mechanical disturbances enhanced by human activity. Although generally not considered to be a significant pathway of human exposure it may become an important secondary source of airborne exposure for example during or after mining activities because of the larger amounts of dust produced and the increased amounts of radionuclides that can be inhaled. Therefore, when calculating human exposure related to strong dusty activities this process should not be neglected.

7.2.4 Suggested methodology in radioecology

Based on the methodology proposed by (Refsgaard et al., 2006) and the techniques used in other disciplines described in Section 7.2.2, the following options can be considered for carrying out a quantitative analysis of the conceptual model uncertainty in radioecology, especially in case the model in use is not in a development phase but rather included in a software.

1. If a single model is available together with experimental data:
    a. Use a split-sample approach for calibrating and validating the model and increase the parameter uncertainty to implicitly account for structural uncertainty.
    b. Estimate the total predictive uncertainty with a statistical analysis of the residuals and subtract the propagated parameter uncertainty from the total uncertainty.
    c. Carry out a sensitivity analysis (MC simulations) within a wrapper framework.

2. If multiple models are available together with experimental data:

    d. Apply techniques a, b or c.
    e. Use advanced statistical tools such as MIM, BMA and GLUE.

3. If multiple models are available but experimental data are not available or not sufficient to carry out a statistical analysis:
    f. Carry out a model intercomparison. If models have a “similar parameterisation” and/or parameter uncertainty can be assessed, the difference in the model outputs can be seen as the conceptual model uncertainty.

4. If a single model is available but no data are available:
    g. Only a qualitative analysis is possible, e.g. pedigree analysis or expert elicitation.

8 Test cases

8.1 Parameter uncertainty analysis using the CROM tool and data from Belgian Site

How propagation of parameter uncertainty (and input uncertainty) can be handled by means of Monte Carlo methods is demonstrated in the present section by applying the CROM tool (Mora et al., 2015) to simulate concentrations of U-238, Ra-226, Pb-210 and Th-228 that were measured in the soil of Belgian forest site (Vanhoudt, 2015) in order to determine the internal and external dose rates for pine trees. The truncated log-normal concentration ratio distributions from (IAEA, 2018) were used to describe such concentrations (Figure 8.1-1). Data from the Belgian forest site is available in the TLD (cf. CONCERT-TERRITORIES deliverable report D9.59).

10^6 Monte Carlo simulations were carried out to produce the distribution of output dose rates.

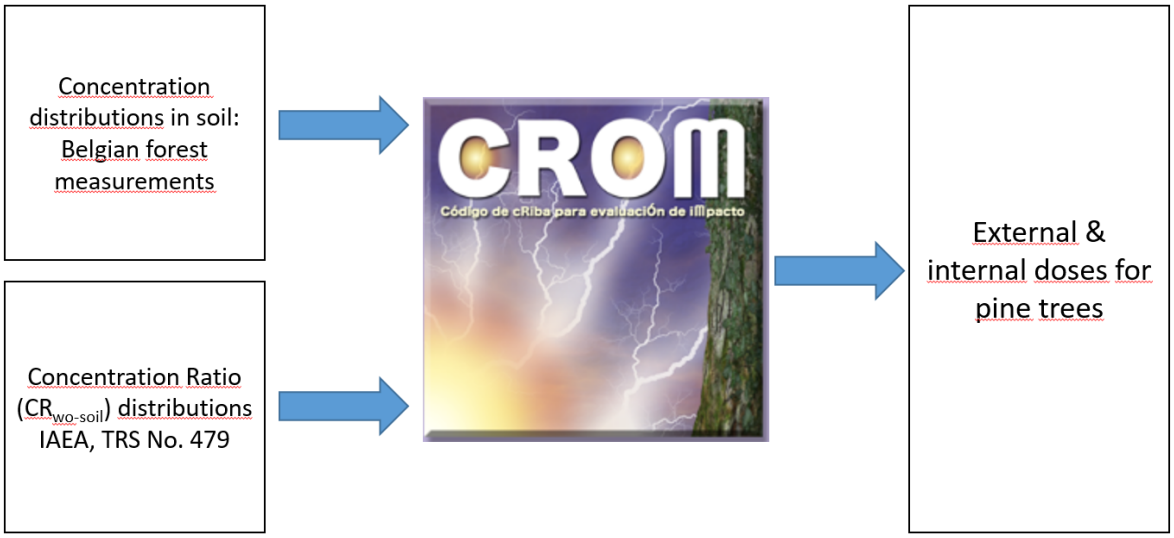

Figure 8.1-1: Flowchart of Monte Carlo simulations using CROM (Mora et al., 2015)

The activity concentration data in soil were measured in 27.04.2016, 13.10.2016, 13.02.2017, 28.11.2017 in soil top layer, which includes upper 4 cm or 20 cm in certain samples. The summary statistics of samples is given in Table 8.1-2. All the distributions of measured concentrations have clear maxima and roughly symmetric tails towards low and high values.

The applied log-normal distribution parameters of concentration ratios from (IAEA, 2018) are given in Table 8.1-1.

The normal distribution (with truncated sub-zero values) was fitted to the mean and standard deviation (cf. Table 8.1-2) for all four nuclides. The histograms and fitted distributions are shown in Figure 8.1-2.

Table 8.1-1: Applied truncated log-normal distribution of concentration ratio ($CR_{wo\text{-}soil}$) for trees.

Nuclides	Distribution parameters, Bq kg^{-1}			
	Geometric mean	Geometric standard dev.	Minimum	Maximum
U-238	$2.9 \cdot 10^{-3}$	3.7	$1.4 \cdot 10^{-5}$	$3.2 \cdot 10^{-2}$
Ra-226	$4.5 \cdot 10^{-4}$	2.5	$1.1 \cdot 10^{-4}$	$2.4 \cdot 10^{-3}$
Pb-210	$4.3 \cdot 10^{-2}$	2.9	$6.5 \cdot 10^{-3}$	$5.8 \cdot 10^{-1}$
Th-228	$7.6 \cdot 10^{-4}$	2.3	$1.0 \cdot 10^{-5}$	$3.0 \cdot 10^{-3}$

Table 8.1-2: Summary statistics of samples from Belgian forest soil.

Nuclides	N (samples)	Activity concentration, Bq kg^{-1}			
		Minimum	Maximum	Mean	Std. dev.
U-238	18	538	6100	6420	1190
Ra-226	19	590	5900	2880	1310
Pb-210	19	26	3030	1880	704
Th-228	12	8.7	65	41.9	15.9

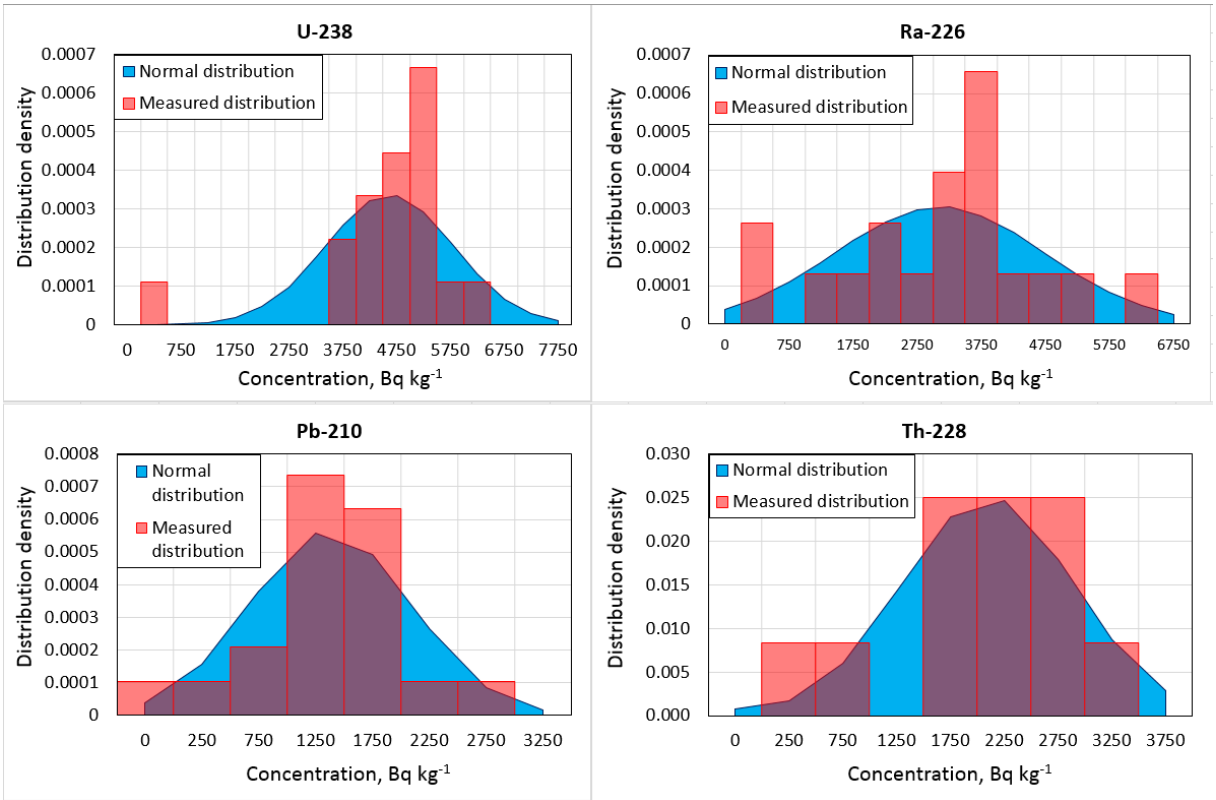

Figure 8.1-2: Activity concentration distribution histograms and fitted normal distributions in the topsoil layer of Belgian forest site.

The concentrations in the whole tree were calculated by using Argos (cf. Chapter 10), coupled in Excel spreadsheets. These were obtained for each radionuclide by using the PDFs for each value of soil concentration given in Table 8.1-2, and by assuming lognormal distributions for CRs with the parameters given in Table 8.1-1. Results are presented in Figure 8.1-3.

Table 8.1-3: Distribution parameters of internal and external dose rates.

Nuclides	Internal dose rate, μGy h^{-1}		External dose rate, μGy h^{-1}	
	Mean	St. dev.	Mean	St. dev.
U-238	0.5494	0.6793	0.00003	0.000008
Ra-226	0.2528	0.2358	0.7904	0.3391
Pb-210	0.0357	0.0439	0.0002	0.00009
Th-228	0.0073	0.0061	0.0097	0.0036
Total	0.8451	0.7204	0.8003	0.3391

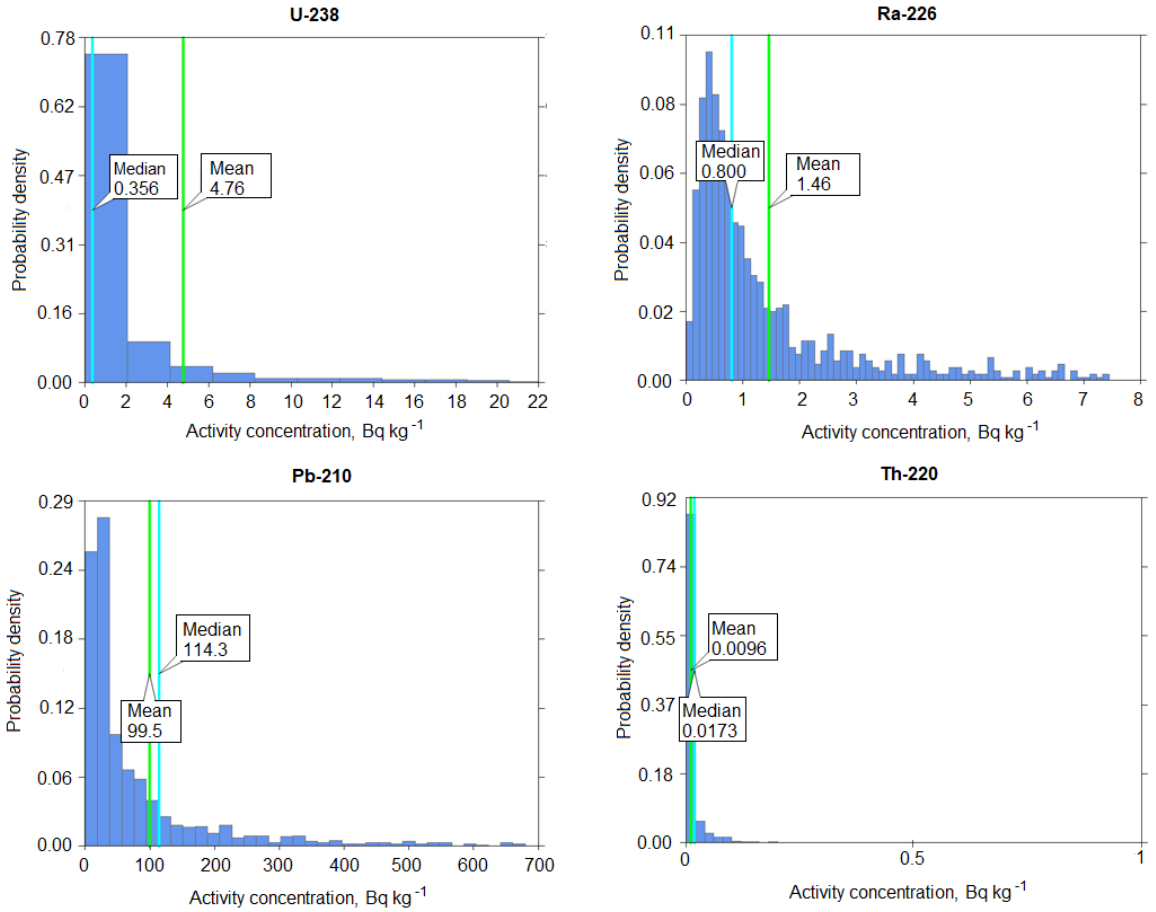

Figure 8.1-3: Distribution of concentrations of radioisotopes in pine trees in Belgian forest site, based on Monte Carlo modelling, output of Excel with Argos. Light blue lines indicate medians, green lines mean concentrations.

Although Argos also allows performing sensitivity analysis, in this case, as the model uses only 1 parameter, the information provided is not very useful (cf. Figure 8.1-4 for one example performed with U-238 concentrations). Obviously, the concentration in U-238 tree depends strongly on the CR for U-238 and then on the concentration in the soil (not so strongly). For the rest of the parameters, there is no dependence.

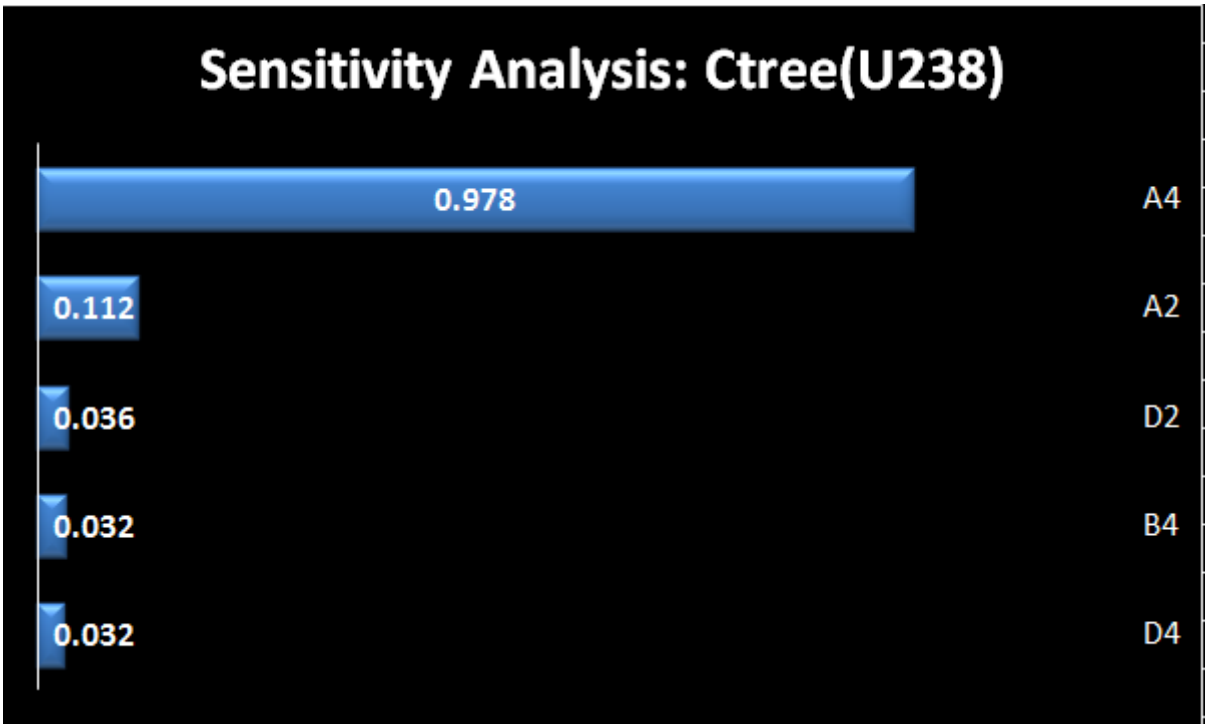

Figure 8.1-4: Results of sensitivity analysis using Pearson method implemented in Argos coupled with Excel spreadsheets.

Applying CROM, the whole-tree dose rates were calculated, assuming the trees are placed on the earth. The internal and external dose rates by nuclide resulting from MC simulations are given in Table 8.1-3. It appears that the total dose rate on average is nearly equally distributed between external and internal path. The graphical distribution of total dose rate is given Figure 8.1-5. Depending on both normally distributed activity concentrations and log-normally distributed concentration ratios, the dose rate has a slightly asymmetric distribution with a heavier tail towards high values.

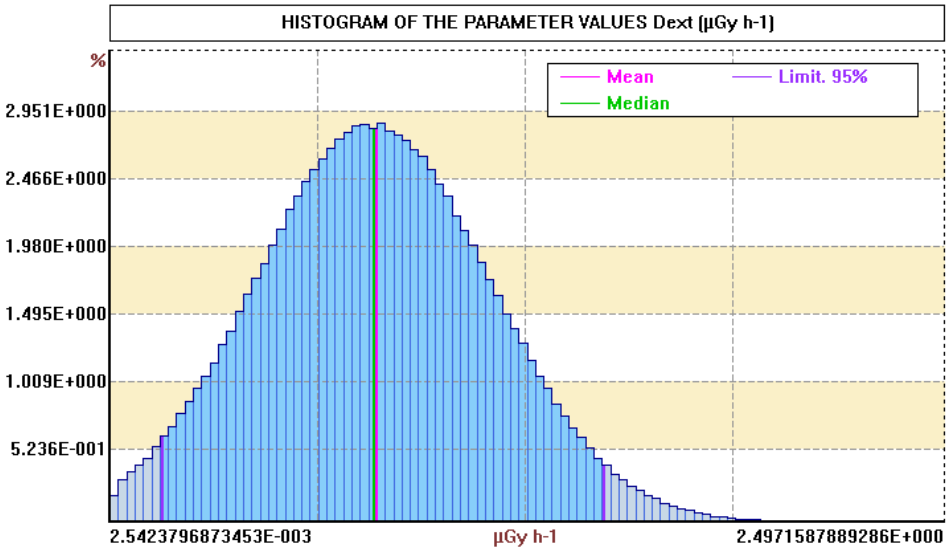

Figure 8.1-5: Distribution of dose rates for pine trees in Belgian forest site, based on Monte Carlo modelling, output of CROM tool.

A model simulation with deterministic parameters (using average activity concentrations and geometric mean concentration ratios only) was also performed. The results are presented in Table 8.1-4. The concentration trees calculated by deterministic method are about three times higher than Monte Carlo means for U-238 and three times lower for Th-228, which both have strongly asymmetric concentration distributions (cf. Figure 8.1-3). Differences for Ra-226 and Pb-210 are around 20%. The deterministic internal and external dose rates are slightly lower than Monte Carlo means, fitting all in factor of 1.5. The total internal dose rate is about 20% lower and external dose rate marginally lower.

Table 8.1-4: Deterministic activity concentrations and dose rates in pine trees. Mean concentrations and geometric mean $CR_{wo\text{-}soil}$ are used for calculation.

Nuclides	Activity concentration, Bq kg^{-1}	Internal dose rate, µGy h^{-1}	External dose rate, µGy h^{-1}
U-238	13.39	0.4468	0.00004
Ra-226	1.30	0.1822	0.7776
Pb-210	80.86	0.0210	0.0002
Th-228	0.03	0.0061	0.0096
Total	95.6	0.6561	0.7875

8.2 Uncertainty analysis of modelled air kerma rates in Fukushima coniferous forests using TREE4-advanced

In the present section, the uncertainty analysis (UA) of modelled air kerma rates (AKR) in coniferous forests contaminated by Fukushima atmospheric fallouts is presented. This analysis aims at quantifying the uncertainties on the predicted evolution of radiocaesium (Cs-137) recycling and AKR in a representative coniferous forest stand over the period 2011-2017 using the IRSN's TREE4-advanced model.

In a first part, the TREE4-advanced model (Transfer of Radionuclides and External Exposure in FORest systems) is described, focusing on the dosimetry calculation module which has been implemented for this test case. The other modules are described in details in CONCERT-TERRITORIES deliverable report D9.61. In a second part, sources of uncertainties are identified for our case study. Beside the 'usual' parameter uncertainty, specific work has been dedicated to quantifying monitoring uncertainties. In fact, the Cs-137 deposits used in many Fukushima related studies originate from monitoring –such as airborne surveys. Airborne measurements which have been acquired along a series of (often parallel) flight lines at a typical altitude of 200m above ground ABG are to be interpolated in space for use in risk assessment studies. This can be done through either deterministic or stochastic methods. In this study, we selected geostatistical techniques because these techniques enabled to quantify the spatial uncertainties on the interpolated deposit, with the view of introducing them in uncertainty calculations, along with other kinds of uncertainties. Our UA was achieved by propagating both

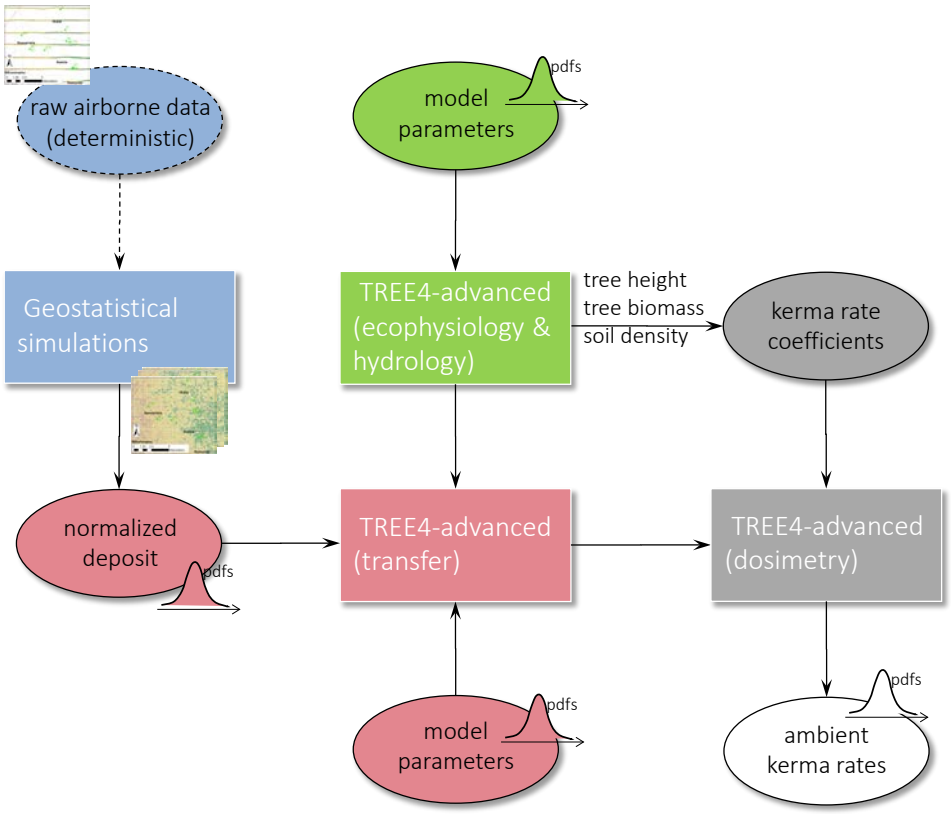

Figure 8.2-1: Model structure (TREE4-advanced) and sources of uncertainties accounted for in the uncertainty analysis of air kerma rates in Fukushima coniferous forests. See main text for description.

monitoring and parameter uncertainties through Monte Carlo simulations (cf. Figure 8.2-1). The results are presented and discussed in the last part.

8.2.1 Model description

The TREE4-advanced model which aims at predicting the dynamics of radiocaesium in a contaminated forest medium has been described and used in CONCERT-TERRITORIES deliverable report D9.61. It consists of 3 different modules: one transfer module dedicated to the prediction of Cs-137 recycling within the soil-tree subsystem, based on the outputs from the eco-physiological and hydrological modules. The transfer module is responsible for assessing the daily evolution of Cs-137 inventories (Bq m^{-2}), fluxes (Bq m^{-2} d^{-1}) and concentrations (Bq kg^{-1} dry mass) from days to decades after an initial atmospheric deposit, the characteristics of which must be specified (i.e. deposition rate, dry deposition fraction, characteristics of the rainfall events if any). TREE4-advanced notably estimates the time evolution of Cs-137 contents in the above-ground vegetation (tree canopy and trunk), as well as in the organic and mineral layers of the forest soil. The mineral profile is discretised into 60 sub-layers down to 30 cm depth, each being 0.5 cm thick, in order to better resolve the downward migration of radiocaesium into the soil profile.

The “transfer” module relies on the estimation of the annual growth/decay of some eco-physiological characteristics such as the forest stand density (trees m^{-2}), the trunk volume (m^3 m^{-2}), the bulk density of the vegetation layer (kg fresh biomass m^{-3}), or the dominant tree height (m). The tree species and the age of the forest stand at start date must be specified. The calculation also relies on the prediction of mean annual water fluxes such as evapotranspiration fluxes or water uptake by vegetation, based on the mean annual climatic characteristics.

The dosimetric modelling approach described in (Gonze et al., 2016), has been implemented in the TREE4-advanced model as a new module within the frame of this work. AKRs (in mGy h^{-1}) are estimated from radiocaesium inventories within the forest medium through the use of pre-calculated kerma rate coefficients (in mGy h^{-1} per Bq m^{-2}). The AKRs are simulated for two altitudes of the detector: 1 m ABG, of interest for subsequent human/biota dose calculations, and 200 m ABG, of interest to mimic measurements at a characteristic flying altitude. The available external kerma rate coefficients at 1 m and 200 m were pre-calculated with MC simulations (Pelowitz et al., 2011). They are given for various soil densities, bulk densities and dominant heights of the vegetation layer, and increasing depths of the radiocaesium source in the soil column (in m). Examples of AKR coefficients as a function of vegetation characteristics and radiocaesium depth in soil are displayed in Figure 8.2-2 and Figure 8.2-3.

As the TREE4-advanced model simulates the ageing of the forest stand characteristics, the kerma rate coefficients change with time.

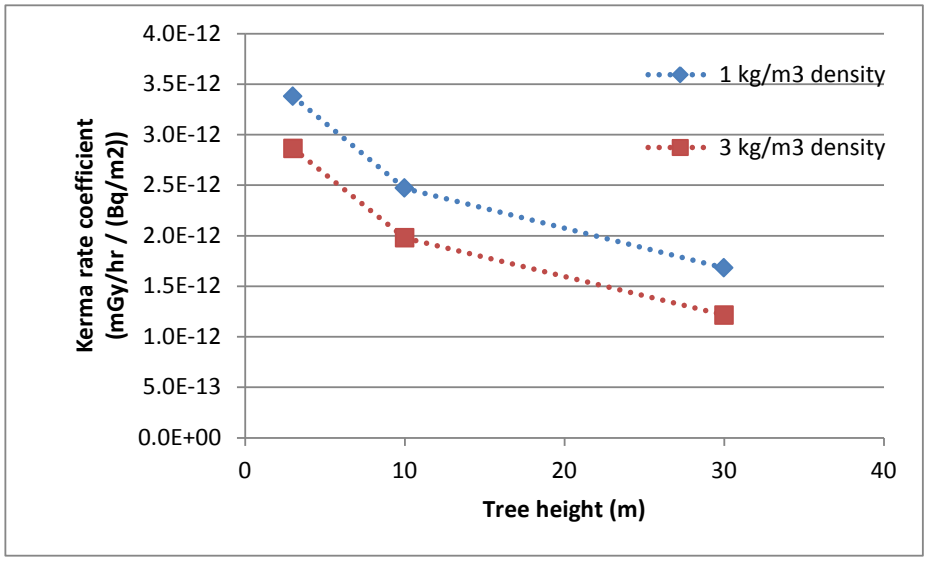

(a) 1 m above ground

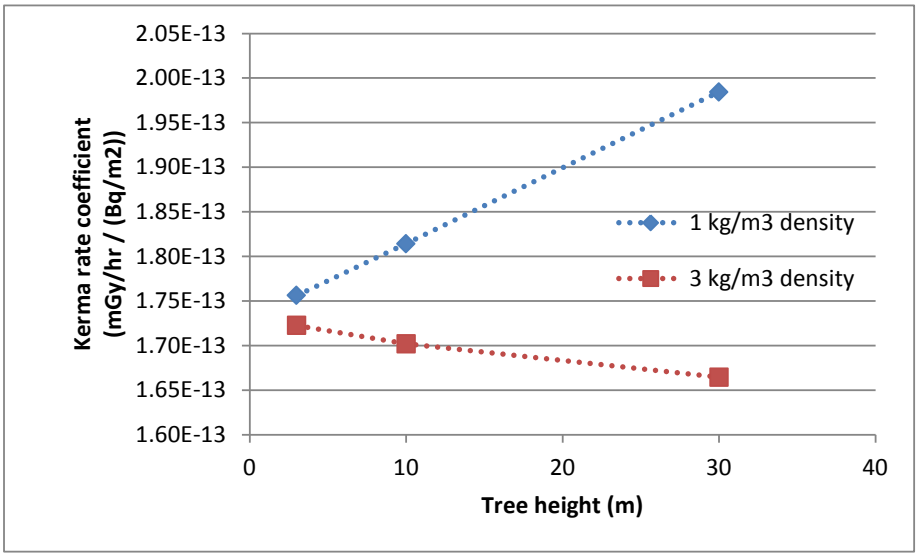

(b) 200 m above ground

Figure 8.2-2: Air kerma rates for a source of Cs-137 located in the above-ground vegetation as a function of tree height (3 values) and bulk vegetation density (2 values), for a detector located at: (a) 1 m above ground and (b) 200 m above ground.

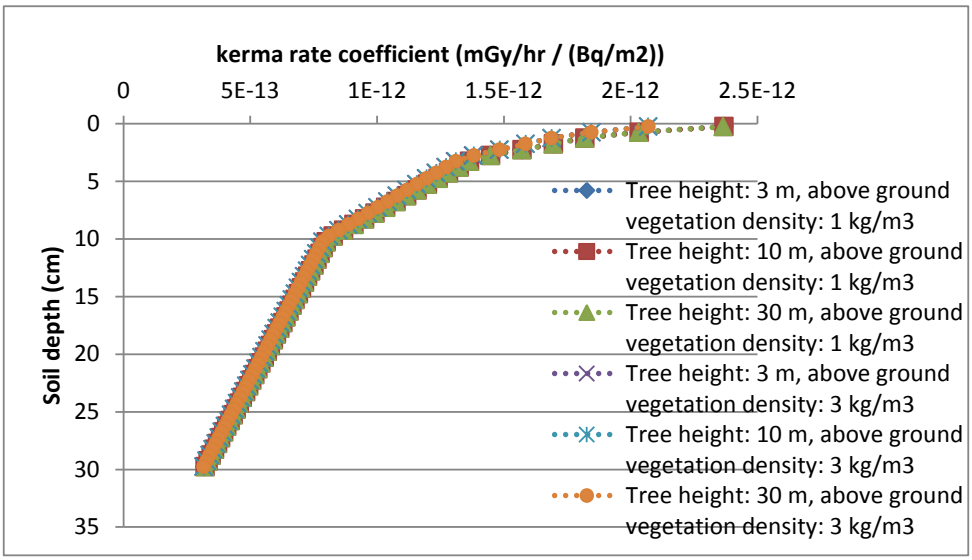

(a) 1 m above ground

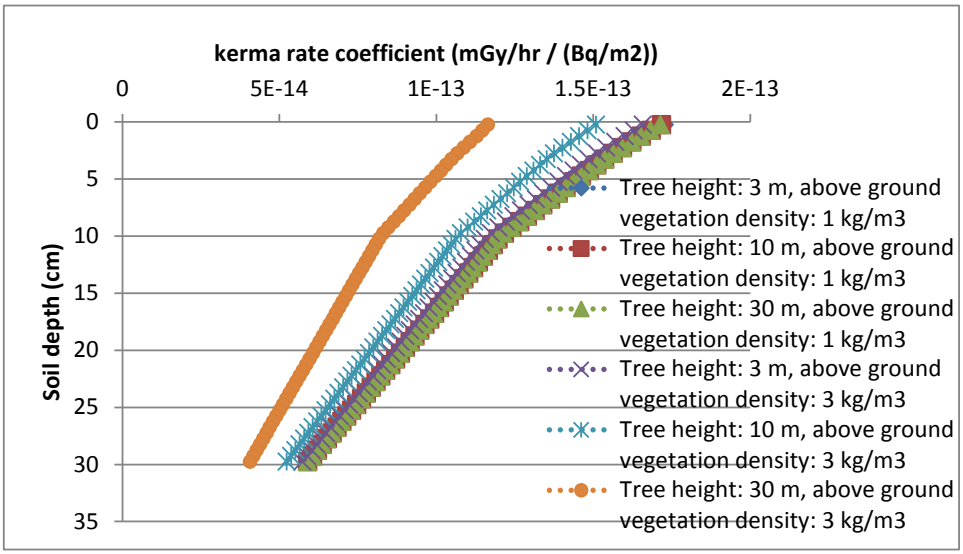

(b) 200 m above ground

Figure 8.2-3: Air kerma rates for a source of Cs-137 located in the soil as a function of soil depth, for various tree heights and above-ground vegetation densities, for a detector located at: (a) 1 m above ground and (b) 200 m above ground.

8.2.2 Characterisation of uncertainties

In this section, we identify the various sources of uncertainties affecting the model predictions. When possible, these uncertainties have been characterised.

8.2.2.1 Parameter uncertainty

The characterisation of parameter uncertainties for the TREE4-advanced model (excluding dosimetry) has already been performed and described in the CONCERT-TERRITORIES deliverable report D9.61 chapter dedicated to its application to Fukushima forests. These parameters concern hydrology, ecophysiology and Cs-137 transfers within the soil-vegetation system. It should be noted that considering a representative forest of the Fukushima area induces spatial variability, especially concerning hydrology and forest ecophysiology. This has been dealt with as a source of uncertainty for the parameters of the related modules, though the uncertainty in its epistemic sense typically concerns parameters of the radiocaesium transfer module.

Let us notice that the uncertainty on the estimated atmospheric deposit was not estimated in the modelling study described in CONCERT-TERRITORIES deliverable report D9.61. This contribution will be estimated and discussed in the next paragraph.

As depicted in Figure 8.2-1, the uncertainties on the AKR coefficient values are not explicitly considered in this study but the uncertainties originating from the eco-physiological module (e.g. height and density of the vegetation layer) are propagated towards the dosimetry module as they are accounted for in the calculation of AKR coefficients.

8.2.2.2 Scenario uncertainty

The application of the TREE4-advanced model to Fukushima forests documented in CONCERT-TERRITORIES deliverable report D9.61 considered a variety of scenarios, depending on the type of plantation (i.e. stand age at the time of deposition) and the type of atmospheric deposits (i.e. dry/wet deposition ratio rainfall height during deposition). These are unknown and vary over the contaminated land, and as such represent a source of uncertainty.

Though acknowledged, these sources of uncertainty have not been taken into account in this case study due to resource limitations. They could have been, by running a discrete number of scenarios, built with identified sets of conditions (such as minimum/maximum values for instance for the forest stand age or the dry/wet deposition ratio).

In our case study, we investigated the scenario of a 40 years forest stand (with variability around this average age considered by a PDF), a wet deposition and a 1.5 mm rainfall height during the deposition event.

8.2.2.3 Monitoring uncertainty

In the present document, we wish to quantify these types of monitoring uncertainties and introduce them into the UA. To achieve this, we use geostatistical simulations of Cs-137 deposit maps based on raw airborne monitoring data (cf. Figure 8.2-1). We thus consider spatial monitoring uncertainty of deposits, only type of monitoring uncertainty tackled in our case study, but the contribution of which to overall uncertainty is deemed important, notably in the case of a wide scale nuclear accident such as Fukushima.

Monitoring data

The airborne survey chosen for this case study is the one carried out by the Japanese Ministry of Education, Culture, Sports, Science and Technology in October/November 2011. The raw data from the detector, count rates (in counts per second), were converted to Cs-137 ground deposits after undergoing three transformations: (1) an altitude correction function for extrapolating count rates to 1-m height above ground; (2) a dose-rate conversion coefficient for converting then count rates into dose rates and (3) a coefficient for converting dose rates into ground deposit (Gonze et al., 2014). Each of the steps comes with some uncertainty, though they have not been explored in the frame of this work. The 'measured' deposit values were (radioactive) decay corrected to the 15th of March 2011, date of the main deposition event. The area studied was chosen to be a 20 x 20 km^2 square tile, centred approximately 30 km to the Northwest of the Fukushima Daiichi NPP. In this tile, the flight lines for the airborne survey were typically 2 km apart from one another.

Geostatistical modelling and simulation

The geostatistical simulations were performed in the selected tile on a 250x250 m^2 mesh grid consisting of 6400 meshes. The mesh size was chosen as it matches a typical field of view size of the airborne measurement device for a flight roughly 250m above ground.

The deposit values along the flight lines were first interpolated to the grid meshes using a kriging equation system (Masoudi, 2019). Uncertainty of the interpolated values was then quantified by Sequential Gaussian Simulation (SGS), using the Isatis commercial software, for each mesh, following seven steps: Gaussian transformation of the data, trend removal, Gaussian transformation of the residual, variography analysis, SGS, back transformation and trend adding. In the end, the SGS provided 1.000 possible deposit values for each grid mesh.

A map of the mean deposit predicted by these SGSs is provided in Figure 8.2-4 a, along with the flight lines available and used over the studied tile.

Investigation of the effect of spatial resolution of monitoring

An interesting question is that of the influence of the spatial resolution of the airborne monitoring. One way to investigate this is to iterate the previous work, starting with a poorer monitoring data set. To achieve this, we have built two additional scenarios, first keeping the raw airborne monitoring data of one out of two flight lines, then keeping the data of only one out of 4 flight lines. For each of these scenarios using downgraded input information, the complete methodology previously described was carried out; uncertainty was thus generated for the interpolated deposits of the grid, with a batch of 1.000 values for each mesh and for each scenario. The maps of the mean predicted deposits mesh are given in Figure 8.2-4 b (using one out of two flight lines) and Figure 8.2-4 c (using one out of 4 flight lines), along with the remaining flight lines used.

Geostatistical simulations can predict negative values, as shown by the mean predicted deposit in Figure 8.2-4 c, for the scenario using one out of four flight lines. Ending up with negative mean values on a significant area of the tile underscores the limitations of performing geostatistical simulations with scarce data and should be seen as a want for a higher monitoring spatial resolution for the considered simulation grid.

Comparing the maps from Figure 8.2-4 a, b and c shows that the spatial resolution of monitoring has an effect on the mean deposit estimated, and therefore certainly greater influence on the uncertainties accompanying it. The quantification of these uncertainties is the object of the next paragraph.

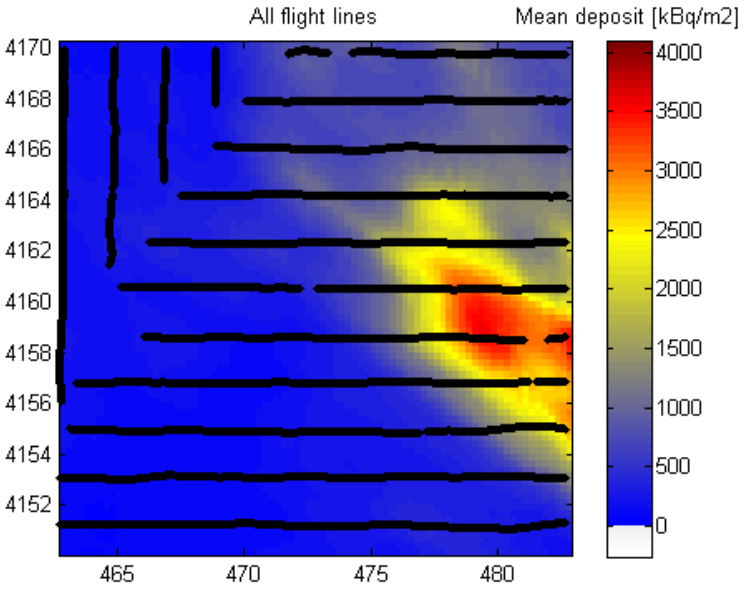

(a) all flight lines

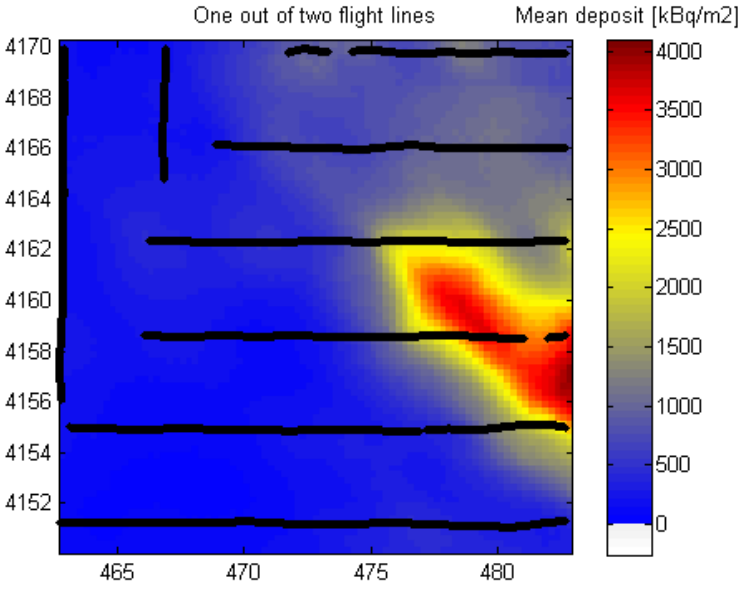

(b) 1 out of 2 flight lines

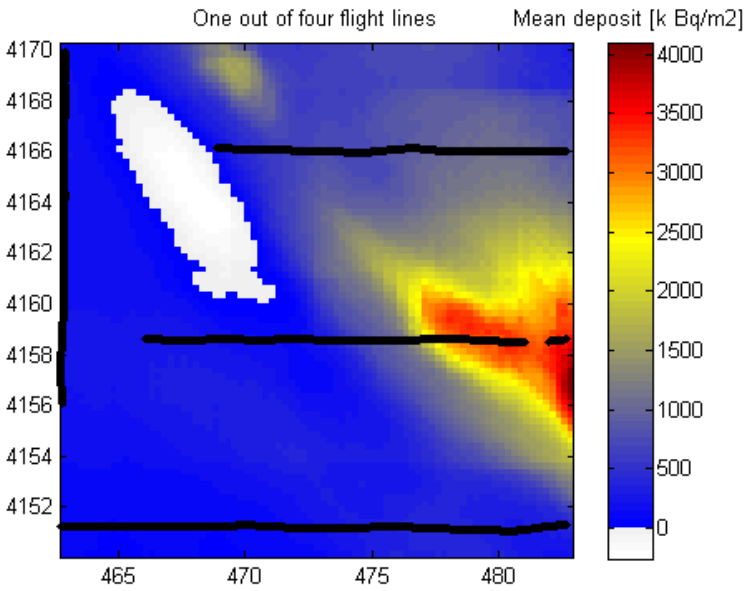

(c) 1 out of 4 flight lines

Figure 8.2-4: Mean deposits (in kBq m^{-2}) of 1.000 geostatistical simulations on the studied area, considering: (a) all flight lines, (b) 1 out of 2 flight lines, (c) 1 out of 4 flight lines.

Quantification of a relative spatial uncertainty

We try to quantify a relative uncertainty for the Cs-137 deposit, considering that this uncertainty is more or less proportional to the level of contamination encountered (for zones with deposits significantly greater than 10 kBq m^{-2}). We assume that this relative uncertainty depends on the spatial density and configuration of the flight lines, for a given flying altitude.

To quantify the spatial uncertainty and inject it in our case study using TREE4-advanced, we therefore work on normalised deposits, for which we build an empirical distribution function (EDF). For each mesh of the tile (6.400) and each geostatistical simulation (1.000), we calculated the variable D*(x)/D(x), where D*(x) is the simulated deposit on the mesh *x* and D(x) is the "true" deposit on the mesh – the value of which we do not know. In a first approach, we assumed that the « true » deposit D*(x) was more or less equal to the average of the simulations in *x*.

Originally, it was planned to sort all the tile's meshes into bins according to their distance to the closest flight line, and to derive EDFs for these bins. However, it appeared that the uncertainty on the deposit estimation depends on other factors than this distance to the closest flight line, and that it could not be simply quantified as a function of known factors.

We therefore chose to estimate the EDF of this normalised deposit over the considered tile by sorting all the D*(x)/D(x) values (6.400*1.000). The resulting function is shown with the green curve in Figure 8.2-5.

Similarly, EDFs were built for normalised deposits calculated starting from the geostatistical simulations run for the two scenario investigating the effect of the spatial resolution of monitoring. The corresponding functions are shown in the Figure 8.2-5, with the blue curve when using one out of two flight lines, with a red curve when using one out of four flight lines.

Regarding the negative deposit values possibly produced by SGSs and discussed previously, it should be noted that they were replaced by nil values when building the EDFs. Such values were frequent enough to appear significantly on the EDF using one out of four flight lines, as shown in Figure 8.2-5 with values of normalised deposit for the first few percentiles.

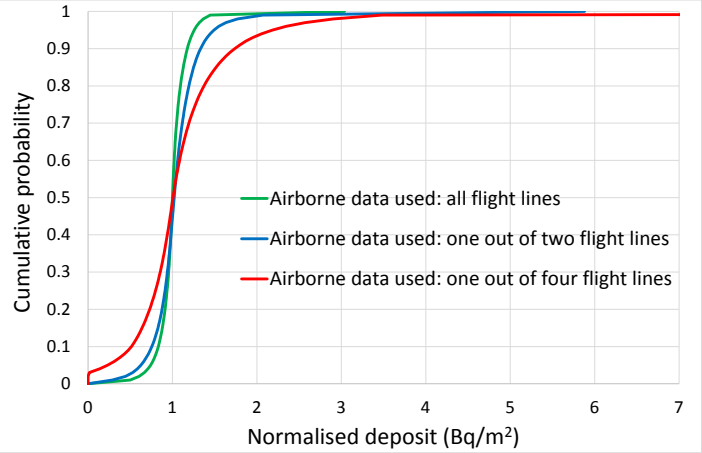

Figure 8.2-5: Empirical distribution function of the normalised Cs-137 deposits (in Bq m^{-2}) for the area of interest, based on 1.000 geostatistical simulations, and for various levels of airborne monitoring information.

8.2.3 Uncertainty analysis

8.2.3.1 Scenarios and simulation settings

The uncertainty analysis was performed for four scenarios. In the first, S1, uncertainty was introduced only for TREE4-advanced model parameters, using a unit Cs-137 deposit, for which no spatial (i.e. monitoring) uncertainty was defined. The second scenario, S2, still performs calculation in a single location, but extends S1 by considering spatial uncertainty on the normalised deposit, using the EDF derived on the selected tile and using all existing flight lines. The third, S3, and fourth, S4, scenarios are built as S2, but with spatial uncertainties derived from incomplete data subsets, i.e. one out of two and one out of four flight lines respectively.

For each scenario, 10.000 probabilistic Monte Carlo simulations were run, using Latin Hypercube Sampling, over a 6 year period, from March 2011 to March 2017.

8.2.3.2 Results and discussion

The time evolution of the AKRs is shown in Figure 8.2-6. For each scenario, the mean (full line), 5th and 95th percentiles (dashed lines) of the simulations are reported. Additionally, at the end of the probabilistic simulation, 6 years after the Cs-137 deposition, the empirical distribution function of the AKR is built for each scenario, shown in Figure 8.2-7.

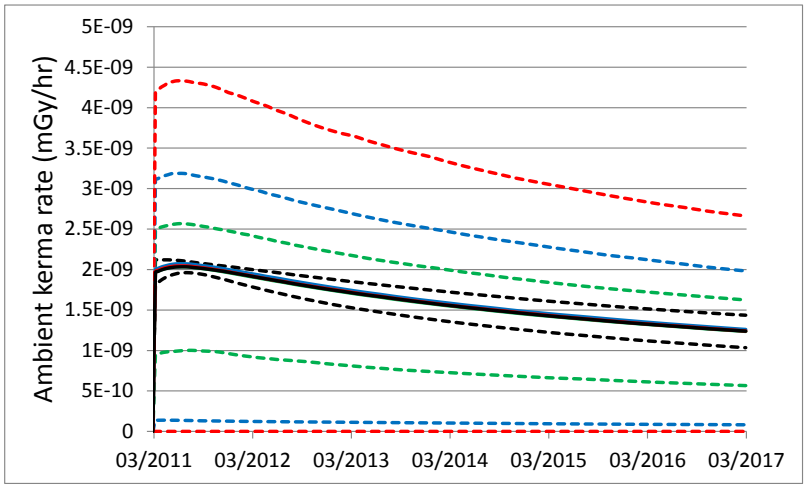

(a) 1 m above ground

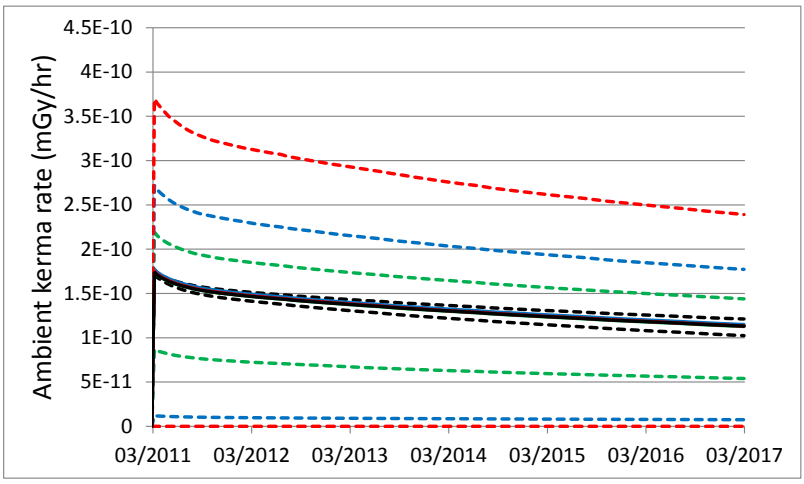

(b) 200 m above ground

Figure 8.2-6: Predicted median (full line), 5th and 95th percentiles (dashed lines) air kerma rates (in mGy/hr) for different input deposit scenarios, considering a detector height of: (a) 1 m, (b) 200 m. The black set is for scenario S1, the green set for S2, the blue set for S3 and the red set for S4. See main text for scenario description.

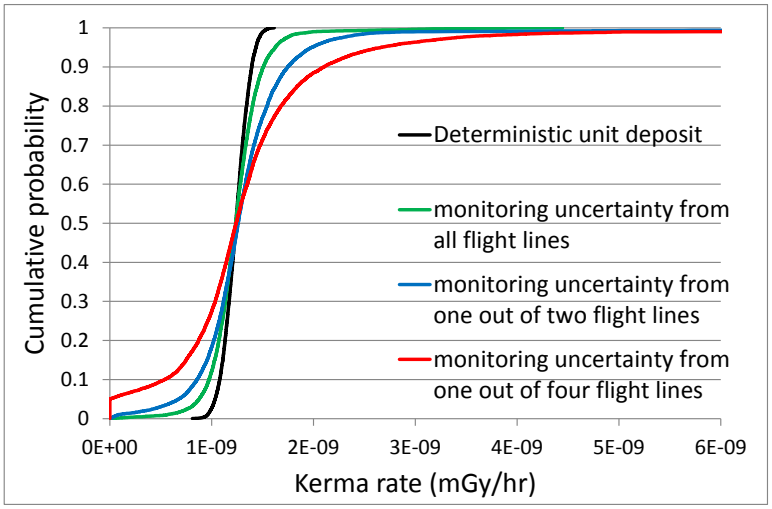

(a) 1 m above the ground

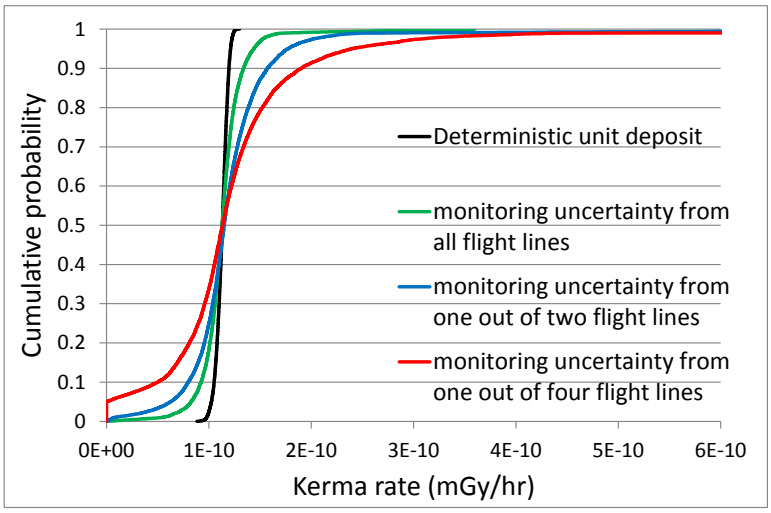

(b) 200 m above ground

Figure 8.2-7 Empirical distribution function of AKR at the end of the simulation, 6 years after deposition, considering a detector height of: (a) 1 m and (b) 200 m.

Before analysing the results on AKRs, general comment on the radiocaesium dynamics in forests must be made. In the scenarios explored, due to the wet deposition hypothesis and the rainfall height during deposition considered, a maximum fraction of the deposited radiocaesium is initially intercepted by the trees, mainly the canopy. Following interception, a sharp decrease of contamination in the vegetation starts due to various depuration processes (i.e. throughfall, litterfall, and stemflow). Contamination is thus transferred to the forest floor, where a slow downward migration starts, first down the organic layer and then down the mineral layers underneath. These findings are described more thoroughly in the chapter of CONCERT-TERRITORIES deliverable report D9.61 dedicated to the TREE4-advanced model application to Fukushima forest, for a similar scenario.

Concerning scenario S1 (no spatial uncertainty in Cs-137 deposit), the time evolution of the median AKR for a detector at 1 m slightly increases over the first months, before steadily decreasing for the rest of the simulation time. The increase can be seen as an effect of the depuration of tree contamination. Indeed, as depicted in Figure 8.2-2 and Figure 8.2-3, the AKR coefficients for a detector at 1 m have the same order of magnitude whether the contamination is in the vegetation or in the soil. For forest stands of approximately 40 years, the tree dominant height typically ranges between 15 m and 20 m over the 6 years, for which the AKR coefficient for contamination in vegetation is less than that for contamination on the soil surface. Therefore, the observed transfer of contamination from the tree to the surface of the soil logically increases the AKR for the detector at 1 m.

Over time, contamination migrates downwards in the soil, implying decreasing AKR coefficients as seen in Figure 8.2-3 a – and therefore decreasing AKRs. The predicted mean at 1 m follows this scheme, with a decrease over this second phase of nearly 30%, when the sole physical decay would lead to a nearly 10% decrease only.

The median AKR for a detector located at 200 m is continuously decreasing, at a rate which is seemingly faster over the first 6 months than over the remaining period, as shown in Figure 8.2-6 b. This is caused by the depuration of tree contamination. While radiocaesium transfer to the ground increases leads to an AKR decrease for a detector at 1 m, this trend is overcome by a competing effect for a detector at 200 m: this transfer increases the thickness of the vegetation layer which is crossed by upward radiations, and increases its subsequent shielding effect - notably for highest vegetation bulk densities. The slower decrease of AKR after these first months reflects the migration of contamination in the soil, given that increasing soil depths of contamination come with decreasing of AKR coefficients (cf. Figure 8.2-3 b). Overall, the predicted mean AKR at 200 m decreases by more than 50% over the six years, when the sole physical decay would lead to a roughly 13% decrease only.

Overall levels of AKRs for a detector at 200 m height are roughly an order of magnitude lower than those for a detector at 1 m height, which is consistent with the ratio of corresponding AKR coefficients, whether for contamination in the vegetation or in the soil (cf. Figure 8.2-2 and Figure 8.2-3).

Concerning the uncertainty analysis, it can be noted from Figure 8.2-6 and Figure 8.2-7 that the range of values for AKRs in scenario 1 at any given date is rather narrow, for both detector locations. The 95^{th} to 5^{th} percentile ratio is less than 1.4 over the six years, and rather smaller at 1 m than at 200 m. The 5%-95% interval is much smaller than that reported in the application of CONCERT-TERRIRORIES deliverable report D9.61 for inventories, concentrations in forest compartments, and fluxes between them. The kerma rates, integrating the contributions of contamination in various forest sub-compartments, tend to 'smooth' the related uncertainties, all the more that the kerma rate coefficients vary mildly with the location of the contamination (in vegetation or soil). Moreover, AKRs are calculated by the simplified dosimetry model implemented in TREE4-advanced, which notably deals with the above ground vegetation as an equivalent homogeneous medium, for which a single kerma rate coefficient is used. It typically does not distinguish kerma rate coefficients for tree sub-compartments (e.g. trunk, branches, leaves), which would enable to address the dependency of AKRs on the vertical profile of contamination in trees, which evolves over time.

Concerning the UA for scenario S2, accounting for spatial uncertainties in the normalised deposits using all flight lines, the trends of AKRs are similar to that of S1, for both detector locations. However, the spatial uncertainties on monitoring induce more uncertainty on AKRs here than the model parameter uncertainties. For the detector at 1m, the 95^{th} to 5^{th} percentile ratio varies between 1.7 and 2, steadily increasing over time; for the detector at 200 m the ratio shows less time variability, staying around 1.7.

For scenarios S3 and S4, similar observations are made for the overall AKR trends over time. For S3, the $95^{th}/5^{th}$ percentile ratio is nearly three-fold during the 6 years, showing that the loss of spatial resolution in the monitoring data has a significantly larger impact on the AKR uncertainty than the uncertainties accompanying model parameters.

Finally, concerning the S4 scenario, the $95^{th}/5^{th}$ percentile ratio is around 1.300 all through the simulation time. This very large uncertainty is mainly due to the lower percentiles of AKRs. In fact, the 95^{th} to median AKR ratio is only two-fold during the 6 years. The lower percentiles, however, present a significant number of simulations with nil or very low AKRs, as shown in the EDFs Figure 8.2-7 a and Figure 8.2-7 b. This is as a consequence of the uncertainties accompanying the normalised deposit for S4, shown in the EDF (Figure 8.2-5) and already discussed in the related paragraph (arising from the negative deposits predicted by SGSs when the monitoring data was too poor).

It should be noted at this point that the numerical stability of the probabilistic calculations has been checked by running the 4 scenarios with another random seed. The predicted 5^{th} and 95^{th} percentiles of AKRs for S1, S2 and S3, and the 95^{th} percentile for S4 have a less than 1% relative difference using one random seed or another. This however, is not the case for the 5^{th} percentile of S4. The use of a second seed leads to a nil normalised deposit for 5% of the simulations, leading to nil AKRs. This is due to the geostatistical simulations providing negative values for many meshes and simulations, as already discussed in the dedicated paragraph. Therefore, it can be argued that it would be no use to perform more Monte Carlo simulations for the UA in scenario S4; it should rather be emphasised that performing geostatistical simulations is of limited use when there is a paucity of the monitoring data. An airborne monitoring with flight lines roughly 8km apart therefore would be insufficient to produce deposit maps at a 250x250 m^2 scale.

8.3 A regional compartment model to quantify the fate of "hot particles" after long-term exposure in the Sellafield intertidal beach region: an attempt to use uncertain information.

The beach areas near the Sellafield nuclear reprocessing facility, UK, have been exposed to radionuclides released over many decades. The present section evaluates the possibility to use a simple modelling approach to predict the consequences to the beach region during a long time of exposure, especially for the fate of the Sellafield Ltd "hot particles" and applies sensitivity analysis on parameters and scenarios (source terms) to identify their relevance and the range of values. Data from Sellafield beaches is available in the TLD (cf. CONCERT-TERRITORIES deliverable report D9.59).

8.3.1 Description of the ARCTICMAR model (the NRPA box modelling approach).

The present model uses a modified approach for compartmental modelling (Iosjpe, 2006; Iosjpe et al., 2002; Iosjpe et al., 2011) which allows the study of dispersion of radionuclides over time (non-instantaneous mixing in the oceanic space). The box structures for surface, mid-depth and deep water layers have been developed based on the description of polar, Atlantic and deep waters in the Arctic Ocean and the Northern Seas and site-specific information for the boxes generated from the 3D hydrodynamic model NAOSIM (Karcher & Harms, 2000). Surface structure of the model is presented in Figure 8.3-1.

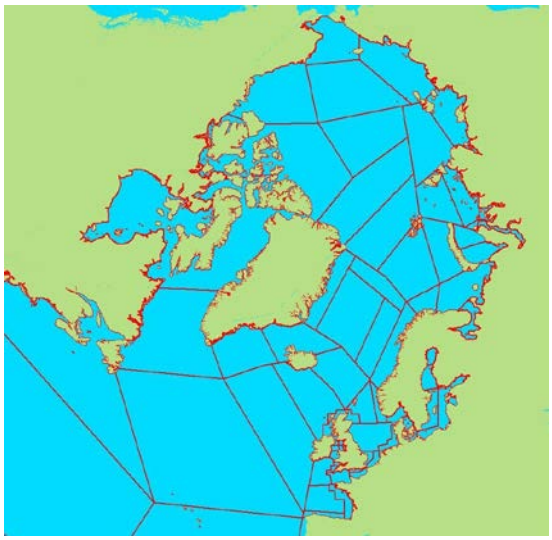

Figure 8.3-1: The structure of the surface water boxes for the NRPA box model (ARCTICMAR) - 345 compartments.

The box model includes the processes of advection of radioactivity between compartments, sedimentation, diffusion of radioactivity through pore water in sediments, particle mixing, pore water mixing and a burial process of radioactivity in deep sediment layers. Radioactive decay is calculated for all compartments. Accumulation of contamination by biota is further calculated from radionuclide concentrations in filtered seawater in different water regions. Doses to humans are calculated on the basis of given seafood consumptions, based on available data for seafood catches and assumptions about human diet in the respective areas. Dose rates to biota are developed on the basis of calculated radionuclide concentrations in marine organisms, water and sediment, using dose conversion factors. Its structure is presented in Figure 8.3-2.

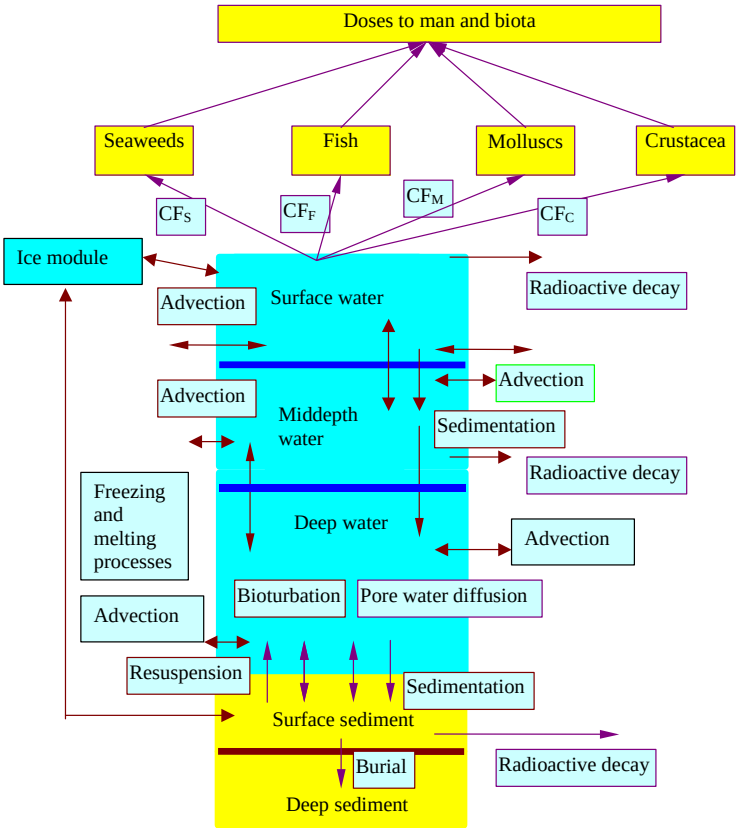

Figure 8.3-2: A schematic structure of the processes involved in modelling.

The equations of the transfer of radionuclides between the boxes are of the form:

$$\frac{dA_i}{dt} = \sum_{j=1}^{n} k_{ji} A_j \gamma\left[t \geq (T_j + w_{ji})\right] - \sum_{j=1}^{n} k_{ij} A_i \gamma\left[t \geq (T_i + w_{ij})\right] - k_i A_i \gamma(t \geq T_i) + Q_i, t \geq T_i \qquad (31)$$

with $A_i = 0, t < T_i$

where $k_{ii} = 0$ for all *i*, A_i and A_j are activities (Bq) at time *t* in boxes *i* and *j*; k_{ij} and k_{ji} are rates of transfer (y^{-1}) between boxes *i* and *j*; k_i is an effective rate of transfer of activity (y^{-1}) from box *i* taking into account loss of material from the compartment without transfer to another, for example radioactive decay; Q_i is a source of input into box *i* (Bq y^{-1}); n is the number of boxes in the system, T_i is the time of availability for box *i* (the first times when box *i* is open for dispersion of radionuclides) and γ is an unit function:

$$\gamma(t \geq T_i) = \begin{cases} 1, t \geq T_i \\ 0, t < T_i \end{cases}$$

The times of availability T_i are obtained from with following formula:

$$T_i = \min_{\mu_m(v_0, v_i) \in M_i} \sum_{j,k} w_{jk}$$

and are calculated as a minimised sum of the weights w_{jk} for all paths $\mu_m(v_0, v_i)$ from the initial box v_0 with discharge of radionuclides to the box *i* on the oriented graph $G = (V, E)$ with a set *V* of nodes v_i correspondent to boxes and a set *E* of arcs e_{ij}, which correspond to the transfer possibility between the boxes *j* and *k* (graph elements as well as available paths are illustrated in Figure 8.3-3). Every arc e_{ij} has a weight w_{jk} which is defined as the time required before the transfer of radionuclides from box *j* to box *k* can begin (without any way through other boxes).The weight w_{jk} is considered as a

discrete function *F* of the water fluxes f_{jk}, f_{kj} between boxes *j* and *k*, geographical information g_{jk} and expert evaluation X_{jk}. M_j is a set of feasible paths from the initial box (v_0) to the box *i* (v_i).

The traditional box modelling is a particular case of the present approach when all times of availability in Equation (31) are zero: $\{T_i\} = 0$ with $i = 1, \ldots n$.

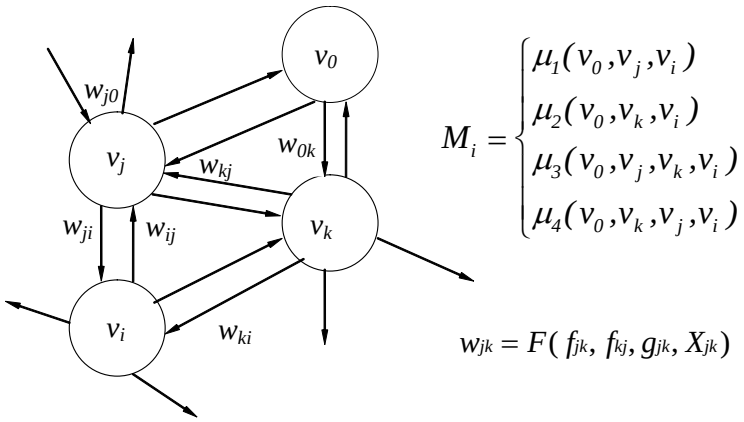

Figure 8.3-3: Graph elements.

Expressions for the transfer rates of radioactivity between the bottom water and sediment compartments will be useful in the present analysis and are listed here (the transfer rates are shown in Figure 8.3-4):

$$k_{WS} = \frac{SR \cdot k_d}{d \cdot (1 + k_d \cdot SSL)} + \frac{D}{d \cdot h_S (1 + k_d \cdot SSL)} + \frac{R_T \cdot \omega \cdot h_S}{d \cdot (1 + k_d \cdot SSL)} + \frac{R_W \cdot \rho \cdot k_d \cdot (1 - \omega)}{d \cdot (1 + k_d \cdot SSL)}$$

$$k_{SW} = \frac{D}{h_S^2 \cdot [\omega + k_d \cdot \rho \cdot (1 - \omega)]} + \frac{R_T \cdot \omega}{\omega + k_d \cdot \rho \cdot (1 - \omega)} + \frac{R_W \cdot \rho \cdot k_d \cdot (1 - \omega)}{h_S \cdot [\omega + k_d \cdot \rho \cdot (1 - \omega)]}$$

$$k_{SM} = \frac{D \cdot \omega}{h_S^2 \cdot [\omega + k_d \cdot \rho \cdot (1 - \omega)]} + \frac{k_d \cdot SR}{h_S \cdot [\omega + k_d \cdot \rho \cdot (1 - \omega)]}$$

$$k_{MS} = \frac{D \cdot \omega}{h_S h_{SM} \cdot [\omega + k_d \cdot \rho \cdot (1 - \omega)]}$$

$$k_{MD} = \frac{k_d \cdot SR}{h_{SM} \cdot [\omega + k_d \cdot \rho \cdot (1 - \omega)]}$$

Here k_{WS} is composed of expressions describing the transfer of activity by sedimentation, molecular diffusion, pore water mixing and particle mixing, respectively. Similarly, k_{SW} is composed of expressions describing the transfer of radioactivity by molecular diffusion, pore water mixing and particle mixing. k_{SM} is composed of expressions describing the transfer of radioactivity by sedimentation and molecular

diffusion. k_{MS} corresponds to the transfer by molecular diffusion. Finally, k_{MD} corresponds to the transfer of radioactivity by sedimentation. R_W (m y^{-1}) is the sediment reworking rate; R_T (y^{-1}) is the pore-water turnover rate; K_d (m^3 t^{-1}) is the sediment distribution coefficient; SSL (t m^{-3}) is the suspended sediment load in the water column; SR (t m^{-2} y^{-1}) is the sedimentation rate; D (m^2 y^{-1}) is the molecular diffusion coefficient, h_S (m) and h_{SM} (m) are the surface and middle sediment thickness respectively; ω is the porosity of the bottom sediment; ρ (t m^{-3}) is the density of the sediment material and d is the depth of the water column.

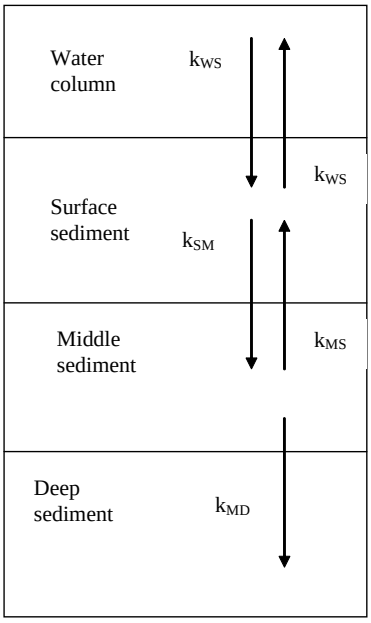

Figure 8.3-4: Generic vertical structure of the water-sediment compartments.

8.3.2 Modification of the ARCTICMAR box model: the regional compartment model for the Cumbrian waters (AMIS).

The AMIS model uses the same modified approach for the box modelling described in the previous section of the present report.

8.3.2.1 Structure of the AMIS model

To better describe the marine environment near the Sellafield facilities the local model for the Irish Sea regions (AMIS) has been developed. The model is a modification of the NRPA box model. Surface structure of the local model is presented in Figure 8.3-5. The structure of the boxes in the model AMIS for the Irish Sea are similar to the ARCTIMAR model. In addition, the model includes the surrounding box “Rest of seas”. The intertidal beach region is part of the Cumbrian Water box and is also shown in Figure 8.3-5 (the red star).

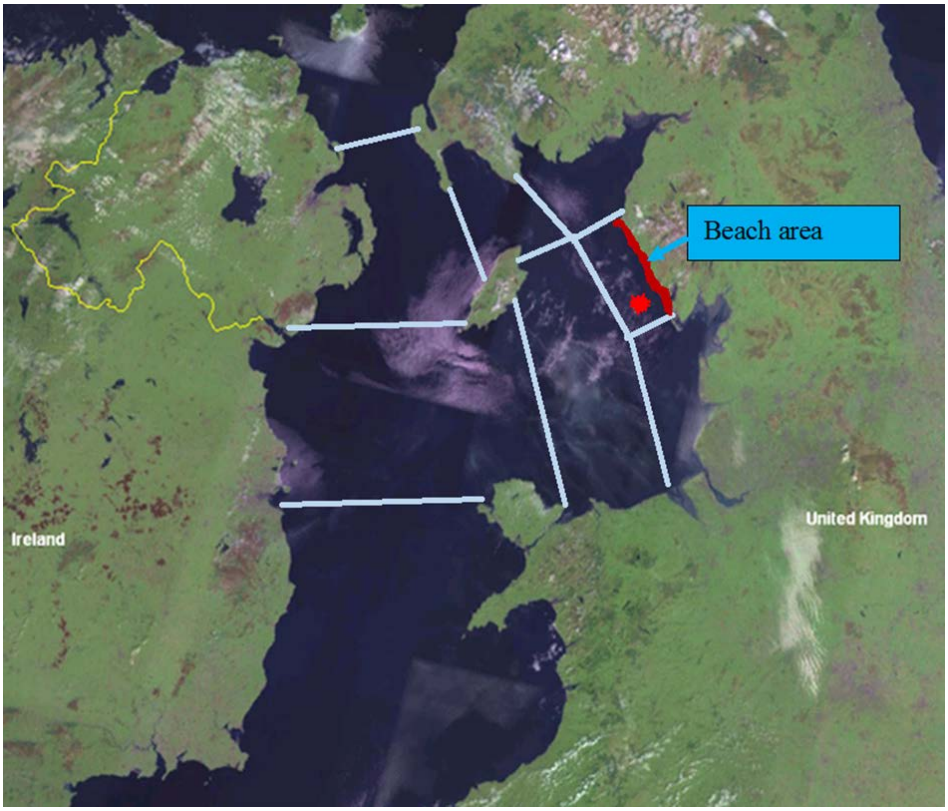

Figure 8.3-5: The structure of the surface water boxes for the regional compartment model AMIS (30 compartments).

8.3.2.2 The choice of the environmental parameters of the AMIS model

Based on the published information about the parameters used in the AMIS model, their values can vary up to 2-3 orders of magnitude (IAEA, 2004; Iosjpe et al., 2002; MacKenzie & Nicholson, 1987; Mitchell et al., 1999; Nielsen & Hou, 2002; Nielsen et al., 1997; Periáñez, 2003; Periáñez, 2005).

The liquid discharges of the radionuclides Cs-137, Pu-239 and Am-241 have been selected for the potential improvement of the AMIS model parameters by comparing the results of the simulations with the available monitoring data for the "Cumbrian Waters" box.

It has been previously shown that the choice of appropriate model parameters has a powerful impact to the results of the radioecological analysis (Iosjpe, 2011b). The selection of parameters has been performed with the help of a sensitivity analysis (similarly to (Iosjpe, 2011a, 2011b)) with the following sensitivity index (Jørgensen & Bendoricchio, 2001):

$$S^{(L)}(P) = \frac{dP^{(S)}}{dP}\frac{P_0}{P_0^{(S)}} \qquad (32)$$

where $P^{(S)}$ and P correspond to state parameters (for example, concentrations of radionuclides in water and sediment phases, doses to man and biota, etc.) and parameters which are under evaluation; P_0 and $P_0^{(S)}$ correspond to the basic values.

According to Equation (32): $S^{(L)} > 0$ when the state parameter $P^{(S)}$ increases with the increase of the evaluated parameter P. $S^{(L)} < 0$ when $P^{(S)}$ decreases with the increase of the parameter P.
There is no influence of the parameter P to the state parameter $P^{(S)}$ when $S^{(L)} = 0$.

Figure 8.3-6 and Figure 8.3-7 show examples of calculations of the local sensitivity indices for the Cs-137 concentrations in the filtered water for parameters reworking rate (Rw), sedimentation rate (SR) and apparent sediment distribution coefficient (K_d). All calculations correspond to liquid discharges of radionuclides into the Cumbrian Waters.

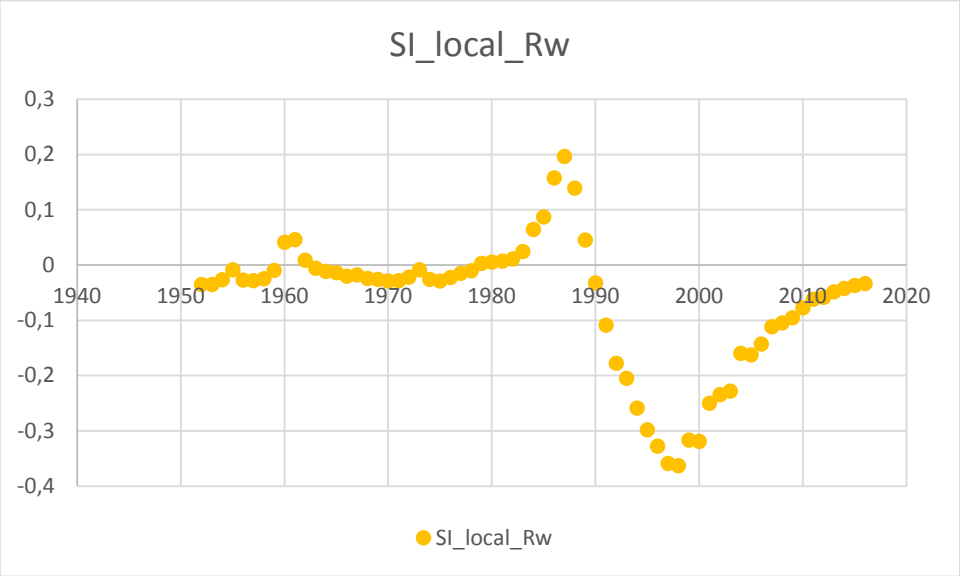

Figure 8.3-6: Dynamic of the local sensitivity index for the reworking rate.

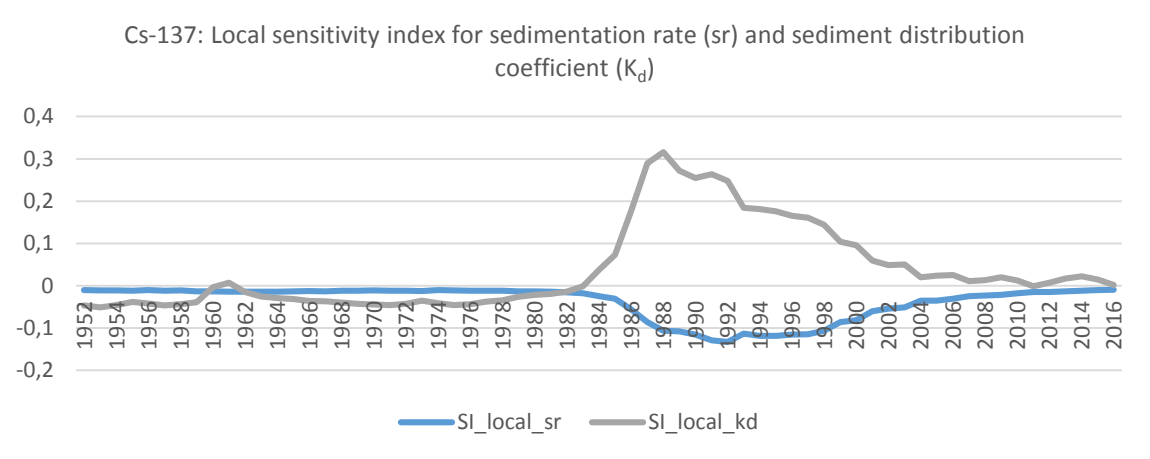

Figure 8.3-7: Dynamic of the local sensitivity indices for the sedimentation rate and sediment distribution coefficient.

The simulations presented in Figure 8.3-6 and Figure 8.3-7 demonstrate the complexities encountered when modelling dispersion of the radioactivity in the marine environment. The results show that the radionuclide concentration can either increase or decrease with the increase of the evaluated parameters. It is also shown that the results can strongly depend on the time of analysis.

The use of the sensitivity indices improves our knowledge about the influence of parameters to the model end points.

The most suitable set of model parameters have been selected for all three radionuclides (Cs-137, Pu-239 and Am-241) simultaneously according to the following equation:

$$\min_{\{\vec{P}_\mu\}} \left\{ \sum_{l=1}^{3} \sum_{i=1}^{n^{(l)}} \left[C_i^{(\vec{a}_\mu, K_d^{(\mu,l)})} - \hat{C}_i^{(l)} \right]^2 \right\} \quad (33)$$

Here $\{\vec{P}_\mu\} = \{\vec{a}_\mu, K_d^{(\mu,l)}\}$ are the sets of different model parameters, which have been used for parameterization (μ=1,..,M, where M is the number of different sets in the present investigation); each set of parameters $\vec{P}_\mu$ consists of the set of environmental parameters $\vec{a}_\mu$ and the set of "apparent" sediment distribution coefficients $K_d^{(\mu,l)}$ (i= 1,2,3 for radionuclides Cs-137, Pu-239 and Am-241, respectively); i=1,… , $n^{(l)}$, where $n^{(l)}$is number of measurements of the concentration of radionuclide *l* in water and sediment; $C_i^{(\vec{a}_\mu, K_d^{(\mu,l)})}$and $\hat{C}_i^{(l)}$ are concentrations of radionuclide *i* in the water and sediment phases, calculated by the model, and experimental data, respectively.

It is necessary to note some important points concerning the sediment distribution coefficients. The definition of the sediment distribution coefficients (K_d) is based on assumptions about the equilibrium balance between dissolved and particulate phases (IAEA, 2004). This assumption is not generally supported by the real conditions in marine environments (Periáñez et al., 2018). Therefore, terms "site-specific" and "apparent" K_d are used in some investigations (Iosjpe, 2011b; Periáñez et al., 2018). Kinetic sub-models for the exchange of radionuclides between water and sediment phases require K_d to be under equilibrium conditions in order to define the system of kinetic coefficients (Periáñez, 2003). Additionally the kinetic sub-models can construct "apparent" K_d during numerical simulations. In particular, it was shown, that (i) "apparent" K_d value near the source of contamination can be 2-3 times less than the equilibrium value and (ii) apparent K_d value in the sediment can be 10-1000 times less than the equilibrium value (Periáñez et al., 2018).
Figure 8.3-8 and Figure 8.3-9 show a reasonable correspondence between the results of the simulations and the experimental data. The environmental parameters of the model are therefore deemed suitable.

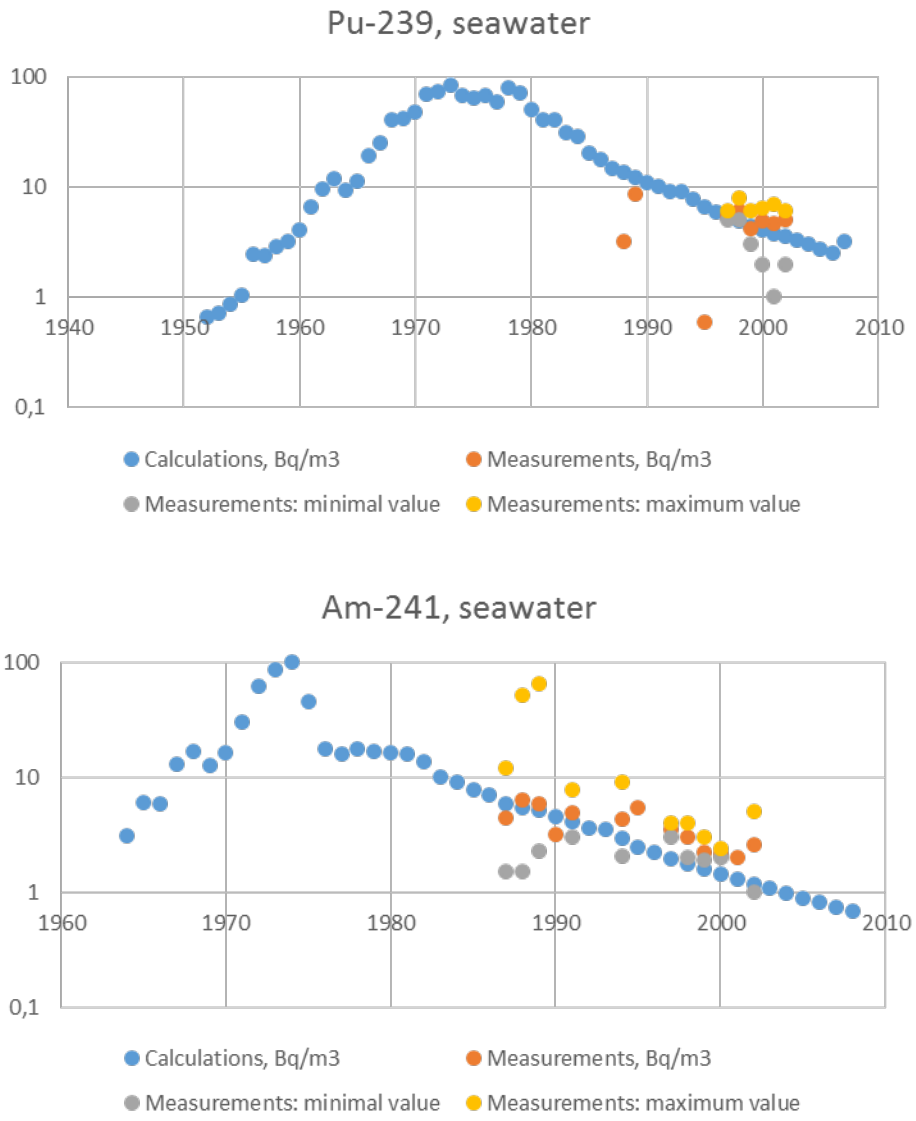

Figure 8.3-8: Comparison of the simulation results with experimental data in filtered water for Pu-239 (top) and Am-241 (bottom).

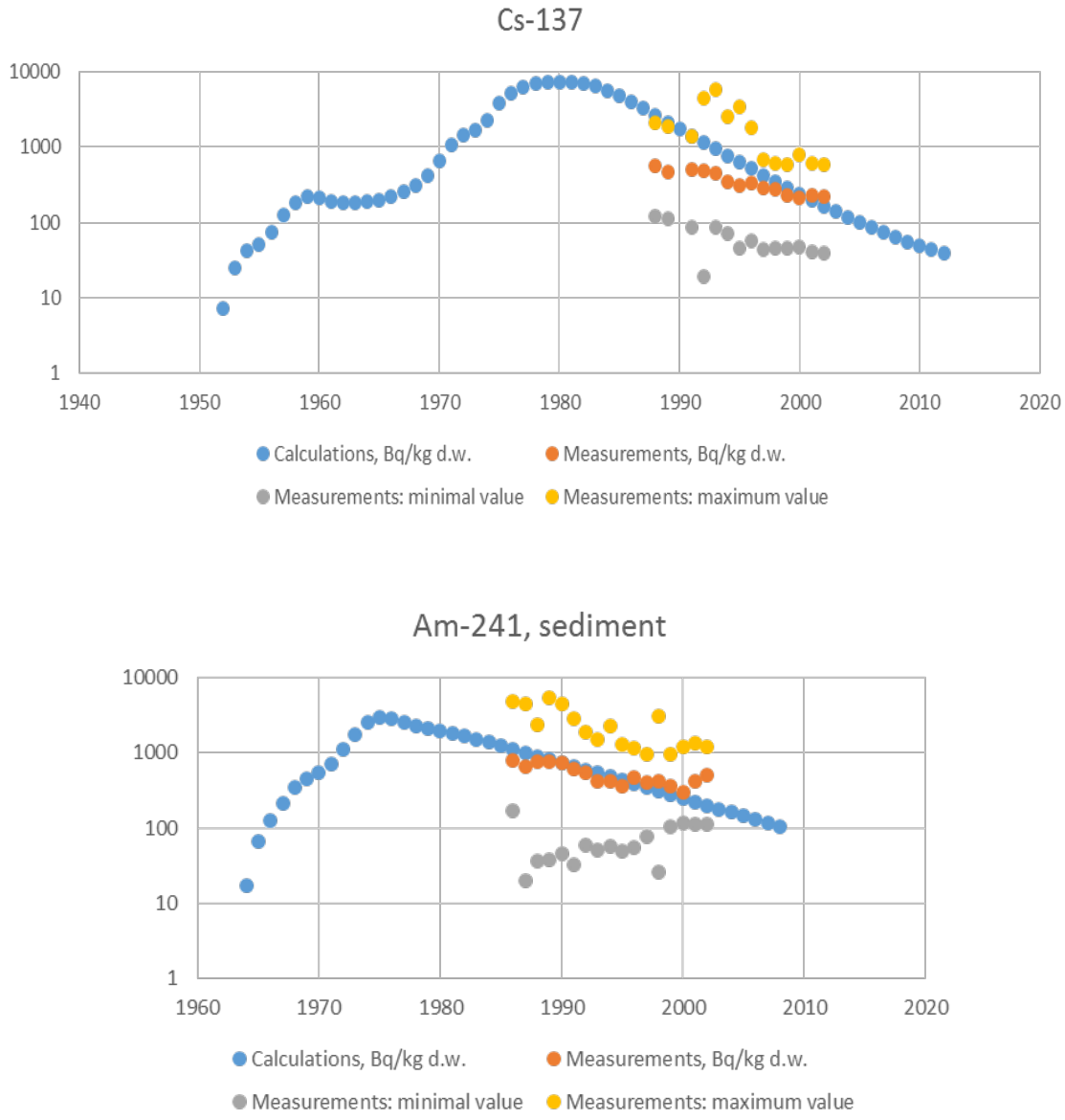

Figure 8.3-9: Comparison of the simulation results with experimental data in sediment for Cs-137 (top) and Am-241 (bottom).

8.3.3 Implementation of the AMIS model to quantify the fate of "hot particles" after long-term exposure in the Sellafield intertidal beach region.

8.3.3.1 Assumptions and peculiarities of the release scenarios for "hot particles".

Discharges of "hot particles" from the Sellafield nuclear facilities are not well understood. According to the recently published report (Sellafield, 2018), particle discharges may be (i) discharges via pipeline (for alpha and beta rich particles up to 1983 and 1985, respectively) and (ii) discharges due to debris from the Sealine Recovery Project in the 1990s and in the years 2003-2006 (for all types of particles).

Based on this information the following scenarios have been chosen:

8.3.3.1.1 Scenarios for Cs-137:

Sc_c1L: $\varphi_{1L}^{(c)}$ · Q/y, where Q corresponds to liquid discharges from 1952 to 1985.

Sc_c1: $\varphi_{1}^{(c)}$ ·1 TBq from 1952 to 1985.

Sc_c2: $\varphi_{2}^{(c)}$· 1 TBq from 1990 to 1995.

Sc_c3: $\varphi_{3}^{(c)}$ 1 TBq from 2003 to 2006.

Sc_c4: $\varphi_{41}^{(c)}$ ·Sc_c1 + $\varphi_{42}^{(c)}$ ·Sc_c2 + $\varphi_{43}^{(c)}$ ·Sc_c3

Sc_c5: $\varphi_{51}^{(c)}$ · Sc_1L $\varphi_{52}^{(c)}$ · Sc_2 + $\varphi_{53}^{(c)}$ · Sc_c3

8.3.3.1.2 Scenarios for Am-241

Sc_a1L: $\varphi_{1L}^{(a)}$ · Q/y, where Q corresponds to liquid discharges from 1964 to 1983.

Sc_a1: $\varphi_{1}^{(a)}$ ·1 TBq from 1964 to 1983.

Sc_a2: $\varphi_{2}^{(a)}$· 1 TBq from 1990 to 1995.

Sc_a3: $\varphi_{3}^{(a)}$ 1 TBq from 2003 to 2006.

Sc_a4: $\varphi_{41}^{(a)}$ ·Sa_c1 + $\varphi_{42}^{(a)}$ ·Sc_a2 + $\varphi_{43}^{(a)}$ ·Sa_a3

Sc_a5: $\varphi_{51}^{(a)}$ · Sa_1L $\varphi_{52}^{(a)}$ · Sa_2 + $\varphi_{53}^{(a)}$ · Sa_a3

Scenarios Sc_c4, Sc_c5, Sc_a4 and Sa_a5 are prepared for the best comparison with experimental data after MC simulation for parameters $\varphi_{41}^{(c)}$, $\varphi_{42}^{(c)}$, $\varphi_{43}^{(c)}$, $\varphi_{51}^{(c)}$, $\varphi_{52}^{(c)}$, $\varphi_{53}^{(c)}$, $\varphi_{41}^{(a)}$, $\varphi_{42}^{(a)}$, $\varphi_{43}^{(a)}$, $\varphi_{51}^{(a)}$, $\varphi_{52}^{(a)}$, $\varphi_{53}^{(a)}$.

Further, the present modelling approach implements the non-instantaneous mixing of radioactivity in the model compartments. According to the algorithm of the simulations, "hot particles", released into the initial box (the Cumbrian Waters) via the pipeline, can reach the box boundaries within approximately 500 hours if they remain in suspension. However, a rough estimate of the time taken for the "hot particles" to fall to the seabed can be found by rewriting the Stokes law (Mitchell, 1996) for the small spherical particles in a fluid medium:

$$t = \frac{4.5L\eta}{(\rho-\rho_w)gr^2} \quad (34)$$

where *r* is a radius of the spherical particle, which will reach the bottom in time *t*; *L* is the distance to

the bottom; η is the dynamic viscosity of seawater; ρ and ρ_w are the density of the particle and seawater, respectively, and *g* is the gravitational constant.

Complete information about dimensions of the "hot particles" is not available. Nevertheless, according to the report (Sellafield, 2017), almost 19% of "hot particles" have diameters more than 2 mm (such particles are classified as "objects"). It is easy to find from expression (3) that for relatively large particles with diameters 0.5 – 1 mm, residence time in the water column will be 0.4 – 1.6 seconds. Even for "very fine sand" (Krumbein & Aberdeen, 1937) with diameters 62.5–125 µm, this residence time will be approximately 7 – 27 min. Only particles with diameters less than 0.9 µm will have a residence time in the water column for more than 500 hours.

Based on the present assessment and acknowledging the approximations used in this approach, an assumption that almost all particles will reach the bottom sediment before they can reach the boundaries of the Cumbrian waters box seems reasonable. As such, the assumption of particles releasing directly into the sediment will be used as the release scenario for the "hot particles".

Further, unlike the usual process of absorption and desorption of radioactivity on the surface of the suspended sediment particles in the water column, "hot particles" may include radioactivity within their bodies as soon as they come into the marine environment. Therefore, "apparent" K_d for the "hot particles" can be much higher than similar K_d for the usual particles suspended in the water column and sediment. For the following calculations values of $2 \cdot 10^4$ $m^3 t^{-1}$ and $5 \cdot 10^6$ $m^3 t^{-1}$ have selected for Cs-137 and Am-241, respectively. It is important to note that the set of other environmental parameters $\vec{a}_\mu$ is the same as those selected based on the liquid discharges.

8.3.3.2 Results for "hot particles" activity in the intertidal beach region.

Calculations of hot particle activities in the intertidal beach region, where the monitoring program has been conducted, use the following expression:

$$A_S^{(MR)} = A_S^{(CW)} \frac{S_{MR}}{S_{CW}} P \qquad (35)$$

where $A_S^{(MR)}$ and $A_S^{(CW)}$ are predicted activities of the "hot particles" in sediment in the monitoring regions and in the Cumbrian Waters, respectively; S_{MR} and S_{CW} are areas of the monitoring regions and the Cumbrian Waters compartment, respectively; *P* is the probability that all particles in the monitoring regions have been detected (It is assumed that *P*=1 for the present calculations).

Figure 8.3-10, Figure 8.3-11 and Figure 8.3-12 show simulation results for the beach region of the "Cumbrian Waters" sediment compartment. Results corresponded to the best fit for parameters $\varphi_{1L}^{(c)}$ and $\varphi_1^{(c)}$ for scenarios Sc_c1L and Sc_c1. Experimental data for the "hot particles" have been prepared based on information about the monitoring programme, published by Sellafield Ltd. Figure 8.3-10 shows results of scenarios Sc_c1L and Sc_c1.

Figure 8.3-11 shows the comparison of predicted Cs-137 activity with experimental data for Sc_c1L (top) and Sc_c1 (bottom).

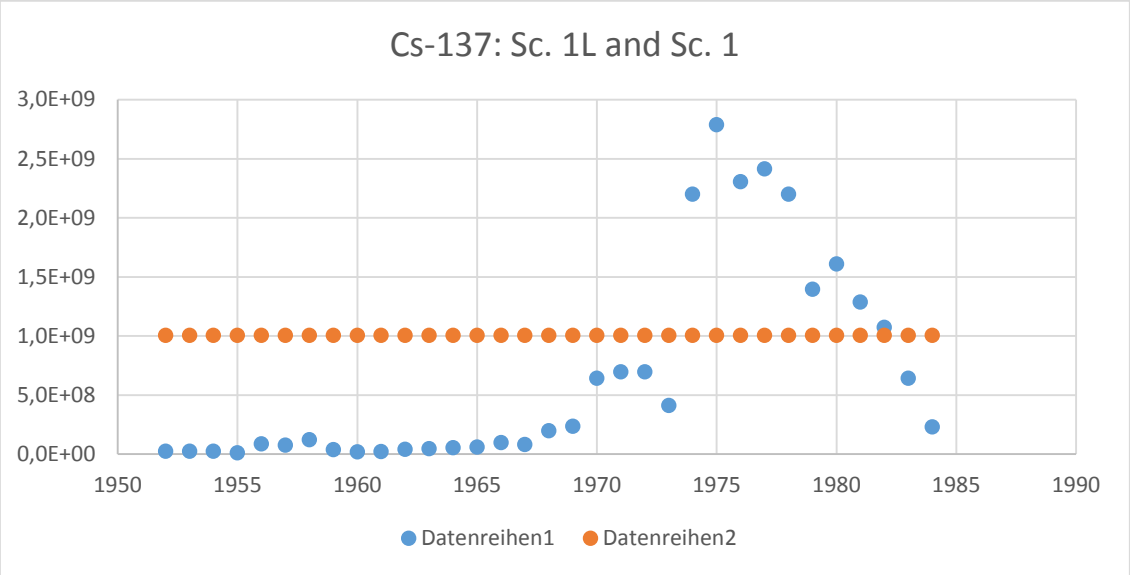

Figure 8.3-10: Scenarios Sc_c1L and Sc_c1. Activities of Cs-137 are shown in Bq.

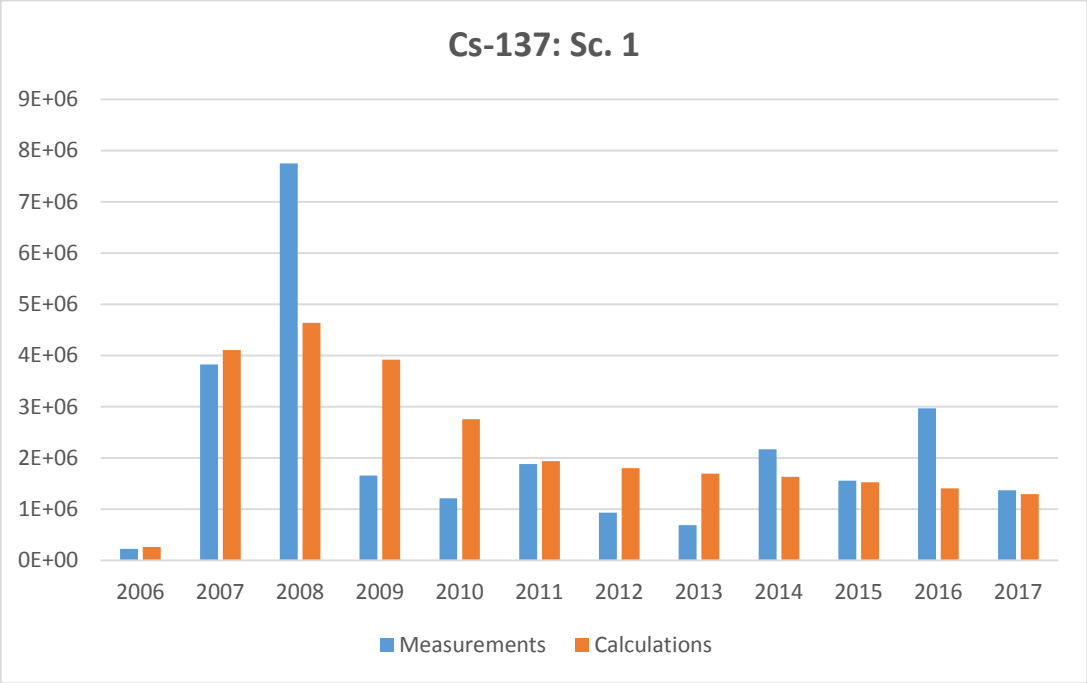

Figure 8.3-11: Comparison of the simulation results with the monitoring data for the sediment of the intertidal beach region according to scenario Sc_c1L. Activities of Cs-137 are shown in Bq.

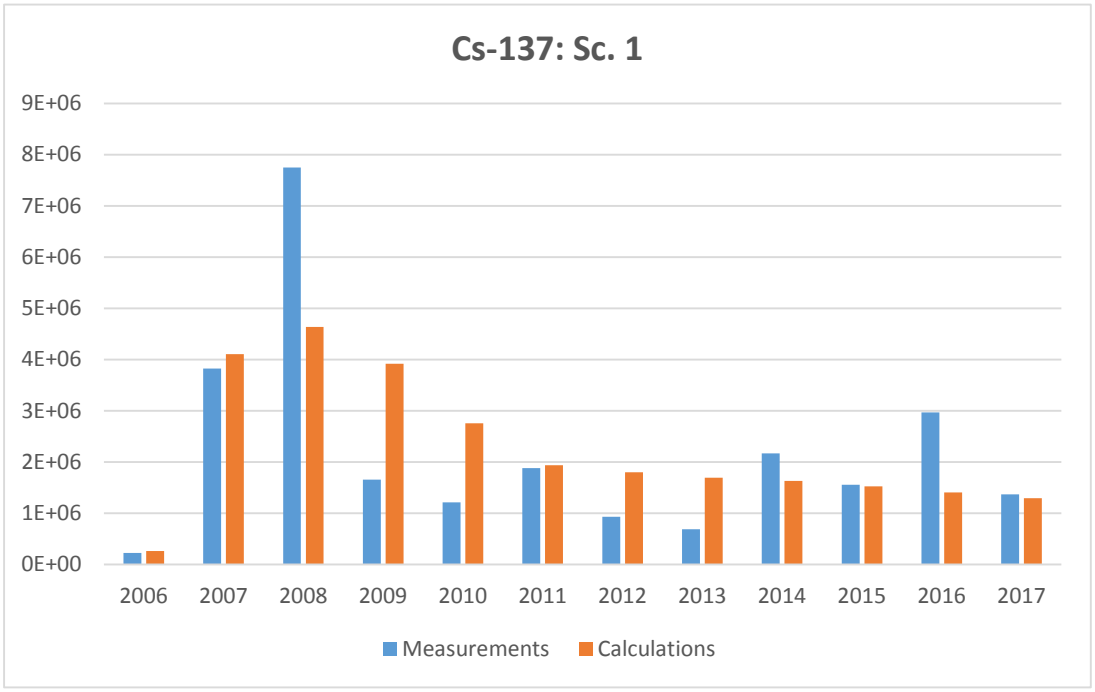

Figure 8.3-12: Comparison of the simulation results with the monitoring data for the sediment of the intertidal beach region according to scenario Sc_c1. Activities of Cs-137 are shown in Bq.

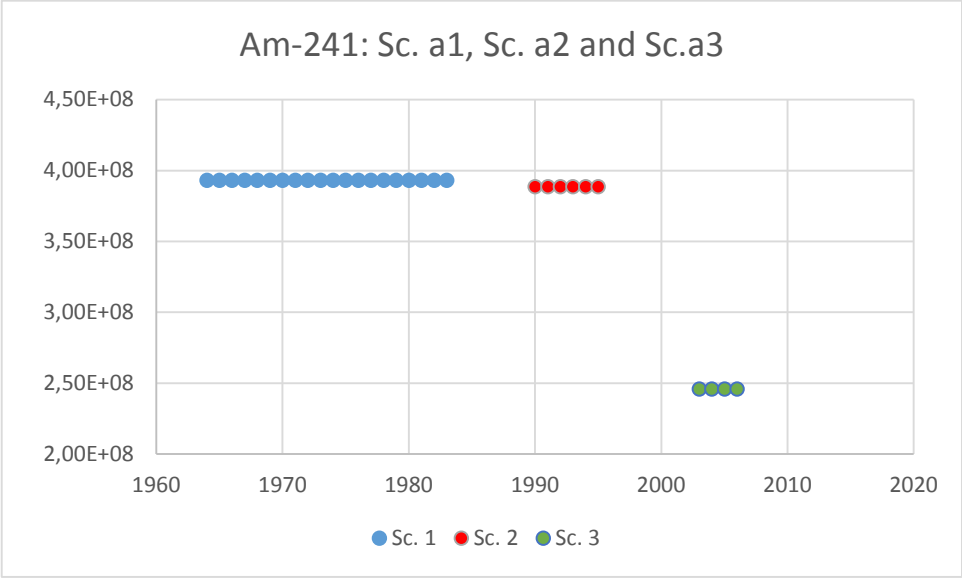

Figure 8.3-13: Scenarios Sc_a1, Sc_a2, Sc_a3. Activities of Am-241 are shown in Bq.

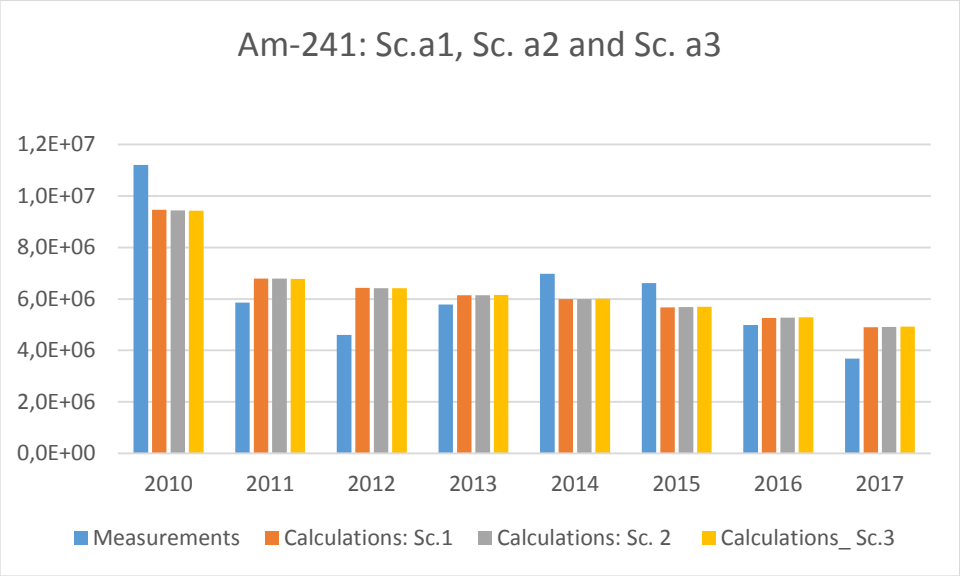

Figure 8.3-14: Comparison of the results of simulations with monitoring data for the sediment of the intertidal beach region according to scenario Sc_a1, Sc_a2 and Sc_a3. Activities of Am-241 are shown in Bq.

Figure 8.3-11, Figure 8.3-12 and Figure 8.3-14 show a reasonable agreement between experimental data.

It is important to note that according to (Sellafield, 2017), at the end of 2009 the monitoring process of "hot particles" was improved, in part with regards to the detection of particles containing Am-241. This information has cast some doubt on the possibility to assume that *P=1* in Figure 8.3-14 before 2010. Therefore, Figure 8.3-14 shows comparisons between prediction and monitoring data for Am-241, but only for experimental data from the monitoring program after 2009.

Similar calculations have been executed for all scenarios. The best comparison with experimental data for Cs-137 corresponds to scenario Sc_c5 with the total released activity of $1.6 \cdot 10^{10}$ Bq. Similarly, the best results for Am-241 corresponds to scenarios Sc_a1 with the total released activity of $8.3 \cdot 10^{9}$ Bq.

8.3.3.3 Estimation of uncertainties.

Calculations have demonstrated that very different scenarios can provide similar results because of the complexity of the model / system (Iosjpe, 2011b; Iosjpe, 2014). In such conditions, additional information about scenarios seems necessary.

As mentioned in Chapter 6, it is possible to estimate the relevance of the parameters by using the global sensitivity index (Hamby, 1994; Saltelli et al., 2008):

$$S^{(G)}(P) = 1 - \frac{P^{(S)}_{min}}{P^{(S)}_{max}} \quad (36)$$

where $P^{(S)}_{min}$ and $P^{(S)}_{max}$ are minimum and maximum absolute values of the state parameter $P^{(S)}$ within the range of parameter P, which have been described in Equation (32). According to construction, $S^{(G)} = 0$, when there is no influence of the evaluated parameters to the state parameter. $S^{(G)} = 1$, when evaluated parameter has strongest influence to the state parameter.

$P^{(S)}_{min}$ and $P^{(S)}_{max}$ can be estimated with help of the local sensitivity indices. One example for the Am-241 hot particles is shown in Figure 8.3-15.

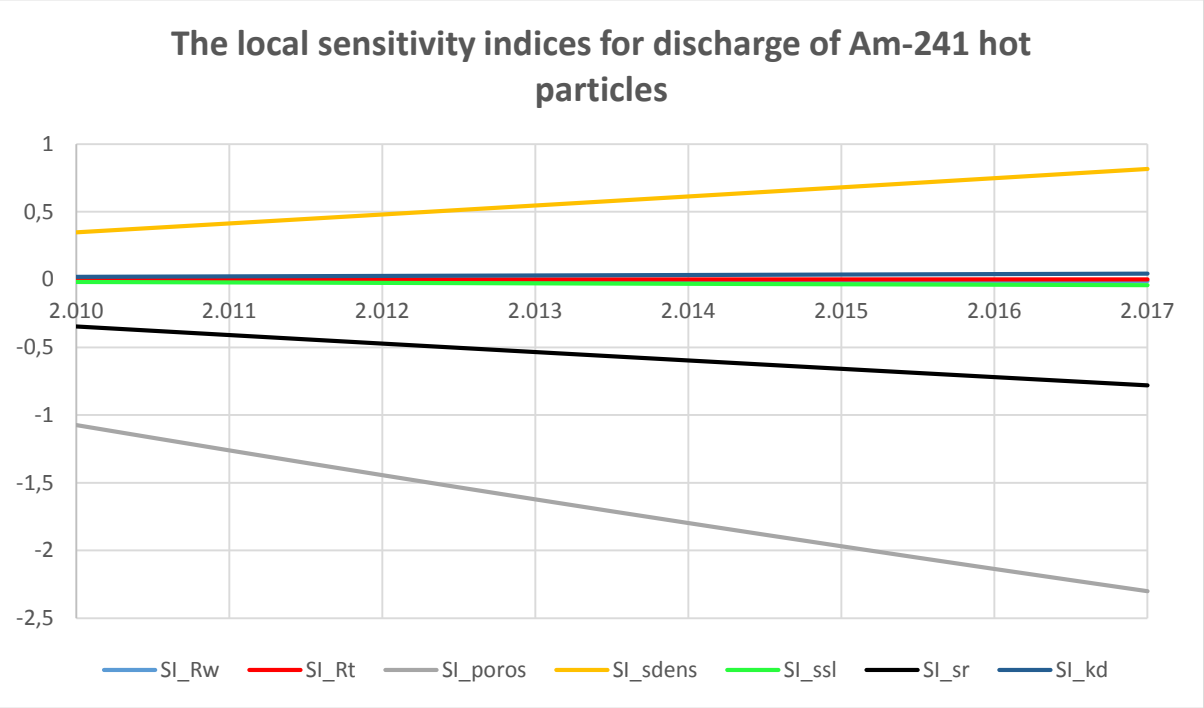

Figure 8.3-15: Influence of the model parameters to average concentration per year for Am-241.

Further, the most suitable set of the environmental model parameters has been selected. Therefore, the range for the parameters has been chosen to be 10%, similar to (Nielsen et al., 1997). The range for the apparent sediment distribution coefficient has been chosen from standard K_{d0} by to K_{d0}·10 according to recommendation from (IAEA, 2004).

Calculations for Cs-137 indicate that the global sensitivity index $S^{(G)}_p$ is $S^{(G)}_p = 0.928$, which is associated with parameters' uncertainties for the best release scenario for Cs-137. The global sensitivity index $S^{(G)}_{Sc}$ is $S^{(G)}_{Sc} = 0.987$ and is associated with scenario uncertainty. The total release for the Cs-137 can be estimated in the range $6.9 \cdot 10^8 < 1.6 \cdot 10^{10} < 7.6 \cdot 10^{10}$ Bq.

The calculated global sensitivity index $S^{(G)}$ associated with parameters' uncertainties for the best release scenario and for scenario uncertainty for Cs-137 is $S^{(G)} = 0.991$.

Similarly, the calculated global sensitivity index $S^{(G)}_p$ associated with parameters' uncertainties for the best release scenario for Am-241 is $S^{(G)}_p = 0.921$, whereas the index $S^{(G)}_{Sc} = 0.897$ is associated with scenario uncertainty. The total release for Am-241 can be estimated in the range $9.8 \cdot 10^8 < 8.3 \cdot 10^9 < 4.4 \cdot 10^{10}$ Bq.

The calculated global sensitivity index $S^{(G)}$ associated with parameters' uncertainties for the best release scenario and for scenario uncertainties for Am-241 is $S^{(G)} = 0.978$.

These results show that to assess the overall activity for the best release scenarios it is important to assess the uncertainties associated with both the model parameters and the choice of a possible release scenario.

8.3.3.4 Conclusion

A specific regional model for the Cumbrian Waters (AMIS) has been constructed to investigate the fate of radionuclides (especially those associated with “hot particles”) in the intertidal beach region near the Sellafield nuclear facilities. Corroboration of the model has been provided based on the comparison of the results of the calculations with experimental data for the liquid discharges of Cs-137, Pu-239 and Am-241 into the Cumbrian waters.

Assumptions for the release scenarios for Cs-137 and Am-241 associated with “hot particles” have been proposed. The comparison of the results of the calculations with monitoring data for “hot particles” demonstrates that the present modelling approach for the constructed regional model can be used to quantify the fate of the “hot particles” after long-term exposure in the intertidal beach region.

Sensitivity analysis has been used for the evaluation of the influence of the model parameters to the end points of modelling and selection of the suitable environmental parameters.

The uncertainty analysis was used to estimate the released total activity of the Cs-137 and Am-241 hot particles. The results show that to assess the overall activity for the best release scenarios it is important to assess the uncertainties associated with both the model parameters and the choice of a possible release scenario.

8.4 Characterisation of conceptual model uncertainty for the quantification of radioecaesium contamination in wild boar and wet deposition of airborne radionuclides.

In this section a description of two cases in radioecology in which conceptual model uncertainty plays an important role is provided. The first case deals with the impact that using a simple model structure (transfer factor) compared to a more complex structure has on the prediction of wild boar meat contamination due to radiocaesium from the Chernobyl accident. The second example deals with the impact that two different model structures, which are obtained by accounting either for equilibrium or for kinetic assumptions, have on the quantification of wet interception of radionuclides. In the first example a description of how correlations among parameters is implemented in the more complex model is also provided. In the second example, one method (introduced in Section 7.2) to quantitatively deal with conceptual model uncertainty is applied.

8.4.1 Quantification of radiocaesium contamination in wild boar meat.

The contamination levels of wild boar meat with Cs-137 in the Bavarian Forest show a very characteristic frequency distribution. Contamination values for the Bavarian Forest are shown in Figure 8.4-1. The reported values vary by about two orders of magnitude while the peak values are higher than 10.000 Bq kg^{-1} fw. The process leading to this large variation is the stochastic nature of the uptake of highly contaminated food items by the wild boar (deer truffle). Deer truffles are highly contaminated fungi which account for a small percentage of the total food intake. Nevertheless, due to their extremely variable and sometimes high contamination, deer truffles account almost exclusively for the total intake of Cs-137 of the wild boars.

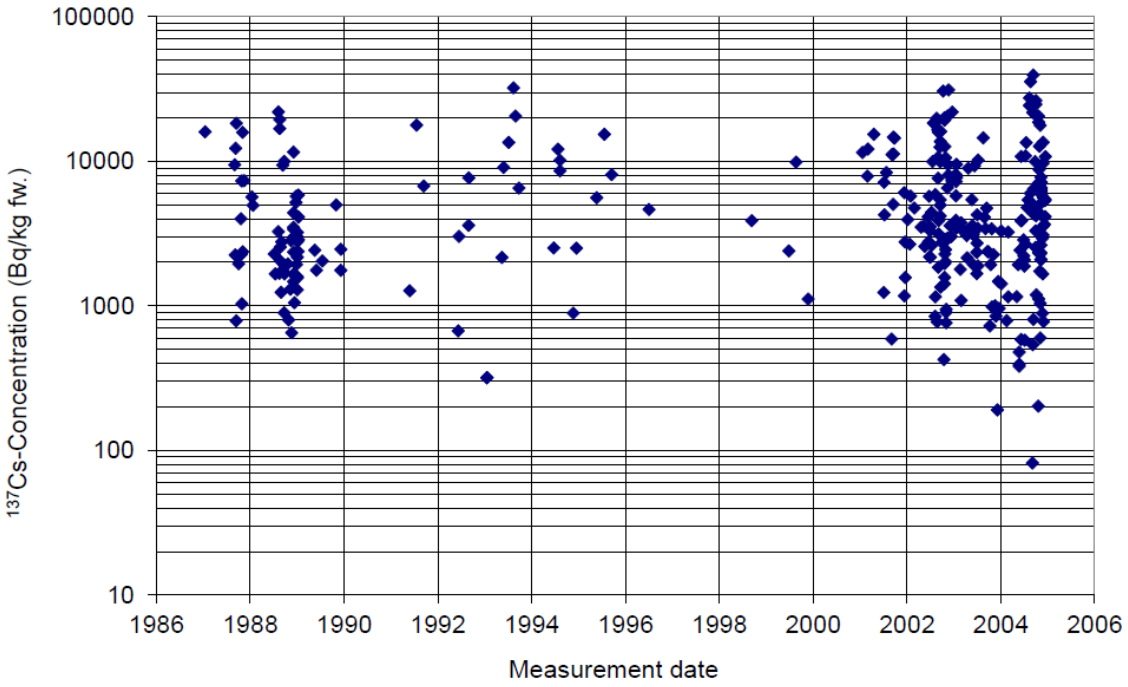

Figure 8.4-1: Wild boar contamination in the Bavarian Forest between 1987 and 2005.

One common way to quantify contamination of radiocaesium in food is the use of the so-called aggregated transfer factors (Diener et al., 2017). The contamination values for wild boar are then calculated as follows:

$$C_{boar} = T_{agg} \cdot C_{surface} \quad (37)$$

where T_{agg} is the aggregated transfer factor in $m^2 kg^{-1}$ and $C_{surface}$ is surface contamination in $Bq\ m^{-2}$. A schematic visualisation of the model is given in Figure 8.4-2.

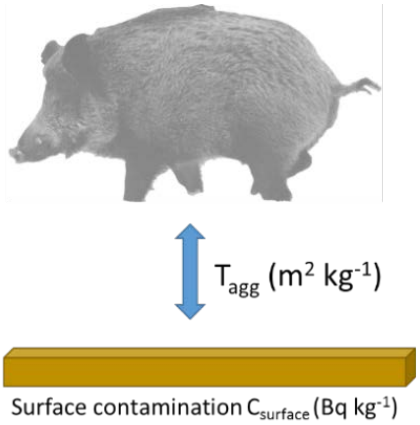

Figure 8.4-2: Schematic visualisation of the aggregated transfer model

However, due to its non-stochastic nature, the aggregated transfer factor model always gives a point estimate and cannot reproduce the distribution of contamination values for wild boar meat. In other words, by applying such a simple model and, hence such a simple mathematical structure, it is not possible to predict the large variability of the radiocaesium concentration in wild boar meat: the extremely simplified model structure causes large uncertainty in model predictions.

On the other hand, a process-based model is available (Hartmann et al., 2016) which can reproduce the distribution of contamination values for wild boar and which delivers results with considerable less uncertainty. In this model the variability of the contamination of deer truffles, the variability of the consumption of said deer truffles and the variability of the mass of the animals is considered.

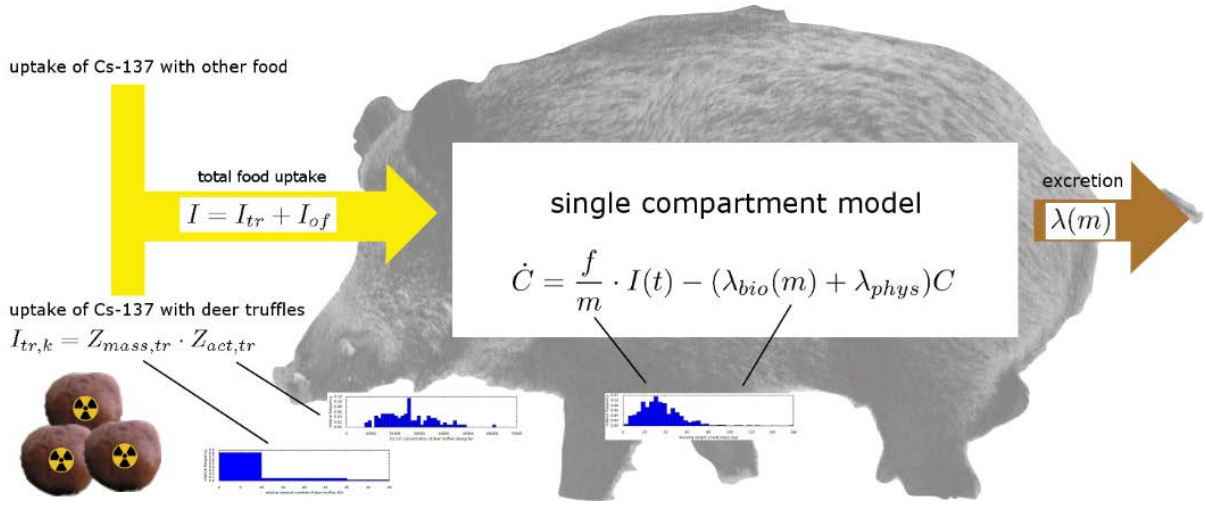

Figure 8.4-3: Schematic of the process oriented model for wild boar contamination with Cs-137.

The activity *A* of Cs-137 in a wild boar is expressed by a one-compartment-model:

$$\dot{\mathrm{A}} = \mathrm{f} \cdot \mathrm{I(t)} - (\lambda_{\mathrm{bio}} + \lambda_{\mathrm{phys}}) \cdot \mathrm{A} \tag{38}$$

where A(t) is the activity of Cs-137 in wild boar (Bq), I(t) is the intake rate of Cs-137 (Bq d^{-1}), *f* is the fraction of Cs-137 absorbed in the gastro-intestinal tract, $\lambda_{\mathrm{bio}} = \ln 2 \cdot \mathrm{T}_{\mathrm{bio}}^{-1}$ is the rate constant for the excretion of Cs-137 (d^{-1}) and $\lambda_{\mathrm{phys}} = \ln 2 \cdot \mathrm{T}_{\mathrm{phys}}^{-1}$ is the rate constant for the physical decay of Cs-137 (d^{-1}). $\mathrm{T}_{\mathrm{bio}}$ is the biological and $\mathrm{T}_{\mathrm{phys}}$ is the physical half-life of CS-137. Considering the body mass m, the concentration C of Cs-137 in wild boars can be expressed by:

$$\dot{\mathrm{C}} = \frac{1}{\mathrm{m}} \mathrm{f} \cdot \mathrm{I(t)} - \lambda \cdot \mathrm{C} \tag{39}$$

with $\lambda = \lambda_{bio} + \lambda_{phys}$ and C given in Bq kg^{-1} fw. Deer truffles are taken up irregularly. In the model, the total intake rate of Cs-137 is approximated by a stochastic term I_{tr} (*tr* = truffles) representing the intake of Cs-137 via deer truffles and a constant value I_{of} (*of* = other food) representing the contribution of all other food items:

$$\mathrm{I(t)} = \mathrm{I_{tr}(t)} + \mathrm{I_{of}} \tag{40}$$

Food uptake is considered as a time-discrete process, where food is taken up once per day at points in time $\mathrm{t_k} = \mathrm{k} \cdot \Delta\mathrm{t}$:

$$\mathrm{I} = \sum_{\mathrm{k}} (\mathrm{I_{tr,k}} + \mathrm{I_{of}}) \cdot \delta(\mathrm{t} - \mathrm{t_k}) \tag{41}$$

with $\Delta t = 1$ d. Within the approach, food uptake is modelled as discrete events leading to an intake of Cs-137 according to a specific distribution. The contribution to the radiocaesium intake by deer truffles can be written as the product of two random variables:

$$\mathrm{I_{tr,k}} = \mathrm{Z_{mass,tr,k}} \cdot \mathrm{Z_{act,tr,k}} \tag{42}$$

$Z_{mass,tr}$ is a random variable describing the frequency distribution of the mass of deer truffles (kg) taken up per day and $Z_{act,tr}$ is a random variable describing the frequency distribution of the activity concentration of deer truffles (Bq kg^{-1} fw).

While the food uptake varies over time, the mass m of the animals is considered to be constant over time and different for each individual wild boar. In the model, the mass of the animal has two effects on the value of C: the mass of the animal has a "diluting" effect on the specific activity of the meat and it has an effect on the biological half-life. According to (Fielitz, 2005), the biological half-life of wild boars has been calculated using the following allometric relation:

$$T_{biol} = 3.5 \cdot m^{0.24} \quad (43)$$

with T_{biol} and m given in days and grams, respectively. It should be highlighted that, in the model, the mass *m* is a random variable and therefore the biological half-life T_{biol} differs for each animal.

For the calculation of the model results, statistical distributions from measurements for stomach content, radiocaesium contamination of deer truffles and animal mass were used as an input. In Table 8.4-1, statistical properties of the model simulations using the process oriented approach and the measured values are shown (Hartmann et al., 2016). For the model results, statistical properties are shown for the complete set of model results as well as for two distinct sets of heavier and lighter animals. It can be observed, that the median value as well as the 95th percentile of the modelling results are in comparably good agreement with the measurements.

Table 8.4-1: Results of model simulations and measurements (Bq kg^{-1} fw) using the process oriented approach.

	Model simulations			Measurements*
	All animals	$m > 15$ kg	$m \leq 15$ kg	
sample size	-	-	-	169
expected value	7.757	6.843	19.247	6.217
median	6.597	6.126	18.376	3.424
variance	18.774	5.808	39.203	53.821
coefficient of variation	0.56	0.35	0.33	1.18
5th percentile	3.801	3.747	13.039	582
95th percentile	16.294	11.545	27.702	21.886

*Measured values from January 2002 until beginning of October 2004

In the process-based model for quantifying radiocaesium contamination of wild boar meat, parameters are selected in a way that either their correlation is minimised (hence can be neglected as mentioned in Section 5.3) or their correlation is accounted for via a functional dependence.

In the process-based model for radiocaesium contamination in wild boar following assumptions on correlations are made:

- the Cs-137 activity in meat is weakly correlated with the ingested amount of food since Cs-137 activity is mainly due to truffles which are only a limited amount of food intake;
- the caloric intake is not correlated with the weight of the animal since truffles do not contribute largely to the caloric intake;
- the correlation between the mass and the biological decay is considered via Equation (43).

These assumption hold if mast years[2] are not considered and if the area where the animals look for food is not very large.

To conclude the present case study shows that if conceptual model uncertainty is not accounted for the predictions of the transfer factor model can be misleading since (long-term) variability of radiocaesium concentration in wild boar meat cannot be quantified with a reasonable level of uncertainty. In addition the test case shows that correlations can be accounted for in a simple and straightforward way as long as processes and parameters involved are chosen appropriately.

[2] i.e. A mast year is when the trees that produce fruits like acorns and beech seeds have a bumper crop and produce much more fruit than they normally would. In this situation wild boars eat more of these fruit and hence intake of other food items is diminished.

8.4.2 Application of a methodology for quantifying conceptual model uncertainty to equilibrium and kinetic models for interception of wet-deposited radionuclides on plants.

Although in radioecology conceptual model uncertainty has not been quantified so far, systematic analysis of parameter uncertainty and quantification of total uncertainty has been already carried out. The work of (Gonze & Sy, 2016; Skipperud et al., 2017; Sy et al., 2016) for modelling wet interception, dry interception and weathering respectively provide an example of estimating parameter uncertainty and evaluating model performance. As already mentioned in Section 7.2.2, these quantities are often a pre-requisite for quantifying conceptual model uncertainty. Based on the methodology proposed in Section 7.2.4 Point 1b, the quantification of conceptual model uncertainty related to the equilibrium and kinetic models developed in (Gonze & Sy, 2016) is here carried out.

8.4.2.1 Interception of wet deposited radionuclides

Wet interception of radionuclides occurs when airborne contamination and contaminants (e.g. radionuclides) are entrained in rain droplets and washed off onto the plant-soil system (Figure 8.4-4). Quantification of the amount of radionuclides deposited onto the plant is of relevance to determine the level of contamination expected for crops or other vegetation.

Figure 8.4-4: Wet interception process

The so-called mass interception factor f_B is introduced to quantify such amount and is defined as the ratio between the amount of pollutant retained by the plant surface (e.g. activity *A* in Bq) and the total amount of pollutant deposited onto the plant-soil system normalised to the standing biomass density *B* (kg d.w. m^{-2}):

$$f_B = (A_{total}/A_{plant})/B \quad (44)$$

The normalisation is carried out in order to acknowledge the different growth stages of the collected plants. The mass interception factor depends upon several factors, namely on:

- the plant/foliage characteristics such as the water storage capacity (L [mm]) and the capability to drain and absorb the water and the pollutant, the specific foliage area (SLA [m^2 kg^{-1} d.w.]) ,
- the precipitation characteristics such as rainfall height ([mm]), rainfall intensity ([mm h^{-1}]) ,
- the properties of the pollutants involved (in particular the valence of chemical elements) since sorption affinity is expected to increase from monovalent cations to divalent ones to inert particles. Anions do not interact as the plant surfaces are negatively charged and hence affinity is expected to be zero.

8.4.2.1.1 Equilibrium and kinetic models for wet interception

(Gonze & Sy, 2016) developed two process-based models for quantifying the mass interception factor: an equilibrium model (EM) and a kinetic model (KM). These models are the result of mass-balance equations for both water and pollutants with explicit parameterisation of the hydrological, biological and chemical mechanisms.

The two models differ in the way the interaction (absorption and drainage on the leaf) between plant surface and chemical element is parameterised. In the EM it is assumed that the interaction is instantaneous and irreversible whereas in the KM the interaction takes place at a given rate and is reversible. Hence in the EM parameterisation of these processes occurs via a concentration ratio at equilibrium (CR [mm]) whereas in the KM the parameterisation occurs in terms of absorption rate (J/K [mm h^{-1}]). Model parameters other than CR and J/K that enter the model equations are also the single-sided leaf area index (LAI [m2 m^{-2}]), the free throughfall coefficient (*p)*, the plant water storage (W [mm]), the plant water storage capacity (SC [mm]).

Details about the numerical derivations of EM and KM are available in (Gonze & Sy, 2016). The major properties of the two models are that for the EM for the interception by plants is weakly dependent on rainfall duration or intensity whereas in the KM wet interception depends more strongly on the rainfall intensity and less to rainfall height. For non-interacting elements such as iodine the EM model and KM model are identical (hence CR = 0 and J/K=0). For other elements instead it is expected that EM model and KM model perform differently depending on whether the sorption affinity is small or large.

8.4.2.1.2 Quantification of parameter uncertainty

In (Gonze & Sy, 2016) the inference of model parameters such as SLA, L, CR for EM and SLA, L, J/K for KM is carried out with a Bayesian approach. Within the Bayesian analysis framework following steps are undertaken to calibrate the model:

1. prior distributions on the set of unknown parameters are assigned,
2. the likelihood distribution function is built upon the observed data (dataset calibration) and the modelled output,
3. the Bayes' theorem is applied by using the MCMC algorithm to obtain the joint posterior distribution of all unknown parameters of the EM and KM models respectively.

In the Bayesian approach the f_B is a stochastic quantity, hence it is written in the form:

$$f_B = \mathrm{norm}(\mu, S) \tag{45}$$

where μ is the modelled output value for interception factor and S is the residual standard deviation, which accounts for the residual that is not covered by the uncertainty of the considered parameters. A normal distribution is assigned to f_B and this is a typical convention in the Bayesian methodology. The statistics (e.g. mean, median, 95% credible interval) for inferred parameters is obtained over 15000 realisations for the EM and KM model.

Within the Bayesian approach, the residual variability is accounted for as if it were an 'additional' parameter and hence its statistics is also obtained.

In Figure 8.4-5 the predicted mass interception factor versus observed mass interception factor according to the EM model are presented. Similar results are available in (Gonze & Sy, 2016) also for KM model.

In the Figure 8.4-5 the error bars quantify the 95% credible interval. These error bars are obtained by propagating the uncertainty of the parameters inferred with Bayesian analysis as well as by propagating the inferred *S*.
In the study carried out by (Gonze & Sy, 2016) the variability related to the sorption affinity of the different elements is also considered in the analysis. In fact, the EM and KM models are tested by

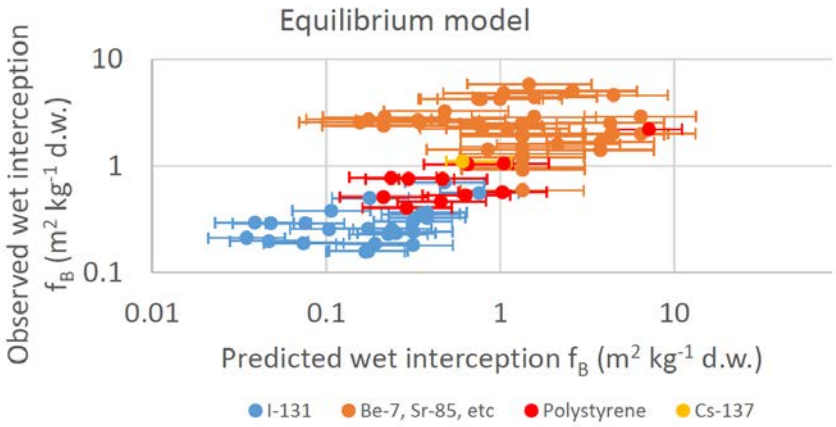

Figure 8.4-5: Observed versus predicted mass interception factor according to EM. Error bars quantify the 95% credible interval.

accounting for several different groupings of elements in order to characterise the effect of variability on the parameters' estimates. In the present study focus is on grouping GEL 2 of (Gonze & Sy, 2016), in which each type of substance is considered separately:

- I-131 (anions),
- Cs-137 (monovalent cations),
- Be-7, Cr-51, Sr-85, Cd-109, Ba-140, Pb-210 (divalent and trivalent cations),
- Polystyrene 1 and 3 (inert micronic particles).

For the grouping GEL 2, the CR and J/K that are obtained from (Gonze & Sy, 2016) are listed in Table 8.4-2.

Table 8.4-2: Median values of the posterior distributions estimated for EM and KM in (Gonze & Sy, 2016).

Model	**Estimated Parameter**	***Type of substance***			
		I	***Cs***	***Be, Sr, Cd, Cr, Ba, Pb***	***Polystyrene***
EM	CR (mm)	0	0.04	0.65	0.96
KM	J/K (mm h^{-1})	0	0.43	3.65	7.04

8.4.2.1.3 Data available for EM and KM testing

The data available for the analysis consists in a set of 363 data points used for calibrating (i.e.

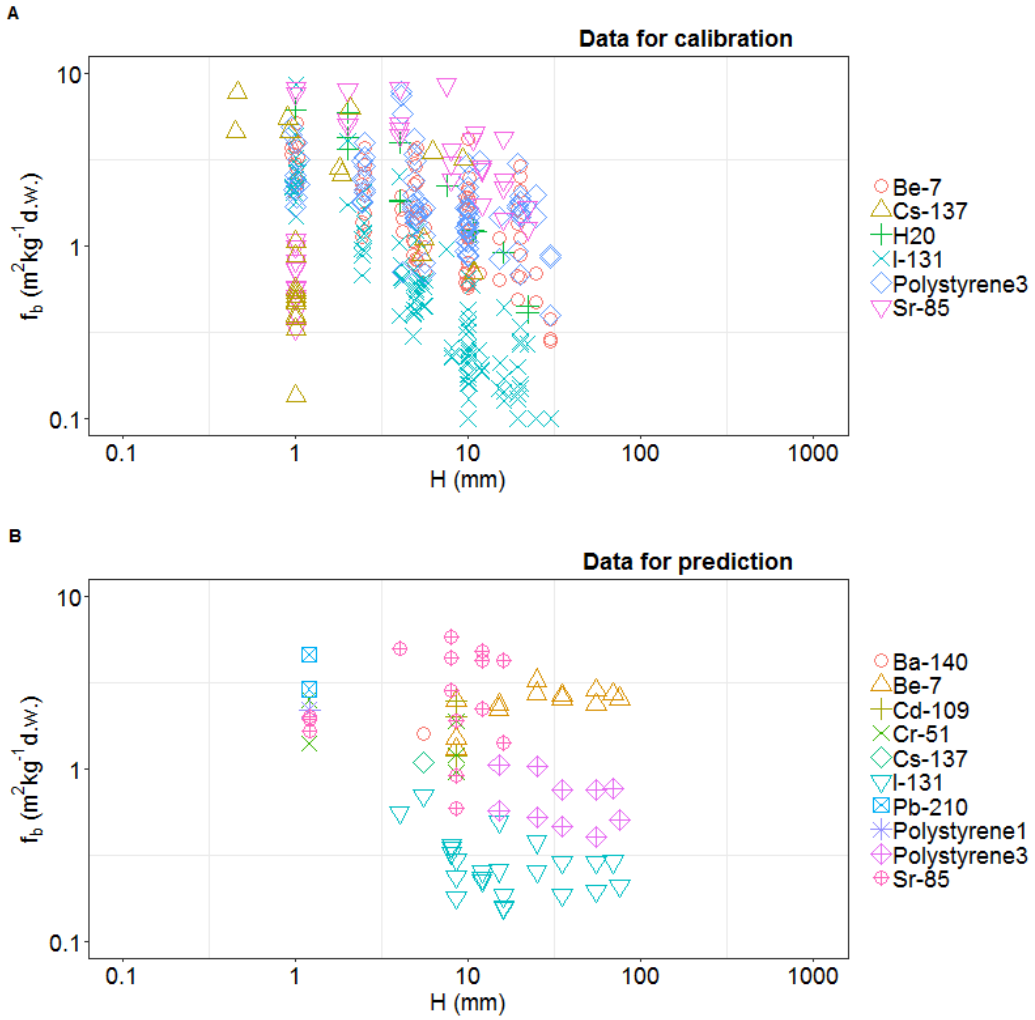

Figure 8.4-6: Available data for wet interception used for calibration (A) and validation (B) of the EM and KM in (Gonze & Sy, 2016).

parameter inference) the EM and KM models (Figure 8.4-6 A) and a set of 77 data points for prediction (Figure 8.4-6 B). The data sets are a collection from various controlled experiments carried out over the years 1974-2014, which include various pollutants (radionuclides), water (H_20) and inert micronic particles (polystyrene) and various types of plants and precipitation characteristics (rainfall height H, rainfall intensity *I*, intermittent rainfall) and biomass density B. The data set available is rather large and comprises ranges of situations that are well suited for the testing of the EM and KM.

The data set for calibration is rather complete and has information available not only about f_B but also about *I* and *H* whereas the data set for prediction misses information on *B* or *I*, which needed to be artificially generated from the calibration data set. Evaporation conditions could not be estimated for the experiments. Hence the models were tested for two "extreme" conditions: a high evaporation rate E_0 = 0.6 mm h^{-1} and no evaporating conditions (E_0 = 0 mm h^{-1}). Since the case with high evaporating conditions produced better results in (Gonze & Sy, 2016), in the present study the assumption E_0 = 0.6 mm h^{-1} is adopted. The model parameters SLA, L, CR and J/K are obtained through model calibration whereas *L* and *p* are set to L=0.3 mm and p=1 respectively.

In Figure 8.4-6 A the general decrease of the mass interception fraction f_B as the rainfall height increases can be observed. This is in agreement with the expectations because once the total water storage capacity of the plant is reached there is a decrease in interception. In Figure 8.4-6 B however it can be observed that this is not the case for some data points on the right side of the plot (some data points referring to Be-7, I-131, Polystyrene 3) which refer to experiments in which rainfall was intermittent.

8.4.2.1.4 Testing of EM and KM performance

Quantification of model performance is carried out by using the Deviance-Information-Criterion (DIC) introduced by (Spiegelhalter et al., 2002) which is a Bayesian alternative to the AIC criteria. The 95% credibility intervals of the model outputs are calculated by means of posterior predictive loss criterion (PPLC) (Gelfand & Ghosh, 1998). The PPLC measures the gap between the observations and the corresponding predictions.
The results of the performance testing with data for calibration confirm the sorption affinity rule mentioned in the introductory part of Section 8.4.2.1: inert particles interact more with the leaf surfaces than divalent cations which themselves are more reactive than monovalent cations. Also EM and KM provide drastically different predictions for cations and inert particles and since sensitivity to rainfall intensity is greater for less reactive substances like monovalent cations (Cs), KM performs better. In general KM predictions for reactive substances are more accurate than EM's. In particular, for divalent cations KM has smaller variance. For all substances taken together, the 95% credible interval encompasses 94% of observations. The authors conclude that the behavior of cations and of micronic particles is better represented by a kinetic absorption model (KM).
Results with data for predictions show that KM model performs well apart from intermittent rainfall conditions. For this set of data the 95% credible interval encompasses 68% of observations. The EM model encompasses 49% of observations due to poorer performance for divalent and trivalent cations. Under intermittent rainfall conditions discrepancy between predicted and observed increases with the number of consecutive rainfall applications.

8.4.2.2 Material and methods for quantification of conceptual model uncertainty

8.4.2.2.1 Methodology to quantify conceptual model uncertainty

Following the methodology suggested in Section 7.2.4, the accumulated conceptual model uncertainty of EM and KM is quantified as the difference between the model output with propagated parameter uncertainty and propagated *S* and model output with only propagated parameter uncertainty. The main assumption of the present study is that the uncertainties are additive and that they are uncorrelated. In this way the propagated conceptual model uncertainty on the model output $\sigma_{CU}(f_B)$ is the residual term *S*, which can be obtained for each predictive data point in analogy to Equation (30) as:

$$\sigma_{CU}(f_B) = \sqrt{\sigma^2_{TOT}(f_B) - \sigma^2_{PU}(f_B)} \quad (46)$$

where $\sigma_{TOT}(f_B)$ is the total uncertainty of the model output and $\sigma_{PU}(f_B)$ is the parameter uncertainty propagated to the model output.

To quantify the conceptual model uncertainty the posterior distributions as well as the cumulative distributions are graphically compared for each predictive data point (cf. Figure 8.4-6 B) and for EM and KM separately. In particular conceptual model uncertainty is quantified by comparing the distributions obtained with both propagated parameter uncertainty and *S* and the distributions obtained only with the propagated parameter uncertainty. The 95% credible intervals of model output

obtained with and without propagation of conceptual model uncertainty are also produced and compared in form of error bars.

8.4.2.3 Results

The analysis on conceptual model uncertainty is applied to the 77 predictive data points. As already mentioned, the EM and KM behave identically for non-interacting substances like I-131. Hence for this element the comparison between posterior distributions with and without *S* is shown for I-131 and for KM (being valid for EM too). In Figure 8.4-7 it can be observed that total uncertainty is higher when conceptual model uncertainty is accounted for.

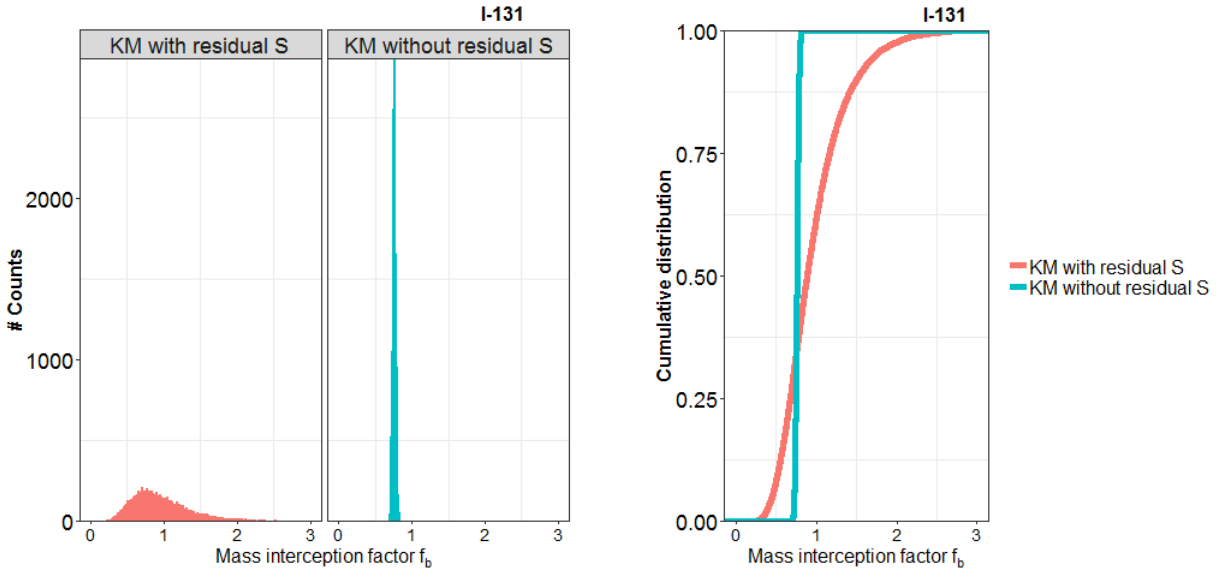

Figure 8.4-7: Posterior distributions with S and without S for KM (left). Cumulative distributions with S and without S for KM (right).

For other particles than I-131, EM and KM models perform differently. For various data points and various types of elements (e.g. for the cations Cd-109, Be-7 and Sr-85) the error bars with and without considering *S* are shown in Figure 8.4-8. The difference between the error bars is an alternative quantification of the conceptual model uncertainty for EM and KM to comparison of PDFs and CDFs. For interacting elements, like the divalent and trivalent cations shown in Figure 8.4-8, the EM has a larger conceptual model uncertainty than the KM. Not by all data points conceptual model uncertainty for KM is smaller than for as this will depend on the performance of the considered model with respect to the specific data point. In general it is observed that the conceptual model uncertainty is larger than the parameter uncertainty.

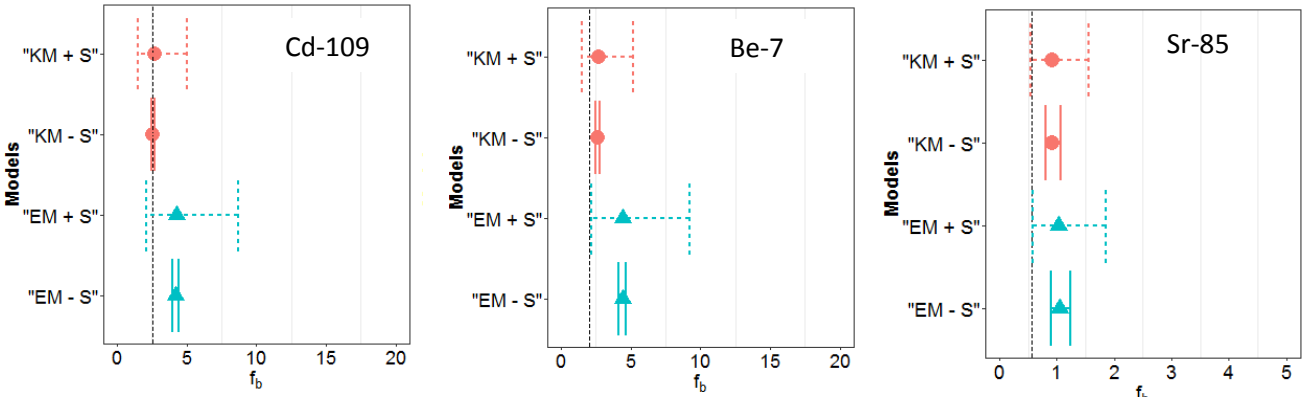

Figure 8.4-8: Predicted mass interception fraction according to EM and EM with propagated conceptual model uncertainty (EM +S; KM+S) and with propagated parameter uncertainty only (EM – S; KM – S). Three data points are shown as an example. Error bars quantify 95% credible intervals. The dotted vertical line indicates the observed mass interception factors.

In the present study a methodology to quantify conceptual model uncertainty has been tested for an equilibrium and a kinetic model developed for quantifying the interception of wet deposited radionuclides.

In the case of EM and KM the conceptual model uncertainty originates in simplification of mathematical formulation of drainage and fixation mechanisms.

In the present study the conceptual model uncertainty is obtained as the difference between the total uncertainty on the predicted model output (obtained from residual analysis) and propagated parameter uncertainty to the model output. The conceptual model uncertainty is the residual difference *S*, obtained from the Bayesian parameter inference analysis.

For each type of particle, the posterior distributions obtained by propagating only parameter uncertainty and both parameter uncertainty and S are obtained and compared.

In general the KM provides a smaller conceptual uncertainty than the EM model (as in general KM performs better than EM). However this depends on valence of the element considered and on the quality of data (i.e. intermittent rain conditions). It is interesting to notice that the total uncertainty budget is larger when conceptual model uncertainty is included.

Two important assumptions underlie the methodology used, namely that data available is adequate and representative of the process under analysis and that parameter uncertainty and conceptual model uncertainty are additive and propagate independently to the model output.

Further steps will be carried out for developing this methodology further, namely:

- to use/develop a metric for distances between probability distributions with all data points (e.g. Kolmogorov-Smirnov test) to quantify the difference between probability distributions.
- to use box plots for inter-quantiles to analyse more in detail the shape of the distributions.

The software tools used for this study is *R* for model implementations and descriptive statistics and R/JAGS for MC simulations (cf. Chapter 10).

8.5 Non-mathematical approach for dealing with uncertainties

In this section, we describe how the NUA and PUA (cf. Section 5.5 for definitions) were applied to improve the advance soil-vegetation-atmosphere ECOFOR model as applied to the Belgian NORM observatory site which is part of TERRITORIES.

8.5.1 Brief introduction of the ECOFOR model

ECOFOR is a model designed to investigate the transfer of radionuclides from an initial atmospheric deposition or from an underground source to vegetation (the model is set-up for pine trees) followed by further translocation to the various structural components of the tree and cycling back to the ground. ECOFOR aims to simplify the hydrological problem by assuming a quasi-steady-state of laminar water flow in a 10-layer heterogeneous soil column with key parameters being porosity, field capacity and a variable (saturation-dependent) hydraulic conductivity. A 'tipping bucket' approach is used whereupon soil layers fill and empty as adjacent layers become filled with water (for extensive description of the ECOFOR model cf. (Søvik et al., 2017))

The vertical transport from above into deeper soil regions is simplified with the Darcy down-flow equation. Capillary transport is described by Newton dynamics' equation for a viscous non-compressible liquid, assuming quasi-steady Poiseuille flow. Plant root water uptake is represented by an exponential root water uptake model that considers root uptake balanced against evapotranspiration. The vertical transport of water within the tree is modelled as the ascent of xylem across a hydraulic potential gradient (Poiseuille equation), while phloem (sucrose) downward transport from leaves back to roots is described as resulting from a downward osmotic pressure gradient. Soil drying (wilting point) and waterlogging (anaerobiosis) are considered. The movement of solutes with respect to water in the soil compartments is assumed to be proportional to retardation, which relates to the empirical parameter K_d. In the plant, selectivity coefficients are applied to calculate the “biological retardation” of solutes with respect to the water fluxes, and it is assumed that radionuclide fluxes can be coupled to element analogue fluxes (Casadesus et al., 2008).

A basic representation of the hydrological and plant parts of the model is given in Figure 8.5-1, and the main parameters are described elsewhere (Vives i Batlle et al., 2014).

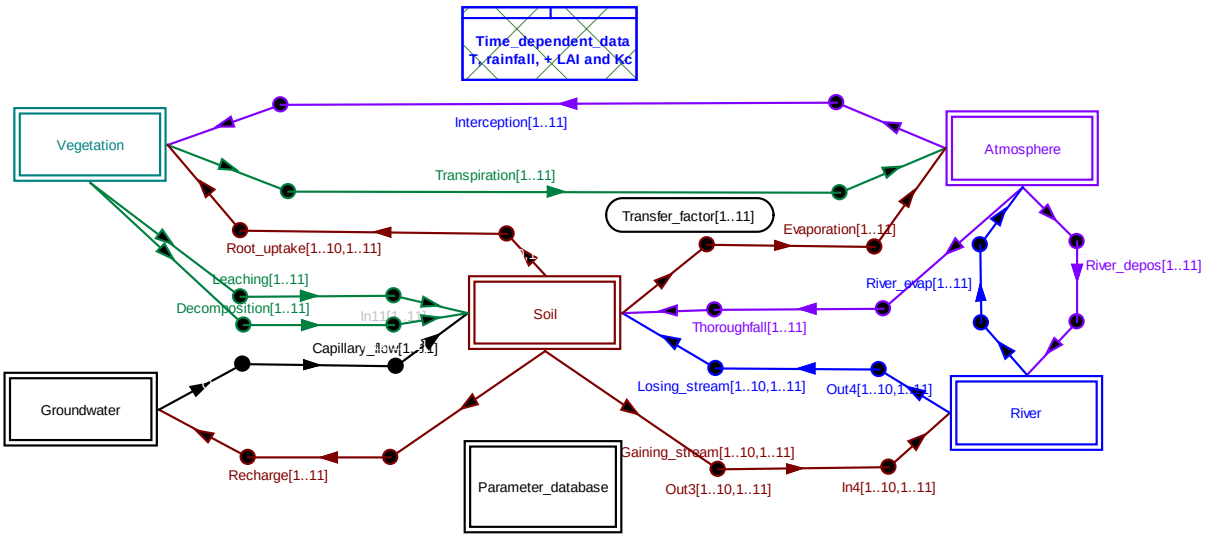

Figure 8.5-1 A basic description of the ECOFOR model

8.5.2 Non-statistical uncertainty analysis

Input parameter values of the model were altered and study the subsequent changes in model output in order to identify the most uncertain parameters and process. By this qualitative method, we were able to obtain valuable conclusions for the model. The essential model parameters are:

a) Plant coefficients. These included (a) time-dependent data for evapotranspiration: temperature (min/max), humidity, leaf area index (LAI), crop coefficient, solar irradiation and precipitation, (b) Selectivity coefficients (SC) for solute fluxes in the plant, and (c) interception, washout, absorption and runoff coefficients.

b) Atmospheric parameters: heat capacity of air, relative humidity, air density, atmospheric pressure, wind speed.

c) Soil parameters: field capacity, saturated hydraulic conductivity, porosity, residual water content, distribution coefficient (K_d).

d) General physics data: Surface tension and viscosity of water, gravity, ideal gas and Van'tHoff constants, acceleration of gravity.

For the hydrology part of the model, which is the most critical set of processes, the most uncertain parameters are the field capacity (FC) and hydraulic conductivity (Hc), which determine soil water hold-up capacity of the soil and the water flows upon which the rest of the model entirely depends. For the transport of elements in soil, the critical and most uncertain parameter is the distribution coefficient (K_d), controlling retardation and the exchange between available and the unavailable fractions of the radionuclides.

For the plant transport, the critical and most uncertain parameter was the selectivity of the plant for different elements. This part is not modelled explicitly as a physico-chemical process because few inputs are available: root architecture and its absorption power with respect to different elements cannot be calculated with simple equations and otherwise this part of the model would be overly complex in relation to the others. That is why we adopted the selectivity coefficients (SC) approach, and these SCs were back-fitted to the model from experimental results i.e. by calibration. In addition LAI, SC, FC and HC were able to be measured experimentally, so this left the K_d as being the most important parameter for the model for which there was difficulty making a determination.

Experimental determination of the K_d *in situ* is fraught with difficulties, due to the impossibility of extracting water from the complex sludge (CaF_2) prevalent at the NORM site (The soil is so compact that we could not mechanically press-out water). The K_d is usually a measured parameter that is obtained from laboratory experiments. Since it is difficult to obtain reproducible K_ds in laboratory experiments based on column methods, we settled for a batch-extraction method in the laboratory.

At the end of this project, with K_d determination being somewhat of an open problem for a complex soil like the sludge from the NORM site, we highlight by way of guidance other possibilities to obtain this parameter:

a) To use a geochemical modelling approach, such as the PHREEQC software, to model the K_d for the environment considered. In order to run PHREEQC model one needs to have many information about the soil properties and water solution. Not having cationic exchange capacity (CEC) and the amount of organic matter (OM) as well as not knowing details about soil mineralogy is a big limitation when using these models.

Incorporating the transport of solutes in the model in a simplified way by means of a parametric K_d approach. The IAEA Technical document 1616 (IAEA, 2009) and, particularly, the papers by Vidal et al. (Vidal et al., 2009) in this document gave us a good basis for this. We also found a particularly good review of regression relationships for many elements (Sheppard, 2011), all of which commonly take the form the following nonlinear polynomial expression:

$$\log(K_d) = A + B \cdot pH + C \cdot \log[\text{ organic carbon}] + D \cdot [clay] + E \cdot [clay] \cdot pH \quad (47)$$

8.5.3 Uncertainty analysis of the ECOFOR model

Following an initial NUA type of analysis (cf. Chapter 5), the process uncertainty analysis was implemented in ECOFOR, for which we defined the following step-wise approach:

a) Identify key processes
b) Identify the candidate mathematical equations from complex (general) to simple (reduced range of application)
c) Set-up the initial model for the required site with all processes thought to be relevant and the most general equations one can possibly use
d) Try to simplify the model by switching-on/off individual processes and keeping/eliminating those who have more/less impact. In other words, vary equations from simple to complex.
e) If the output is uncertain, choose more general equations or include more processes. If the output is good enough, then one has obtained the simplest model that is fit for purpose.

In ECOFOR, we applied the process uncertainty analysis process mainly in the simplified representation of the hydrology. In particular we used the following logic:

- Water infiltration from rainfall: we replaced this process by a switch in which excess water goes to groundwater recharge.
- Balancing hygroscopic, capillary and gravitational water: from an initial application of Richards equation, we considered a range of process simplifications ranging from the different versions of the equation (low flow velocities, relatively saturated conditions) down to simplest pure tipping bucket approach, reaching an intermediary compromise in which tipping bucket switches apply but the water velocities are not instantaneous but defined by the Lucas Washburn equation for upward capillary motion, and the Darcy law with a variable rather than saturated hydraulic conductivity for downward motion.

For the hydraulic conductivity we tried different equations ranging from the Van Genuchten, Brooks and Corey, Campell, Kendy, etc. and settled for the Kendy exponential equation for ease of computation and minimisation of parameters. The selected formula was validated by running soil water profiles as shown in the example below.

The result of PUA (cf. Chapter 5) was a more simplified and practical version of the model with the following added characteristics:

- The tipping bucket switches act now as physical barriers to the passage of water: every compartment can be donor or acceptor of a contiguous compartment leading to four in and out fluxes (two each to and from the above or below compartments).
- Simplified representation of plant transport: implementation of simple root uptake balanced against evapotranspiration (water mass conservation) with Xylem up flow and phloem down flow along the osmotic pressure gradient.

- Water interception, washout, absorption & leaching as well as litterfall and decomposition were simplified from initial processes taking into account penetration through plant stomata to simple transfer factors.
- Simplified representation of elements' linkage to water was adopted through retardation processes in soil (rather than using the complex coupling between transport and advection/diffusion equations). Selectivity coefficients (empirical) were used to link to water fluxes in plants. These were determined by model calibration.
- For the soil transport part, simple retardation was not considered sufficient; in this case the PUA went into the direction of increased complexity from the initial version of the model. For each of the 10 soil layers, we subdivided the existing soil compartment into a fraction available for exchange with pore water and an unavailable fraction, with exchange of solutes between the two fractions regulated by a reversible linear kinetic model. This now takes into account the amount of insoluble elements which gets immobilised in the soil column and does not depend on pore water movement.

The PUA process has led to an optimised ECOFOR model that requires considerably less parameters than the initial model version, and still is fit for the purpose, being able to understand the combined action of soil/vegetation/atmosphere processes for pine trees in the Belgian NORM site. This model has proved successful transferability from the Mol forest (sandy soil – fast circulation), characterised by high permeability - high H_C, heterogeneous 6-layer horizon, low FC and free drainage, to the NORM site (Phosphate CaF_2 sludge – slow circulation), characterised by nearly impermeable – low H_C, 1 humus layer + 9 homogeneous sludge layers, high FC and slow drainage.

9 Good practices for dealing with uncertainty analysis for radioecological models (recommendations).

- Concerning definitions of types of uncertainty: Be aware that there are no generally accepted definitions of types of uncertainty, and that various types of uncertainty are often interrelated, e.g., parameter and input uncertainty, conceptual model uncertainty and scenario uncertainty. Clarify what you mean when using specific terms, ideally providing contextualised definitions (read Chapter 4 for further information).
- Concerning the prioritisation of the types of uncertainty: Distinguish and discuss the various contributions to the overall uncertainty budget and prioritise them for your specific model/available data. Do not restrict yourself to only one type of uncertainty, e.g., measurement uncertainties or propagated parameter uncertainty.
- Concerning sensitivity analyses: Sensitivity analysis usually refers to parameter sensitivity analysis, i.e. the analysis to what extent the different factors/parameters influence the model output. Uncertainties due to different model structures and different types of release scenarios can be analysed in a similar way. Read Chapter 6 for further information and cf. Sections 8.2, 8.3 and 8.4 for examples.
- Concerning the quantification of parameter/input uncertainty: Be aware that selecting an inadequate probability density function (PDF) increases the uncertainty. If high percentiles of the model output(s) have to be calculated, the tails and therefore the shape of the PDFs are essential (read Chapters 6 and 7 for further information).
- Concerning the quantification of conceptual model uncertainty: Identify and discuss if key processes or input variables are excluded from the model due to gaps in knowledge or ignored for simplicity. If this type of uncertainty is neglected, uncertainty bands of model output may not be sufficiently wide. A quantitative methodology that distinguishes between the contribution of the propagated conceptual model uncertainty and propagated parameter uncertainty to the total uncertainty budget of a model should be preferred as it provides more insight into the model's features (cf. Section 7.2). Cf. Section 8.4 for an example of application of such methodology.
- Concerning the quantification of scenario uncertainty: Try to quantify the contributions to uncertainty arising from the model itself, i.e. model structure, the model parameters and the underlying assumptions (e.g. possible variability in the climate conditions assumed in the scenarios, possible range of variation of source term in Bq). This approach helps to select a reasonably simple model that is fit for purpose. Cf. Chapter 7 for further information.
- Concerning the numerical uncertainty related to the numerical approaches used to solve equations: Select appropriate numerical approaches (see Section 4.1.5) and possibly investigate this uncertainty for models involving differential equations. This is usually of minor concern in simple radioecological models (e.g. point scale, equilibrium models).
- Concerning the choice of a specific approach for quantifying uncertainties: Identify the specific requirements of the assessment task and select an easy-to-use approach (e.g. analytical, probabilistic or Bayesian approach) that is fit for purpose for quantifying uncertainties.
- Concerning the choice of different Monte Carlo methods and sampling procedures: Get acquainted with the requirements, advantages and limitations of simple random sampling, the Markov Chain Monte Carlo (MCMC) method or the LHS (Latin Hypercube sampling) method. Cf. Chapters 5, 6 and 7 for further information.
- Concerning correlations among parameters: Be aware of potential correlations between model parameters/factors/input variables and take them into account, at least by discussing them and trying to quantify them even in a simplified way. If a parameter is not sensitive, correlations with other parameters can be neglected. If several equivalent model structures are available, select the model structure that minimises parameter correlations. Approaches

enabling to account for parameter correlations in Monte Carlo methods, such as the Gaussian Copula method or the Iman-Conover method, are described in Section 5.4.3.

- Concerning input data and their representativeness: Unless the contamination is homogeneously distributed, a large set of samples are usually required to assure that the data are representative of the scenario to be reproduced or assessed. Consider discussing and analysing to what extent the data available are representative given the purpose of your assessment.
- Concerning the quantification of uncertainty if data on the endpoints of the model are not available: Identify available data sets or produce new relevant data to validate your model. Carrying out a comprehensive uncertainty analysis allows to understand the quality of the model in detail as well as the impact of its structure, its parameters and the underlying assumptions.
- Concerning the applicability of similar models in related scientific fields: Models in related scientific fields might by applied to radioecology if specific features of radioecological data such as their variability are taken into account.
- Concerning the acceptable level of uncertainty: Clarify and discuss this point together with the stakeholders as a graded approach before developing or applying a model to a given situation or assessment context.
- Concerning the use of process-based models: Be aware that process-based models, in which sensitive, strongly varying empirical parameters are replaced with ideally more robust sub-models, might help to reduce the total uncertainty budget. Sometimes such reduction is not achieved and a validation program as complete as possible should be performed, preferentially in advance of its application to real, different situations. The validation program ensures that an improvement in reducing the uncertainties and/or an improvement of the model performance is really obtained.

10 A list of software for handling uncertainty analysis for radioecological models.

In the present chapter a list is provided of software and tools that are available for dealing with radioecological models and uncertainty analysis. Some of them have been applied in the present guidance.

The tools can be categorised into:

1. Programming languages.
   The programming languages that have been most recently used within the field of radioecology are Python, R and C++.
2. Computational tools for MC calculations. For example:
   - Crystal Ball (Excel plug-in, under a license https://www.oracle.com/middleware/technologies/crystalball.html),
   - @risk (https://www.palisade.com/risk/)
   - ModelRisk (https://www.vosesoftware.com/products/modelrisk/)
   - ARGO (open software http://boozallen.github.io/argo/),
   - Monte Carlo package of CRAN-R (used under free statistical software R, https://cran.r-project.org/web/packages/MonteCarlo/index.html)
3. Radioecological Software
   Specific software for radioecological models with already implemented mathematical equations to model the behavior of radionuclides exist.
   Within the project TERRITORIES/WP1/Task 1.3 the following radioecological software/models have been used that include MC and uncertainty analysis capabilities:
   - NORMALYSA (http://project.facilia.se/normalysa/software.html)
   - CROM (ftp://ftp.ciemat.es/pub/CROM)
   - SYMBIOSE (https://www.irsn.fr/EN/Research/Scientific-tools/Computer-codes/SYMBIOSE/Pages/The-SYMBIOSE-platform-3838.aspx)
   - ERICA (http://www.erica-tool.com/)
4. Design platforms
   Mathematical models can be created using libraries already embedded in the platform. MC tools are usually available for both 1D MC and 2D MC. For example:
   - Ecolego (http://ecolego.facilia.se/ecolego/show/HomePage)
   - GoldSim (https://www.goldsim.com/web/home/)
   - Stella (https://www.iseesystems.com/)
   - Matlab (https://www.mathworks.com/products/matlab.html)
   - SimLab (https://ec.europa.eu/jrc/en/samo/simlab)

11 References

Albrecht, A., & Miquel, S. (2010). Extension of sensitivity and uncertainty analysis for long term dose assessment of high level nuclear waste disposal sites to uncertainties in the human behaviour. *Journal of Environmental Radioactivity, 101*(1), 55-67.

Alderman, P. D., & Stanfill, B. (2017). Quantifying model-structure- and parameter-driven uncertainties in spring wheat phenology prediction with Bayesian analysis. *European Journal of Agronomy, 88*, 1-9. doi: 10.1016/j.eja.2016.09.016

Ali, T., Boruah, H., & Dutta, P. (2012). Uncertainty modeling of radiological risk using probability and possibility methods. *International Journal of Computer Applications, 43*(13), 13-17.

Apostolakis, G., & Kaplan, S. (1981). Pitfalls in Risk Calculations. *Reliability Engineering, 2*(2), Pp.135-145. doi: doi:10.1016/0143-8174(81)90019-6

Arendt, P., W. Apley, D., & Chen, W. (2012). Quantification of Model Uncertainty: Calibration, Model Discrepancy, and Identifiability. *Journal of Mechanical Design, 134*, 100908. doi: 10.1115/1.4007390

Ascough, J. C., Maier, H. R., Ravalico, J. K., & Strudley, M. W. (2008). Future research challenges for incorporation of uncertainty in environmental and ecological decision-making. *Ecological Modelling, 219*(3-4), 383-399. doi: 10.1016/j.ecolmodel.2008.07.015

Barthel, R., & Thierfeldt, S. (2015). Vergleichende Betrachtung der probabilistischen/stochastischen und deterministischen Modellierung von Expositionen im Hinblick auf die Belastbarkeit des Modellergebnisses und die Anforderung an die Qualität der Eingangsdaten (Vol. 101/15): Bundesamt für Strahlenschutz (BfS).

Bastin, L., Cornford, D., Jones, R., Heuvelink, G. B. M., Pebesma, E., Stasch, C., . . . Williams, M. (2013). Managing uncertainty in integrated environmental modelling: The UncertWeb framework. *Environmental Modelling & Software, 39*, 116-134. doi: 10.1016/j.envsoft.2012.02.008

Bayes, T. (1763). An Essay towards solving a Problem in the Doctrine of Chances. *Philosophical Transactions of the Royal Society of London, 53:* , 370–418.

Beresford, N. A., Wood, M. D., Vives i Batlle, J., Yankovich, T. L., Bradshaw, C., & Willey, N. (2016). Making the most of what we have: application of extrapolation approaches in radioecological wildlife transfer models. *Journal of Environmental Radioactivity, 151*, 373-386. doi: 10.1016/j.jenvrad.2015.03.022

Bernardo, J. M. (2003). Bayesian Statistics. 47. Retrieved from EOLSS website: https://www.uv.es/~bernardo/BayesStat2.pdf

Beven, K. (2007). *Environmental modelling: An uncertain future?* : CRC press.

Bogacki, P., & Shampine, L. F. (1989). A 3 (2) pair of Runge-Kutta formulas. *Applied Mathematics Letters, 2*(4), 321-325.

Borgonovo, E. (2008). Sensitivity Analysis of Model Output with Input Constraints: A Generalized Rationale for Local Methods. . *Risk Analysis, 28*(3), pp.667-680.

Breuninger, M. I., Schachtel, G. A., Lührmann, P. M., Hartmann, B., & Neuhäuser-Berthold, M. (2003). Complex correlation structure in consumption rates of major food groups: implications for the assessment of radiation exposure. *Public Health Nutrition, 6*(1), 7.

Bukowski, J., Korn, L., & Wartenberg, D. (1995). Correlated inputs in quantitative risk assessment: The effects of distributional shape. . *Risk Analysis, 15*(2), pp.215-219.

Butts, M. B., Payne, J. T., Kristensen, M., & Madsen, H. (2004). An evaluation of the impact of model structure on hydrological modelling uncertainty for streamflow simulation. *Journal of Hydrology, 298*(1-4), 242-266. doi: 10.1016/j.hydrol.2004.03.042

Casadesus, J., Sauras-Yera, T., & Vallejo, V. R. (2008). Predicting soil-to-plant transfer of radionuclides with a mechanistic model (BioRUR). *Journal of Environmental Radioactivity, 99*(5), 864-871.

Cherubini, U., Luciano, E., & Vecchiatio, W. (2004). *Copula Methods in Finance*.

Ciecior, W., Rohlig, K. J., & Kirchner, G. (2018). Probabilistic biosphere modeling for the long-term safety assessment of geological disposal facilities for radioactive waste using first- and second-order Monte Carlo simulation. *Journal of Environmental Radioactivity, 190-191*, 10-19. doi: 10.1016/j.jenvrad.2018.04.024

Ciffroy, P., Durrieu, G., & Garnier, J.-M. (2009). Probabilistic distribution coefficients (Kds) in freshwater for radioisotopes of Ag, Am, Ba, Be, Ce, Co, Cs, I, Mn, Pu, Ra, Ru, Sb, Sr and Th – implications for uncertainty analysis of models simulating the transport of radionuclides in rivers. *Journal of Environmental Radioactivity*(100), 14.

Ciffroy, P., Siclet, F., Damois, C., Luck, M., & Duboudin, C. (2005). A dynamic model for assessing radiological consequences of routine releases in the Loire river: parameterisation and uncertainty/sensitivity analysis. *Journal of Environmental Radioactivity, 83*(1), 9-48.

Copplestone, D., Beresford, N. A., Brown, J. E., & Yankovich, T. (2013). An international database of radionuclide Concentration Ratios for wildlife: development and uses. . *Journal of Environmental Radioactivity, 126*, pp288-298.

Cox, M. G., & Siebert, B. R. L. (2006). The use of a Monte Carlo method for evaluating uncertainty and expanded uncertainty. *Metrologia, 43*(4), S178-S188. doi: doi:10.1088/0026-1394/43/4/S03

Cukier, R. I., Levine, H. B., & Shuler, K. E. (1978). Non-Linear Sensitivity Analysis of Multi-Parameter Model Systems. *Journal of Computational Physics, 26*(1), 1-42. doi: Doi 10.1016/0021-9991(78)90097-9

Cullen, A. C., & Frey, H. C. (1999). *Probabilistic Techniques in Exposure Assessment: A Handbook for Dealing with Variability and Uncertainty in Models and Inputs*: Springer US.

Diener, A., Hartmann, P., Urso, L., i Batlle, J. V., Gonze, M., Calmon, P., & Steiner, M. (2017). Approaches to modelling radioactive contaminations in forests–Overview and guidance. *Journal of Environmental Radioactivity, 178*, 203-211.

Dowdy, S., Weardon, S., & Chilko, D. (2004). *Statistics for Research*: Wiley-Interscience.

Draper, D. (1997). Assessment and Propagation of Model Uncertainty. *J R Stat Soc Series B, 57*, 45-97. doi: 10.2307/2346087

Efron, B., & Tibshirani, R. J. (1994). *An Introduction to the Bootstrap*: Taylor & Francis.

Ekstroem, P. A., & Broed, R. (2006). Sensitivity analysis methods and a biosphere test case implemented in EIKOS (pp. 84). Finland.

Elster, C. (2014). Bayesian uncertainty analysis compared with the application of the GUM and its supplements. . *Metrologia, 51* (4), S159-S166. doi: doi:10.1088/0026-1394/51/4/S159

Engeland, K., Xu, C. Y., & Gottschalk, L. (2005). Assessing uncertainties in a conceptual water balance model using Bayesian methodology. *Hydrological Sciences Journal-Journal Des Sciences Hydrologiques, 50*(1), 45-63. doi: 10.1623/hysj.50.1.45.56334

EPA, U. S. (1997). Guiding Principles for Monte Carlo Analysis. Washinton, D.C.: U.S. Environmental Agency.

EPA, U. S. (1999). Understanding variation in partition coefficient, Kd, values.

EPA, U. S. (2001). Risk Assessment Guidance for Superfund: Volume III - Part A, Process for Conducting Probabilistic Risk Assessment Washington: U.S. Environmental Protection Agency.

EPA, U. S. (2009). Guidance on the Development, Evaluation and Application of Environmental Models. Washington, D.C.: U.S. Environmental Protection Agency.

EPA, U. S. (2011). Exposure Factors Handbook 2011 Edition (Final Report). Washington, D.C.: U.S. Environmental Protection Agency.

EPA, U. S. (2014). Risk Assessment Forum White Paper: Probabilistic Risk Assessment Methods and Case Studies.

ERICA. (2007). ERICA Assessment Tool Help Function Document. Version 15.

Evans, M., Hastings, N., & Peacock, B. (2000). *Statistical Distributions* (3rd ed.): John Wiley & Sons Inc.

Ferson, S. (1994). *Naive Monte Carlo methods yield dangerous underestimates of tail probabilities.* Paper presented at the High Consequence Operations Safety Symposium, Sandia National Laboratories.

Ferson, S., & Burgman, M. (1995). Correlations, dependency bounds and extinction risks. . *Biological Conservation, 73*, pp.101 - 105.

Ferson, S., & Ginzburg, L. R. (1996). Different methods are needed to propagate ignorance and variability. . *Reliability Engineering & System Safety,, 54(2)*, pp. 133–144.

Fielitz, U. (2005). Untersuchungen zum Verhalten von Radiocäsium in Wildschweinen und anderen Biomedien des Waldes. *Abschlussbericht Forschungsvorhaben StSch, 4324*, 105.

Frey, H. C. (1992). *Quantitative Analysis of Uncertainty and Variability in Environmental Policy Making.* Paper presented at the Fellowship Program for Environmental Science and Engineering, Washington, DC.

Frey, H. C., & Patil, S. R. (2002). Identification and review of sensitivity analysis methods. *Risk Analysis, 22*(3), 553-578.

Gelfand, A. E., & Adrian, F. M. S. (1990). Sampling-Based Approaches to Calculating Marginal Densities. *Journal of the American Statistical Association, 85*(410), 398-409. doi: 10.2307/2289776

Gelfand, A. E., & Ghosh, S. K. (1998). Model choice: a minimum posterior predictive loss approach. *Biometrika, 85*(1), 1-11.

Gelman, A., Carlin, J. B., & Stern, H. S. (2003). *Bayesian Data Analysis, Second Edition*.

Girard, S., Korsakissok, I., & Mallet, V. (2014). Screening sensitivity analysis of a radionuclides atmospheric dispersion model applied to the Fukushima disaster. *Atmospheric Environment, 95*, 490-500. doi: 10.1016/j.atmosenv.2014.07.010

Gonze, M.-A., Mourlon, C., Calmon, P., Manach, E., Debayle, C., & Baccou, J. (2016). Modelling the dynamics of ambient dose rates induced by radiocaesium in the Fukushima terrestrial environment. *Journal of Environmental Radioactivity, 161*, 22-34.

Gonze, M.-A., Renaud, P., Korsakissok, I. n., Kato, H., Hinton, T. G., Mourlon, C., & Simon-Cornu, M. (2014). Assessment of dry and wet atmospheric deposits of radioactive aerosols: application to Fukushima radiocaesium fallout. *Environmental Science & Technology, 48*(19), 11268-11276.

Gonze, M.-A., & Sy, M. M. (2016). Interception of wet deposited atmospheric pollutants by herbaceous vegetation: Data review and modelling. *Science of the Total Environment, 565*, 49-67.

Goossens, L. H., & Harper, F. T. (1998). Joint EC/USNRC expert judgement driven radiological protection uncertainty analysis. *Journal of Radiological Protection, 18*(4), 249-264. doi: 10.1088/0952-4746/18/4/003

Goossens, L. H. J., Boardman, J., Harper, F. T., Kraan, B. C. P., Cooke, R. M., Young, M. L., . . . Hora, S. C. (1997). Probabilistic accident consequence uncertainty analysis: External exposure from deposited material uncertainty assessment. (Washington, DC: NRC and Brussels–Luxembourg: CEC).

Grueber, C. E., Nakagawa, S., Laws, R. J., & Jamieson, I. G. (2011). Multimodel inference in ecology and evolution: challenges and solutions. *Journal of Evolutionary Biology, 24*(4), 699-711. doi: 10.1111/j.1420-9101.2010.02210.x

Hamby, D. (1994). A review of techniques for parameter sensitivity analysis of environmental models. *Environmental monitoring and assessment, 32*(2), 135-154.

Hartmann, P., Urso, L., Fielitz, U., & Steiner, M. (2016). *A probabilistic/stochastic approach for contamination levels of Cs-137 in wild boars.* Paper presented at the 14th International Congress of the International Radiation Protection Association, Cape town, South Africa.

Hastings, W. K. (1970). Monte Carlo Sampling Methods Using Markov Chains and Their Applications. *Biometrika, 57*(1), 97-109. doi: 10.2307/2334940

Heinemeyer, G., Filter, M., Greiner, M., Herzler, M., Lindtner, O., Kurzenhäuser, S., . . . Schümann, M. (2018). Guidance document on uncertainty analysis in exposure assessment. Recommendation of the Committee for Exposure Assessment and Stand-ardisation of the Federal Institute for Risk Assessment (BfR).

Helton, J. C., & Davis, F. J. (2002). Illustration of sampling-based methods for uncertainty and sensitivity analysis. *Risk Analysis, 22*(3), 591-622. doi: 10.1111/0272-4332.00041

Helton, J. C., Hansen, C. W., & Sallaberry, C. J. (2012). Uncertainty and sensitivity analysis in performance assessment for the proposed high-level radioactive waste repository at Yucca

Mountain, Nevada. *Reliability Engineering & System Safety, 107*, 44-63. doi: 10.1016/j.ress.2011.07.002

Hinton, T. G., Garnier-Laplace, J., Vandenhove, H., Dowdall, M., Adam-Guillermin, C., Alonzo, F., . . . Vives i Batlle, J. (2013). An invitation to contribute to a strategic research agenda in radioecology. *Journal of Environmental Radioactivity, 115*, 73-82. doi: 10.1016/j.jenvrad.2012.07.011

IAEA. (2004). *Safety Standards Series No. Rs-G-1.7. Application of the Concepts of Exclusion, Exemption and Clearance.* (Vol. RS-G-1.7).

IAEA. (2009). Quantification of radionuclide transfer in terrestrial and freshwater environments for radiological assessments, IAEA-TECOC-1616, Vienna, 616 pp.

IAEA. (2011). Radioactive Particles in the Environment: Sources, particle characteristics and analytical techniques *IAEA-TECDOC* (pp. 90). Vienna: IAEA.

IAEA (Cartographer). (2018). World Distribution of Uranium Deposits.

ICRP. (2005). Low-dose Extrapolation of Radiation-related Cancer Risk. . *Annals of the ICRP, 35*(4).

ICRP. (2006). Assessing dose of the representative person for the purpose of radiation protection of the public and the optimisation of radiological protection *Annals of the ICRP* (Vol. 36, pp. 71-104): International Commission on Radiation Protection.

ICRP. (2012). Compendium of Dose Coefficients based on ICRP Publication 60. *Annals of the ICRP, 41*(Supplement).

ICRP. (2014). Protection of the Environment under Different Exposure Situations. ICRP Publication 124. *Annals of ICRP, 43*(1), 1-58. doi: 10.1177/0146645313497456

ICRP. (2017). Dose coefficients for nonhuman biota environmentally exposed to radiation. *Annals of ICRP, 46*(2).

Iman, R. L., & Conover, W. (1982). A Distribution-Free Approach to Inducing Rank Correlation Among Input Variates. *Communication in Statistics- Simulation and Computation, 11*(3), pp.311-334. doi: DOI: 10.1080/03610918208812265

Iosjpe, M. (2006). Environmental modelling: modified approach for compartmental models. *Radioactivity in the Environment, 8*, 463-476.

Iosjpe, M. (2011a). Evaluation of the environmental parameters controlling the vulnerability of the coastal marine regions. *Radioprotection, 46*(6), S289-S293.

Iosjpe, M. (2011b). A sensitivity analysis of the parameters controlling water–sediment interactions in the coastal zone: Consequences to man and environment. *Journal of Marine Systems, 88*(1), 82-89.

Iosjpe, M. (2014). *Radioecological assessment of marine environment: complexity, sensitivity and uncertainties.* Paper presented at the ICRER 2014: 3. International Conference on Radioecology and Environmental Radioactivity, Barcelona (Spain).

Iosjpe, M., Brown, J., & Strand, P. (2002). Modified approach to modelling radiological consequences from releases into the marine environment. *Journal of Environmental Radioactivity, 60*(1-2), 91-103.

Iosjpe, M., Karcher, M., Gwynn, J., Harms, I., Gerdes, R., & Kauker, F. (2011). Improvement of the dose assessment tools on the basis of dispersion of the 99 Tc in the Nordic Seas and the Arctic Ocean. *Radioprotection, 44*(5), 531-536.

IPCC. (2001). Climate change: the scientific basis. Contribution of working group I to the third assessment report of the intergovernmental panel of climate change. (pp. 881). Cambridge University press (UK) and New York (USA).

Jang, H.-K., Kim, J.-Y., & Lee, J.-K. (2008). Radiological risk assessment for field radiography based on two dimensional Monte Carlo analysis. *Applied Radiation and Isotopes, 67*, 4.

JCGM. (2008a). Evaluation of measurement data – Guide to the Expression of Uncertainty in Measurement (GUM 2008) (Vol. 100): BIPM.

JCGM. (2008b). *Evaluation of measurement data. Supplement 1 to the GUM. Propagation of distributions using a Monte Carlo method.* .

Jin, X., Xu, C.-Y., Zhang, Q., & Singh, V. P. (2010). Parameter and modeling uncertainty simulated by GLUE and a formal Bayesian method for a conceptual hydrological model. *Journal of Hydrology, 383*(3-4), 147-155. doi: 10.1016/j.jhydrol.2009.12.028

Jørgensen, S. E., & Bendoricchio, G. (2001). *Fundamentals of Ecological Modelling*: Elsevier.

Karcher, M., & Harms, I. (2000). Estimation of water and ice fluxes in the Arctic for an improved box structure of the NRPA box model (Transport Programme). *Report to the Norwegian Radiation Protection Agency (NRPA)*.

Kirkup, L., & Frenkel, R. B. (2006). *An Introduction to Uncertainty in Measurement. Using the GUM (Guide to the Expression of Uncertainty in Measurement)*. Sydney: Cambridge University Press

Klugman, S. A. (1992). The Hierarchical Bayesian Approach. In S. A. Klugman (Ed.), *Bayesian Statistics in Actuarial Science: with Emphasis on Credibility* (pp. 65-79). Dordrecht: Springer Netherlands.

Kraan, B., & Cooke, R. (1997). The Effect of Correlations in Uncertainty Analysis: Two Cases. . In R. Cooke (Ed.), *Technical Committee Uncertainty Modeling: Report on the Benchmark Workshop*. Delft, Netherlands.: European Safety and Reliability Association.

Krumbein, W. C., & Aberdeen, E. J. (1937). The sediments of Barataria Bay [Louisiana]. *Journal of Sedimentary Research, 7*(1), 3-17.

Kruschke, J. K., Aguinis, H., & Joo, H. (2012). The Time Has Come:Bayesian Methods for Data Analysis in the Organizational Sciences. *Organizational Research Methods, 15*(4), 722-752. doi: 10.1177/1094428112457829

Law, A. M. (2015). *Simulation Modeling and Analysis* (5th ed.): McGraw-Hill Education.

Lindenschmidt, K.-E., Fleischbein, K., & Baborowski, M. (2007). Structural uncertainty in a river water quality modelling system. *Ecological Modelling, 204*(3-4), 289-300. doi: 10.1016/j.ecolmodel.2007.01.004

MacKenzie, J., & Nicholson, S. (1987). COLDOS-a computer code for the estimation of collective doses from radioactive releases to the sea: UKAEA Safety and Reliability Directorate.

Maier, H. R. (2008). *Chap. 5: Uncertainty in Environmental decision making: Issues, challenges, and future directions* (Vol. 3). The Netherland: Elsevier.

Martuzzi, M. K. v. K. M. (2006). INTARESE Work Package 1.5: Cross-cutting issues in Risk Assessment - Integrating Uncertainty to integrated Assessment.

Masoudi, P. (2019). Estimation of Fukushima radiocesium deposits by airborne surveys: sensitivity to the flight-line spacing (under review).

McAllister, M., & Kirchner, C. (2002). Accounting for Structural Uncertainty to Facilitate Precautionary Fishery Management: Illustration with Namibian Orange Roughy. *Bulletin of Marine Science, 70*(2), 499-540.

McKay, M. D., Beckman, R. J., & Conover, W. J. (1979). Comparison of Three Methods for Selecting Values of Input Variables in the Analysis of Output from a Computer Code. *Technometrics, 21*(2), 239-245. doi: 10.1080/00401706.1979.10489755

Mercat-Rommens, C., Chojnacki, E., & Baudrit, C. (2006). *Uncertainties: new ways to take them into account TA-6: radiation protection of the public and the environment.* Paper presented at the Second European IRPA Congress on Radiation Protection, Paris.

Metropolis, N., Rosenbluth, A. W., Rosenbluth, M. N., & Teller, A. H. (1953). *Calculation of equations of state by fast computing machines* (Vol. 21).

Mitchell, D. L. (1996). Use of mass-and area-dimensional power laws for determining precipitation particle terminal velocities. *Journal of the atmospheric sciences, 53*(12), 1710-1723.

Mitchell, P., Condren, O., Vintró, L. L., & McMahon, C. (1999). Trends in plutonium, americium and radiocaesium accumulation and long-term bioavailability in the western Irish Sea mud basin. *Journal of Environmental Radioactivity, 44*(2-3), 223-251.

Mora, J. C., Cortes, D., Robles, B., Rodriguez, J., Brown, J. E., & Beresford, N. A. (2015). Generic model for combined TIER-1 assessments for human and wildlife.

Morgan, M. G., & Henrion, M. (1990). *Uncertainty – A Guide to Dealing with Uncertainty in Quantitative Risk and Policy Analysis*: Cambridge University Press.

Morgan, M. G., Henrion, M., & Small, M. (1992). *Uncertainty: A Guide to Dealing with Uncertainty in Quantitative Risk and Policy Analysis*: Cambridge University Press.

Mousavi, J., & Parvini, M. (2016). A sensitivity analysis of parameters affecting the hydrogen release and dispersion using ANOVA method. *International Journal of Hydrogen Energy, 41*(9), 5188-5201. doi: 10.1016/j.ijhydene.2016.01.042

Nelsen, R. B. (2006). *An Introduction to Copulas (Springer Series in Statistics)*: Springer-Verlag.

Nielsen, S., & Hou, X. (2002). MARINA II. Update of the MARINA Project on the radiological exposure of the European Community from radioactivity in North European marine waters. Annex B: Environmental data.

Nielsen, S., Iosjpe, M., & Strand, P. (1997). Collective doses to man from dumping of radioactive waste in the Arctic Seas. *Science of the Total Environment, 202*(1-3), 135-146.

NIST/SEMATECH. (*e-Handbook of Statistical Methods* Retrieved from http://www.itl.nist.gov/div898/handbook/

Oughton, D. H., Aguero, A., Avila, R., Brown, J. E., Copplestone, D., & Gilek, M. (2008). Addressing uncertainties in the ERICA Integrated Approach. *Journal of Environmental Radioactivity, 99*(9), 1384-1392. doi: 10.1016/j.jenvrad.2008.03.005

Özkaynak, H., Frey, H. C., Burke, J., & Pinder, R. W. (2009). Analysis of coupled model uncertainties in source-to-dose modeling of human exposures to ambient air pollution: A PM2. 5 case study. *Atmospheric Environment, 43*(9), 1641-1649.

Pelowitz, D. B., Durkee, J. W., Elson, J. S., Fensin, M. L., Hendricks, J. S., James, M. R., . . . Waters, L. S. (2011). MCNPX 2.7 E extensions: Los Alamos National Lab.(LANL), Los Alamos, NM (United States).

Periáñez, R. (2003). Redissolution and long-term transport of radionuclides released from a contaminated sediment: a numerical modelling study. *Estuarine, Coastal and Shelf Science, 56*(1), 5-14.

Periáñez, R. (2005). *Modelling the dispersion of radionuclides in the marine environment*: Springer.

Periáñez, R., Brovchenko, I., Jung, K., Kim, K., & Maderich, V. (2018). The marine kd and water/sediment interaction problem. *Journal of Environmental Radioactivity, 192*, 635-647.

Pröhl, G. (2003). Chapter 4 Radioactivity in the terrestrial environment. In E. M. Scott (Ed.), *Radioactivity in the Environment* (Vol. 4, pp. 87-108): Elsevier.

Pulkkinen, U., & Huovinen, T. (1996). Model uncertainty in safety assessment (pp. 34). Finland.

Refsgaard, J. C., van der Sluijs, J. P., Brown, J., & van der Keur, P. (2006). A framework for dealing with uncertainty due to model structure error. *Advances in Water Resources, 29*(11), 1586-1597. doi: 10.1016/j.advwatres.2005.11.013

Refsgaard, J. C., van der Sluijs, J. P., Hojberg, A. L., & Vanrolleghem, P. A. (2007). Uncertainty in the environmental modelling process - A framework and guidance. *Environmental Modelling & Software, 22*(11), 1543-1556. doi: 10.1016/j.envost.2007.02.004

Rice, J. A. (2006). *Mathematical Statistics and Data Analysis*.

Risbey, J., van der Sluijs, J., Kloprogge, P., Ravetz, J., Funtowicz, S., & Quintana, S. C. (2005). Application of a checklist for quality assistance in environmental modelling to an energy model. *Environmental Modeling & Assessment, 10*(1), 63-79. doi: 10.1007/s10666-004-4267-z

Salbu, B. (2006). Uncertainties in environmental impact and risk assessment from radionuclides released from different nuclear sources influencing the Arctic. In P. Strand, M. K. Sneve, & A. V. Pechkurov (Eds.), *Radiation and Environmental Safety in North-West Russia* (Vol. 9, pp. 273-284).

Salbu, B. (2016). Environmental impact and risk assessments and key factors contributing to the overall uncertainties. *Journal of Environmental Radioactivity, 151* 352-360. doi: 10.1016/j.jenvrad.2015.09.001

Salbu, B., Teien, H. C., Lind, O. C., & Tollefsen, K.-E. (2019). Why is the multiple stressor concept of relevance to radioecology? *International Journal of Radiation Biology*.

Saltelli, A., & Annoni, P. (2010). How to avoid a perfunctory sensitivity analysis. *Environmental Modelling & Software, 25*(12), 1508-1517. doi: 10.1016/j.envsoft.2010.04.012

Saltelli, A., & Bolado, R. (1998). An alternative way to compute Fourier amplitude sensitivity test (FAST). *Computational Statistics & Data Analysis, 26*(4), 445-460. doi: 10.1016/s0167-9473(97)00043-1

Saltelli, A., Ratto, M., Andres, T., Campolongo, F., Cariboni, J., Gatelli, D., . . . Tarantola, S. (2008). *Global sensitivity analysis. The primer*. The Atrium, Southern Gate, Chichester, West Sussex PO19 8SQ, England: John Wiley & Sons, Ltd.

Saltelli, A., Ratto, M., Tarantola, S., Campolongo, F., Commission, E., & Ispra, J. R. C. (2006). Sensitivity analysis practices: Strategies for model-based inference. *Reliability Engineering & System Safety, 91*(10-11), 1109-1125. doi: 10.1016/j.ress.2005.11.014

Saltelli, A., Tarantola, S., Campolongo, F., & Ratto, M. (2004). *Sensitivity Analysis in Practice: A Guide to Assessing Scientific Models*: Halsted Press.

Sellafield. (2017). Particles in the Environment. Annual Report for 2016/2017 and Forward Programme. Whitehaven: Sellafield Ltd. UK Nuclear Decommission Authority.

Sellafield. (2018). Particles in the Environment. Annual Report for 2017 and Forward Programme. Whitehaven: Sellafield Ltd. UK Nuclear Decommission Authority.

Sheppard, C. S. (2013). Transfer Parameters – Are On-Site Data Really Better? . *Human and Ecological Risk Assessment., 11*, pp.939-949.

Sheppard, S. C. (2011). Robust Prediction of Kd from Soil Properties for Environmental Assessment. *Human and Ecological Risk Assessment, 17*(1), 263-279.

Simon-Cornu, M., Beaugelin-Seiller, K., Boyer, P., Calmon, P., Garcia-Sanchez, L., Mourlon, C., . . . Gonze, M. A. (2015). Evaluating variability and uncertainty in radiological impact assessment using SYMBIOSE. *Journal of Environmental Radioactivity, 139*, 91-102. doi: 10.1016/j.jenvrad.2014.09.014

Sivia, D., & Skilling, J. (2006). Data Analysis: A Bayesian Tutorial (pp. 264): Oxford University Press.

Skipperud, L., Vives I Batlle, J., Thorring, H., Kashparov, V., Beresford, N., Michalik, B., . . . Søvik, Å. (2017). Deliverable (D-No. 3.2), COMET WP3. COMET IRA on improved parameterisation of key processes for transfer and dynamic modelling approaches: results and impact.

Smith, A. E., Ryan, P. B., & Evans, J. S. (1992). The Effect of Neglecting Correlations When Propagating Uncertainty and Estimating the Population Distribution of Risk. . *Risk Analysis, 12*, pp. 467-474.

Sobol, I. M. (1993). Sensitivity estimates for non linear mathematical models. *Mathematical Modelling and Computational Experiments*(1), 7.

Søvik, Å., Vives i Batlle, J., Duffa, C., Masque, P., Lind, O., Salbu, B., . . . Thørring, H. (2017). COMET deliverable (D-No. 3.7). Final report of WP3 activities.

Spiegelhalter, D. J., Best, N. G., Carlin, B. P., & Van Der Linde, A. (2002). Bayesian measures of model complexity and fit. *Journal of the Royal Statistical Society: Series B (Statistical Methodology), 64*(4), 583-639.

Strauss, R. L. a. O. (1997). Coping with Uncertainty: A Naturalistic Decision-making Analysis. *Organisational behaviour and human decision processes, 69*(2), 149-163.

Suter-II, G. W. (2007). *Ecological Risk Assessment*: CRC Press. Taylor & Francis Group.

Sy, M. M. (2016). *Analyse d'incertitude en situation accidentelle. Transfer de radionucleides dans l'environnement et evaluation de l'exposition humaine par voie alimentaire.* (Docteur de l'Universite d'Aix-Marseille), Aix-Marseille Universite Marseille (France).

Sy, M. M., Gonze, M.-A., Metivier, J.-M., Nicoulaud-Gouin, V., & Simon-Cornu, M. (2016). Uncertainty analysis in post-accidental risk assessment models: An application to the Fukushima accident. *Annals of Nuclear Energy, 93*, 94-106. doi: 10.1016/j.anucene.2015.12.033

Symonds, M. R. E., & Moussalli, A. (2011). A brief guide to model selection, multimodel inference and model averaging in behavioural ecology using Akaike's information criterion. *Behavioral Ecology and Sociobiology, 65*(1), 13-21. doi: 10.1007/s00265-010-1037-6

Tian, Y., Huffman, G. J., Adler, R. F., Tang, L., Sapiano, M., Maggioni, V., & Wu, H. (2013). Modeling errors in daily precipitation measurements: Additive or multiplicative? *Geophysical Research Letters, 40*(10), 2060-2065. doi: 10.1002/grl.50320

Till, J. E., & Grogan, H. A. (2008). *Radiological risk assessment and environmental analysis*. Oxford; New York: Oxford University Press.

Tucker, W. T., & Ferson, S. (2003). Probability Bounds Analysis in Environmental Risk Assessment. *Applied Biomathematics Report* (pp. pp.1-63).

Uusitalo, L., Lehikoinen, A., Helle, I., & Myrberg, K. (2015). An overview of methods to evaluate uncertainty of deterministic models in decision support. *Environmental Modelling & Software, 63*, 24-31. doi: 10.1016/j.envsoft.2014.09.017

van der Sluijs, J. P., Risbey, J. S., Kloprogge, P., Ravetz, J. R., Funtowicz, S. O., Quintana, S. C., . . . Huijs, S. W. F. (2003). RIVM/MNP Guidance for Uncertainty Assessment and Communication: Detailed Guidance (RIVM/MNP Guidance for Uncertainty Assessment and Communication Series, Volume 3)

Vanhoudt, N. (2015). Sludge heap 'Kepkensberg' from Belgian phosphate industry. European Observatories for Radioecological Research – Template for the Description of Candidate Sites *EC STAR Project Report* (pp. 20).

Vidal, M., Rigol, A., & Gil-Garcia, C. J. (2009). Soil radionuclide interactions. In: IQuantification of radionuclide transfer in terrestrial and freshwater environments for radiological assessments, IAEA-TECOC-1616, Vienna, pp. 71-102.

Vives i Batlle, J., Vandenhove, H., & Gielen, S. (2014). Modelling water and ^{36}Cl cycling in a Belgian pine forest. In: Proc. ICRER 2014 - 3rd International Conference on Radioecology & Environmental Radioactivity, 7-12 September 2014, Barcelona, Catalonia. Electronic proceedings Extended Abstract. Available from: http://radioactivity2014.pacifico-meetings.com/.

Vose, D. (2008). *Risk Analysis: A Quantitative Guide*: John Wiley & Sons.

Walker, W. E., Harremoës, P., Rotmans, J., Van Der Sluijs, J. P., Van Asselt, M. B., Janssen, P., & Krayer von Krauss, M. P. (2003). Defining Uncertainty A Conceptual Basis for Uncertainty Management in Model-Based Decision Support. *Integrated assessment, 4*, 5-17.

Walsh, L., & Kaiser, J. C. (2011). Multi-model inference of adult and childhood leukaemia excess relative risks based on the Japanese A-bomb survivors mortality data (1950-2000). *Radiation and Environmental Biophysics, 50*(1), 21-35. doi: 10.1007/s00411-010-0337-6

Zadeh, L. A. (1965). Fuzzy sets. *Information and control, 8*(3), 338-353.